Electronic Supplementary Material (ESI) for Dalton Transactions.

Supporting information

GSH resistant and highly cytoselective Ruthenium(II)-*p*-cymene-imidazo[4,5-f][1,10]phenanthrolin-2-yl)phenol complexes as potential anticancer agent‡

Binoy Kar,[a] Utpal Das,[a] Sourav De,[a] Sudhindra Pete,[a] Ajay Sharma S,[a] Nilmadhab Roy,[a] Ashok Kumar S K,[a] Debashis Panda,[b] Priyankar Paira*[a]

CHARACTERIZATION OF LIGANDS (L1-L7)

^{1}H NMR of ligand L1:

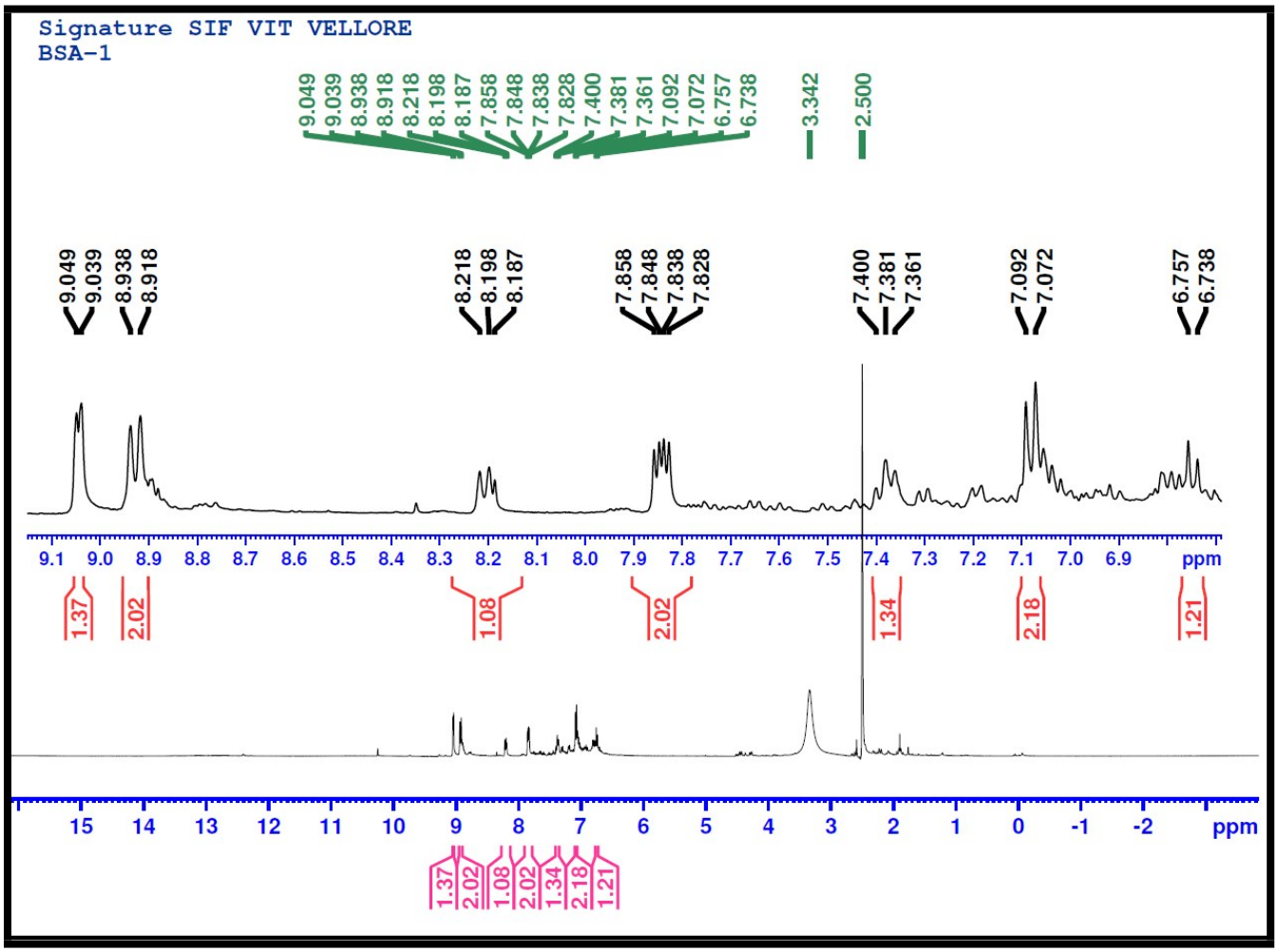

^{1}H NMR of ligand L2:

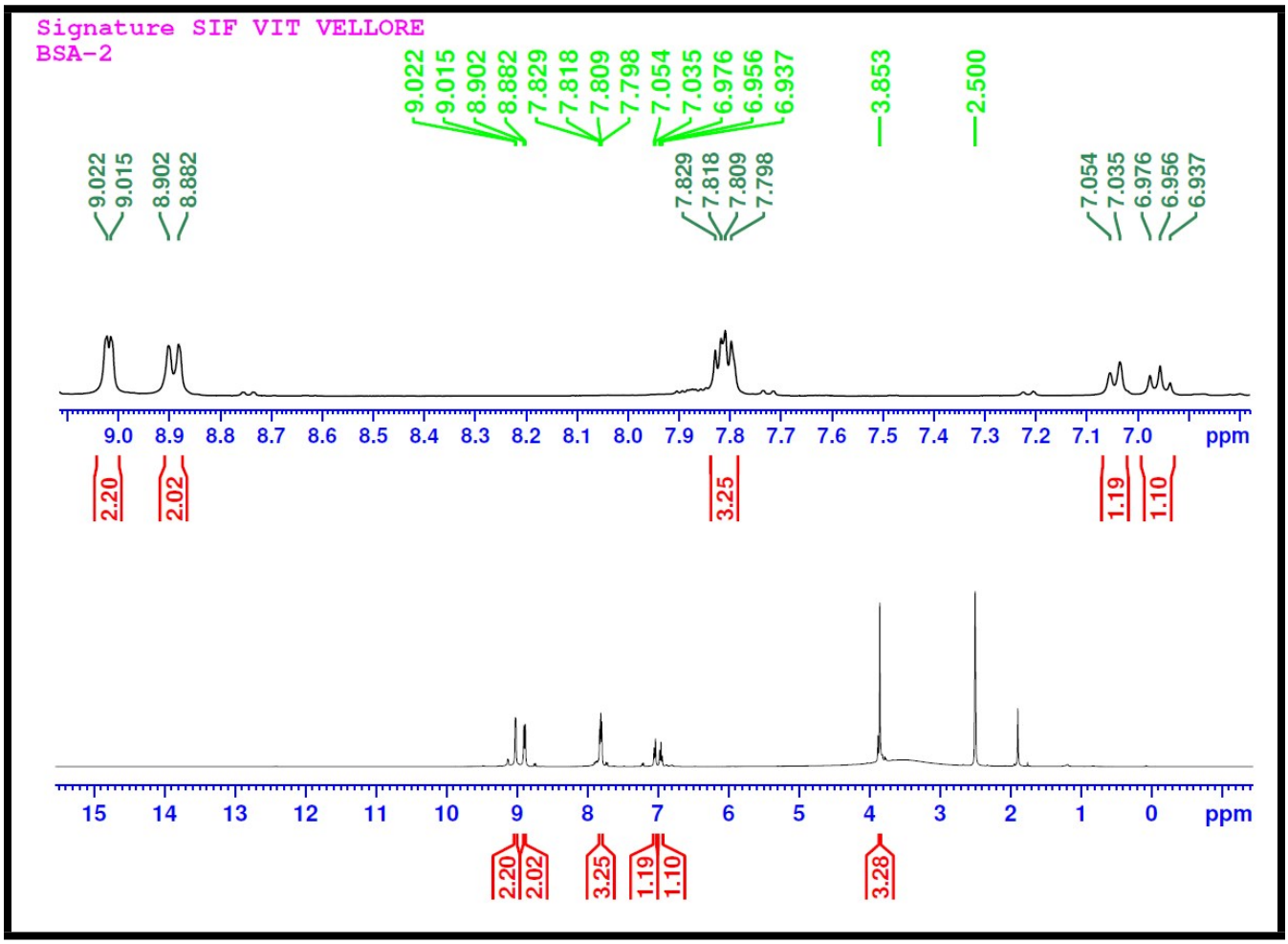

^{1}H NMR of ligand L3:

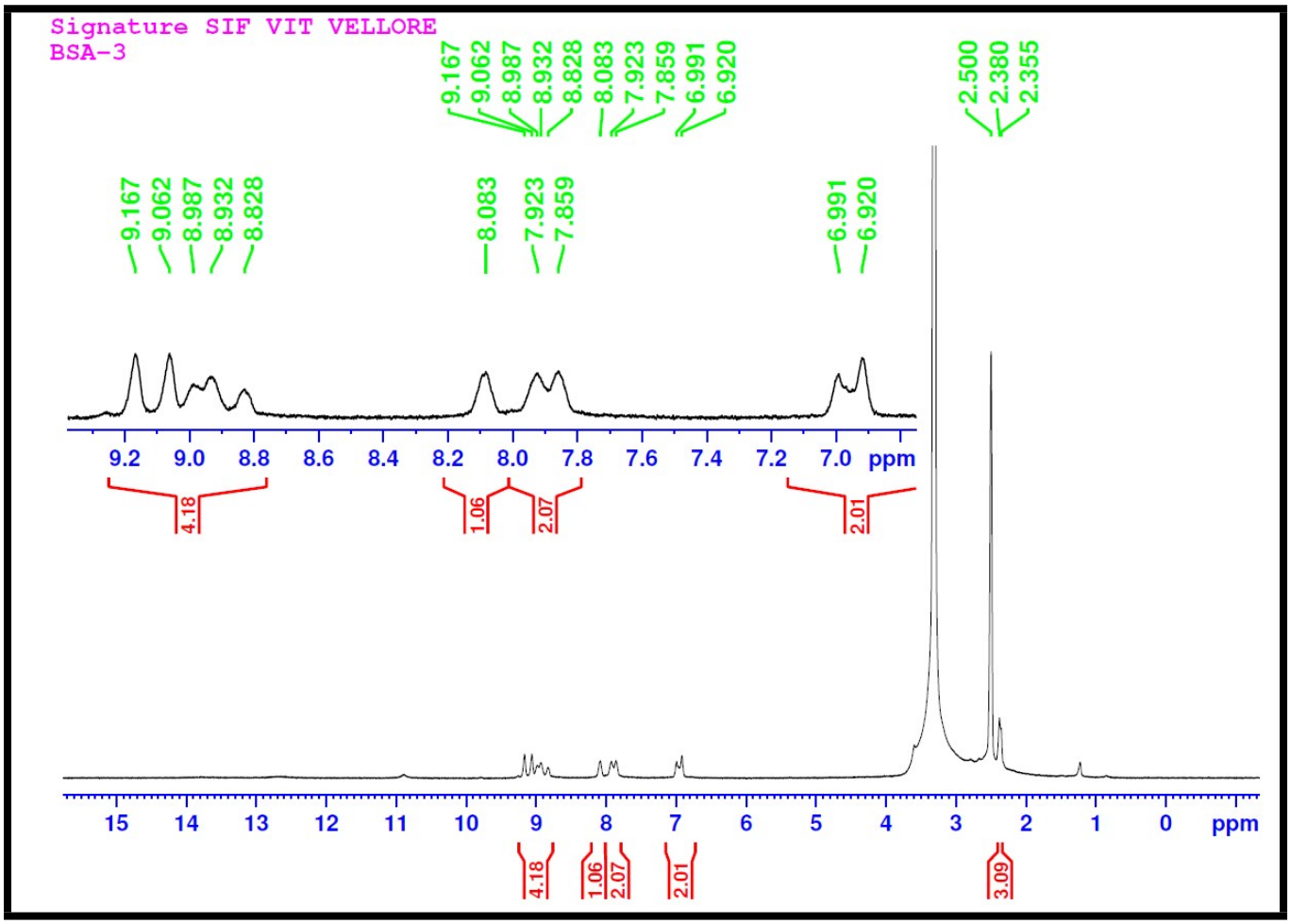

^{1}H NMR of ligand L4:

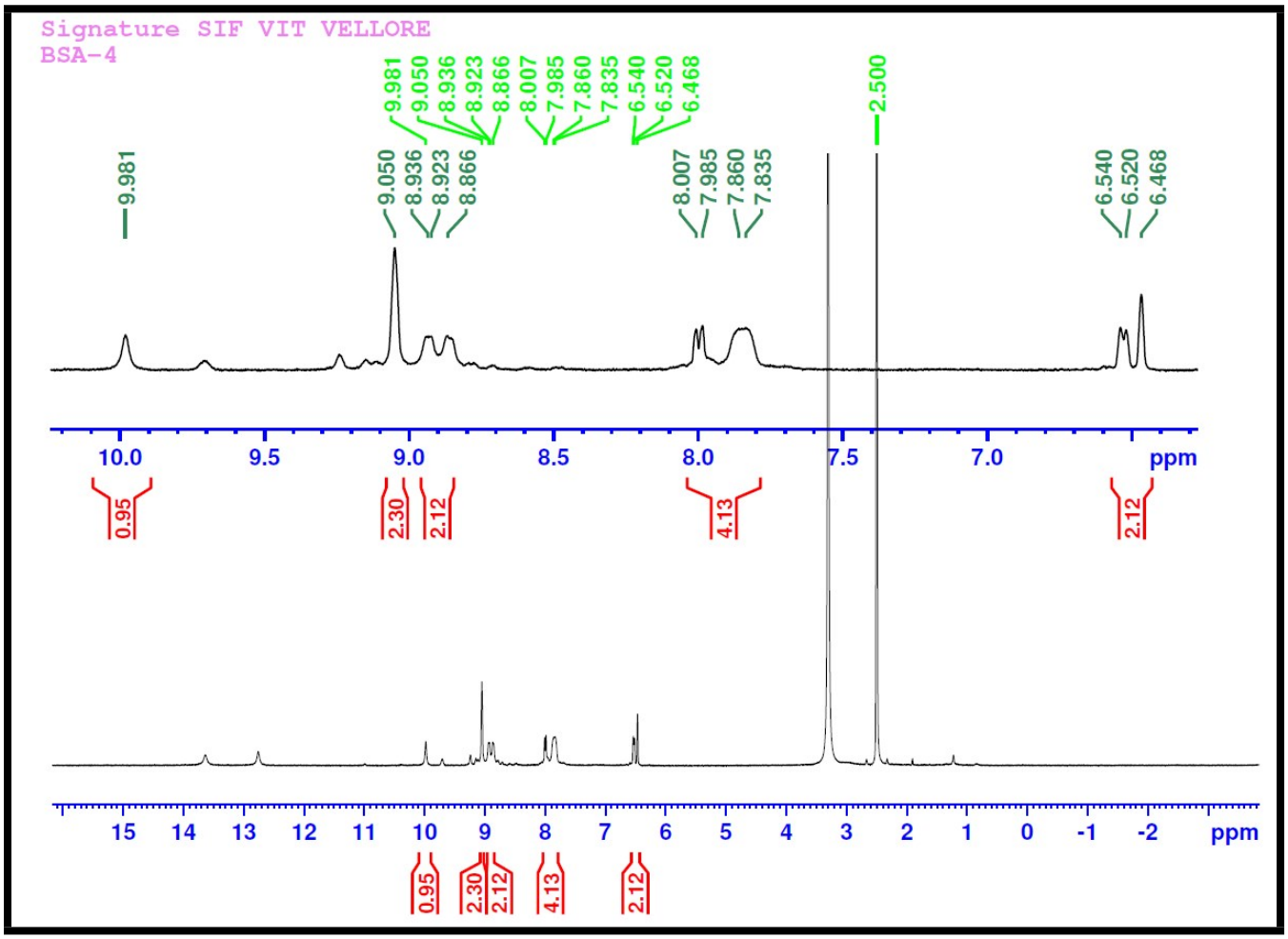

^{1}H NMR of ligand L5:

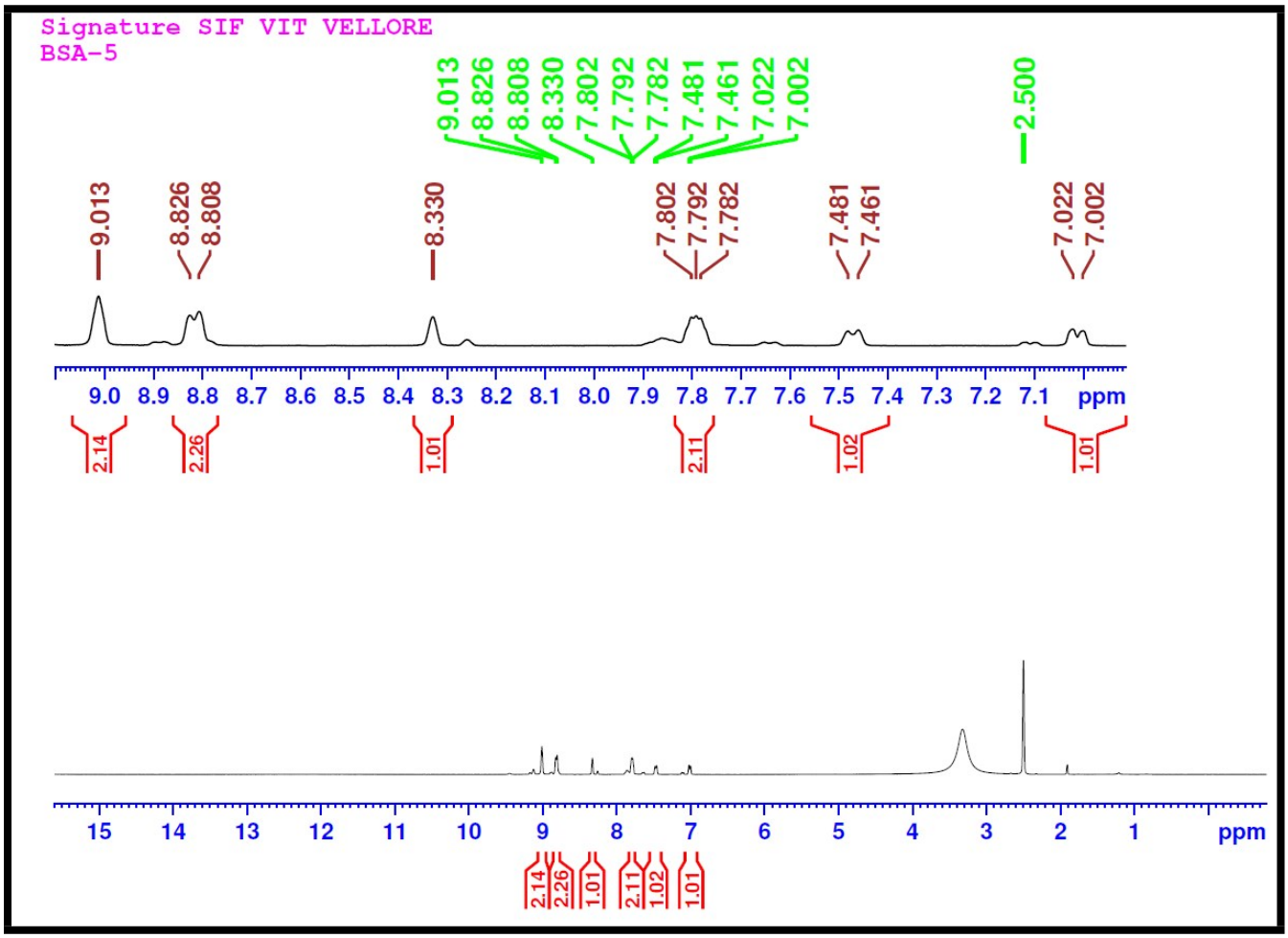

^{1}H NMR of ligand L6:

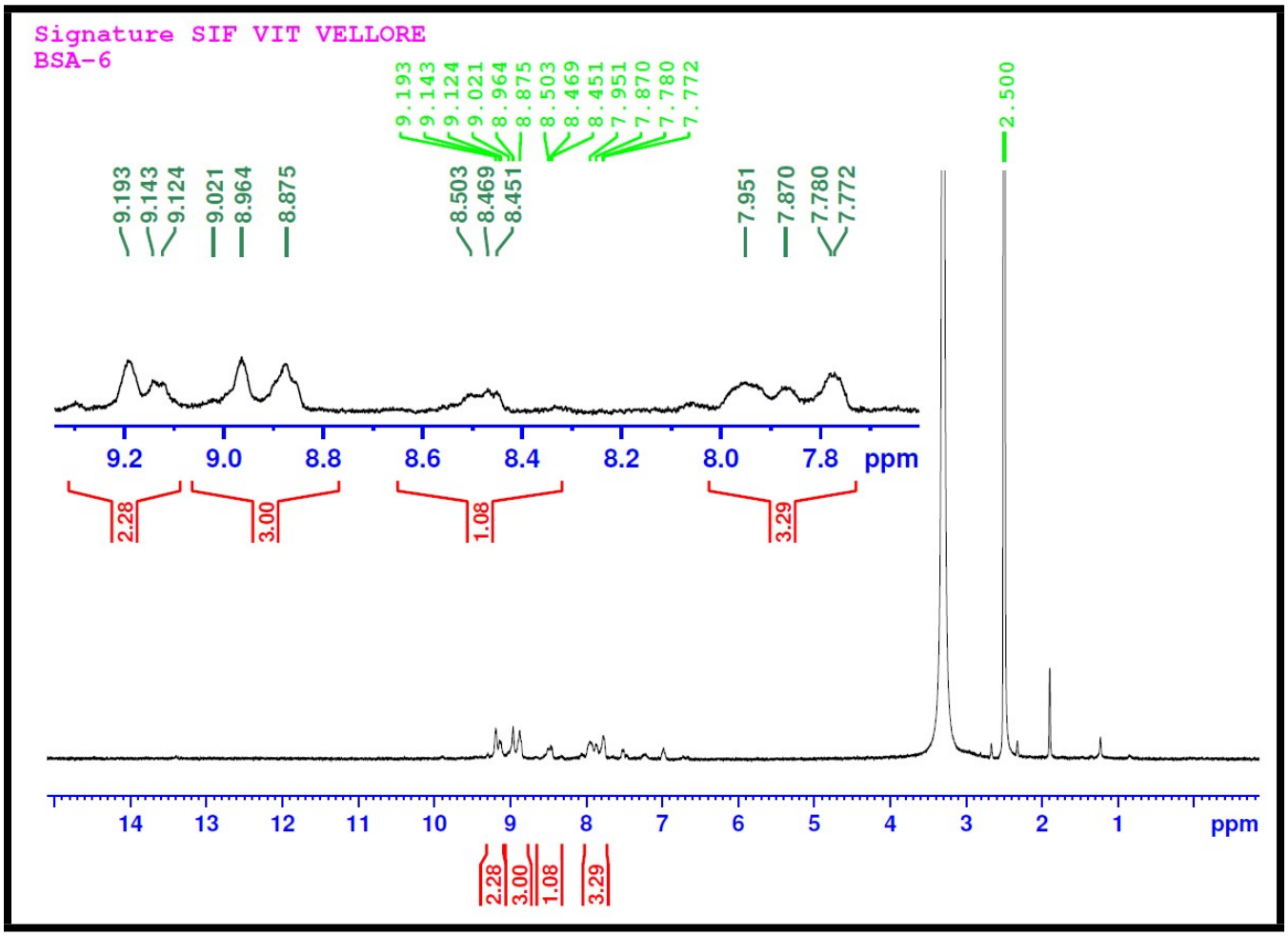

^{1}H NMR of ligand L7:

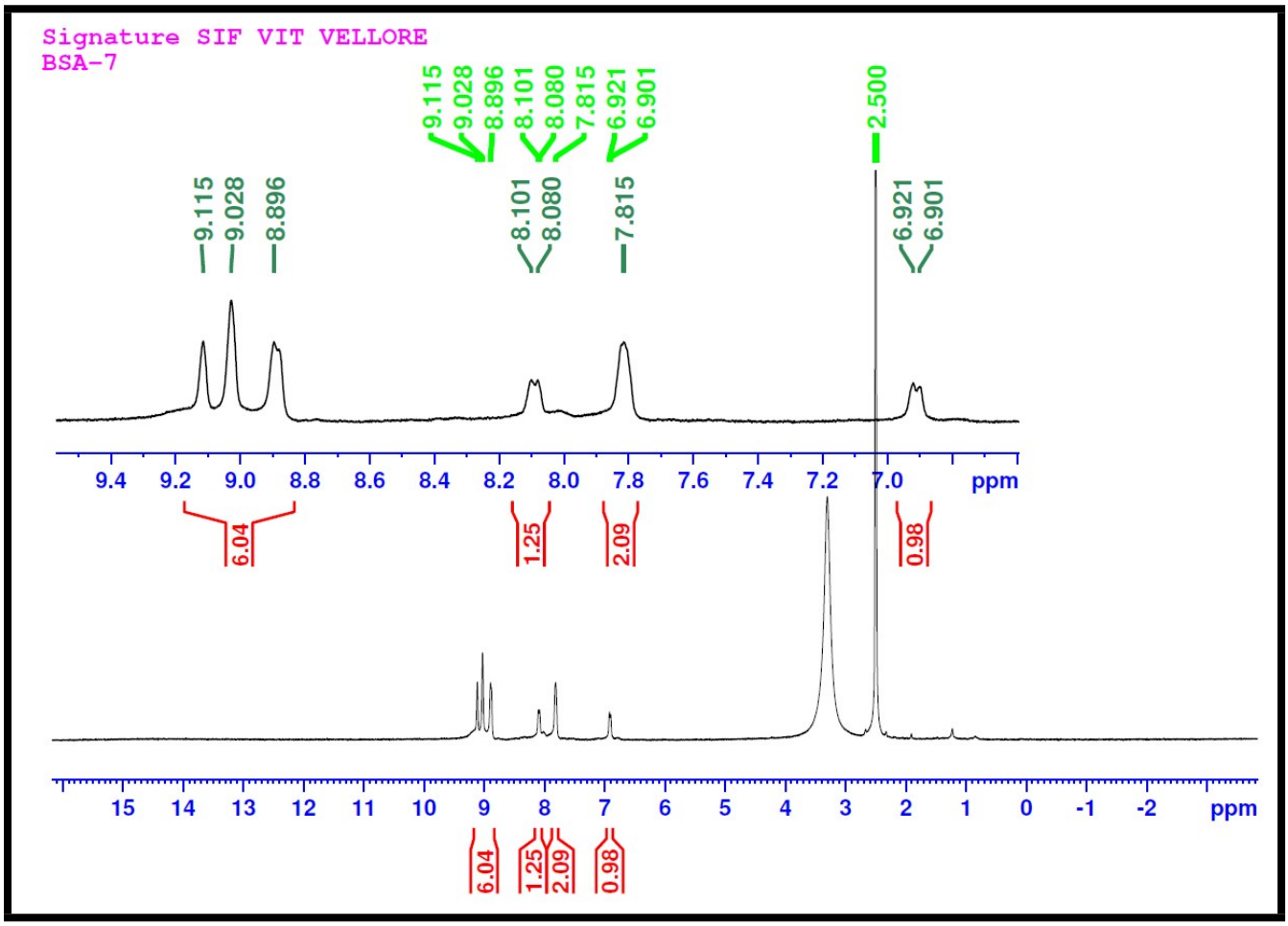

CHARACTERIZATION OF COMPLEXES (RuL1-RuL7):

^{1}H NMR of complex RuL1:

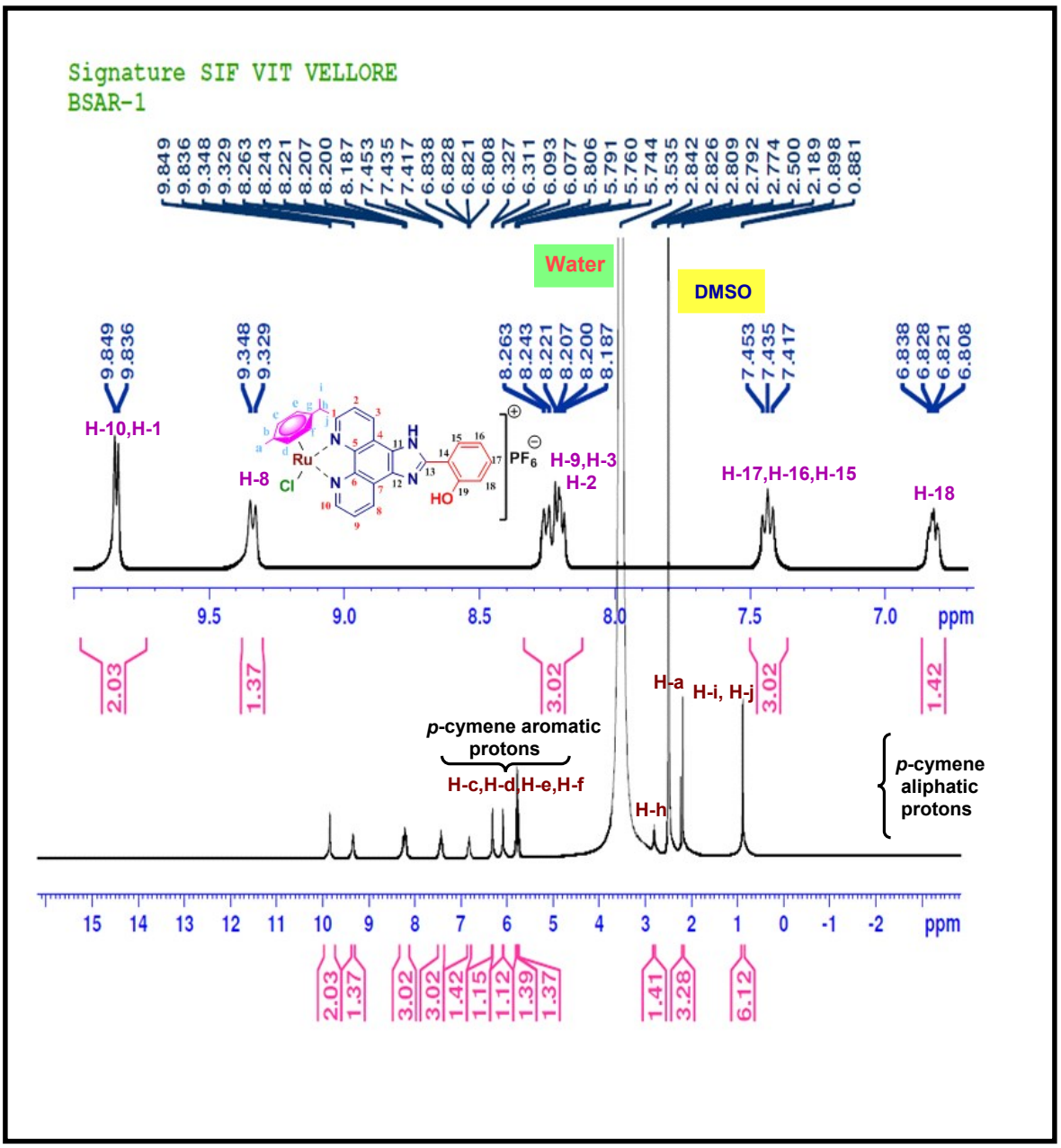

^{13}C NMR of complex RuL1:

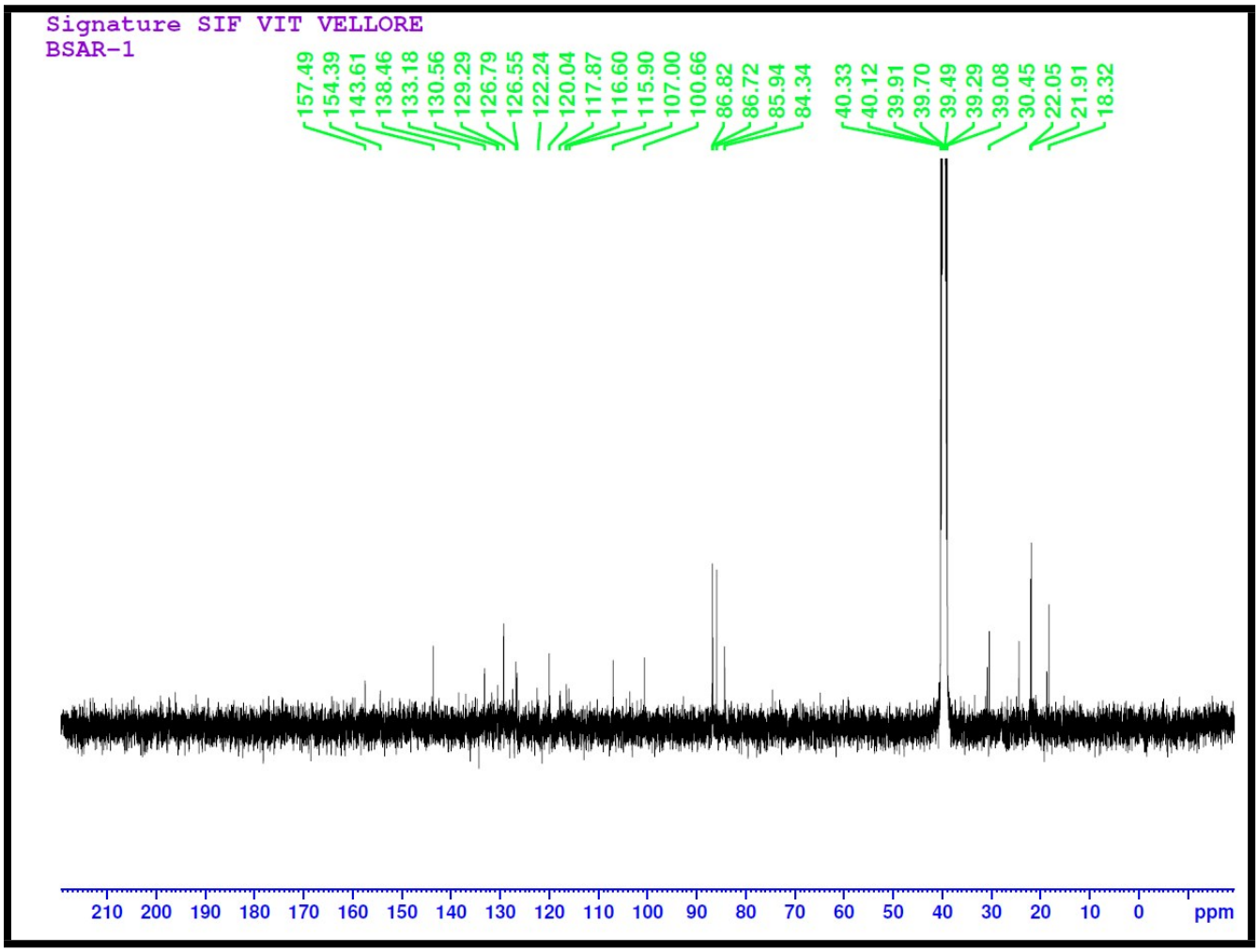

^{19}F NMR of complex RuL1:

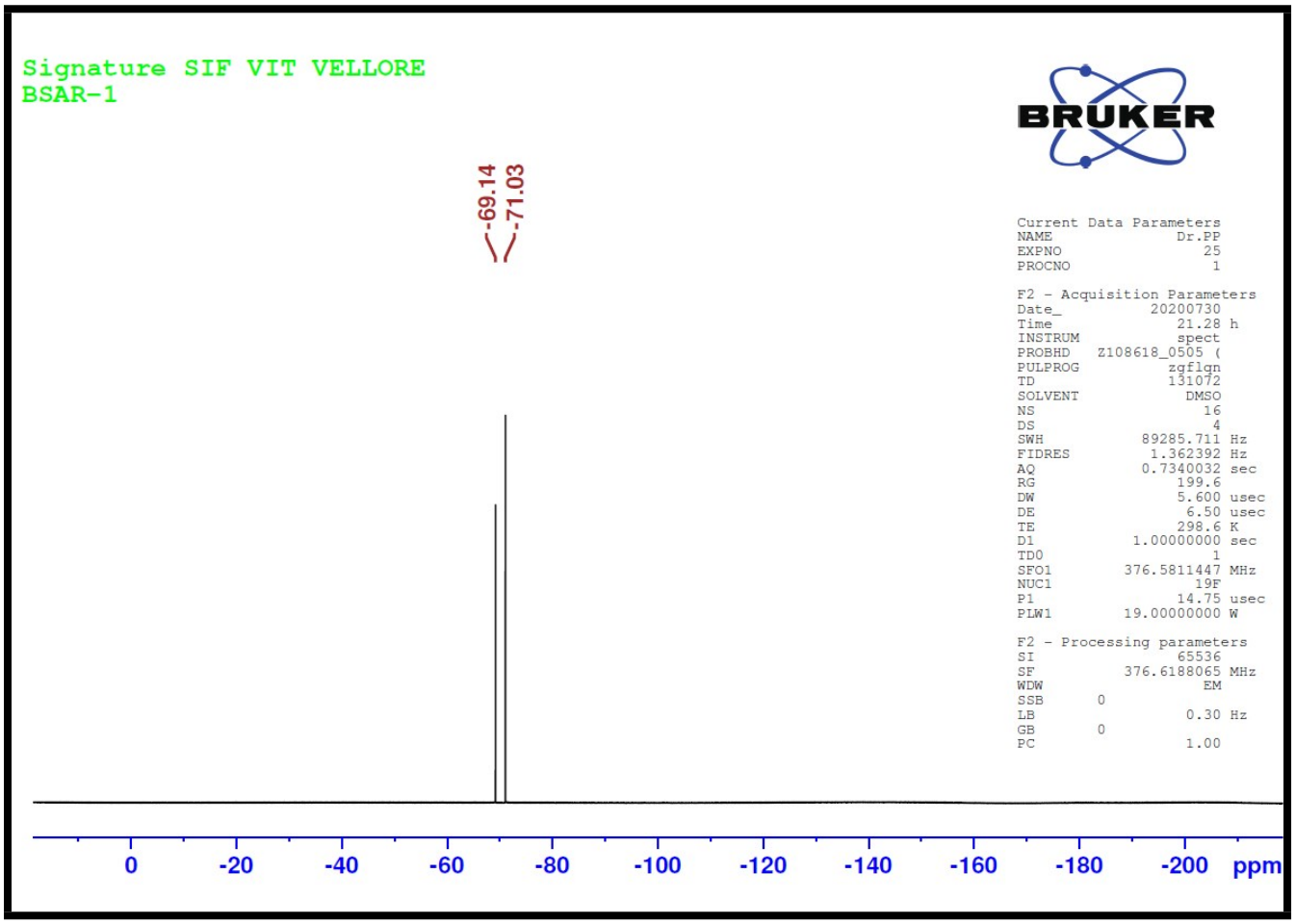

^{31}P NMR of complex RuL1:

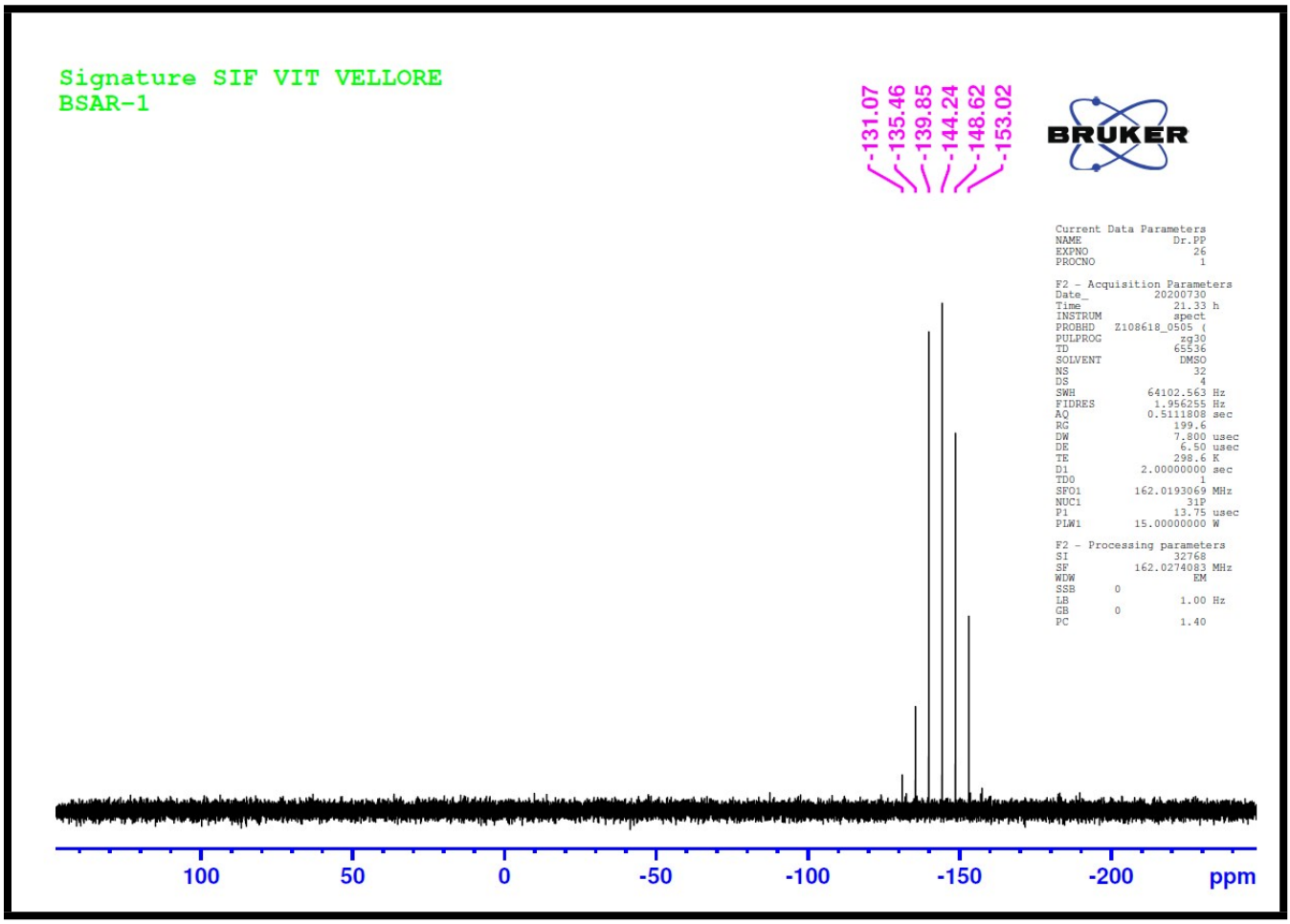

IR spectrum of RuL1

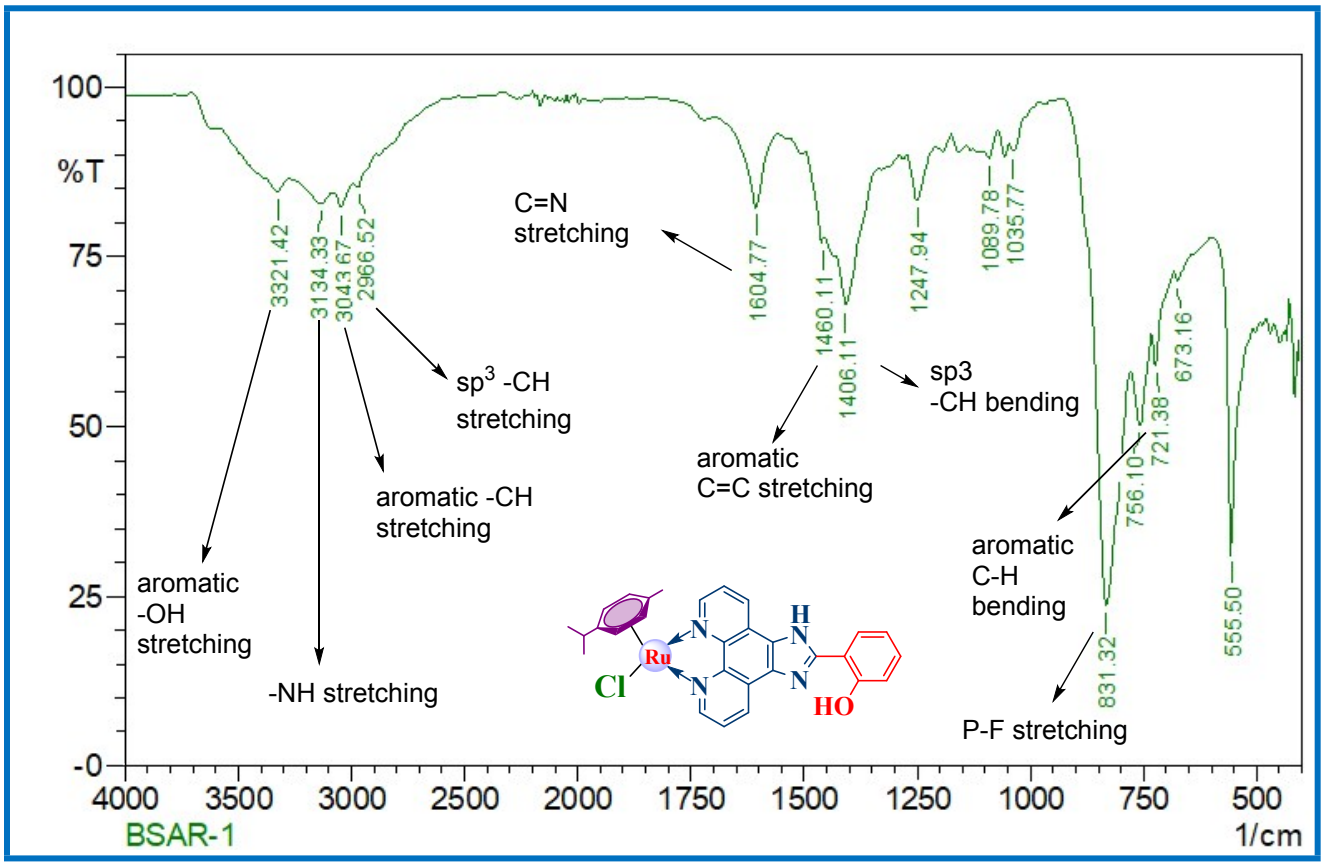

^{1}H NMR of complex RuL2:

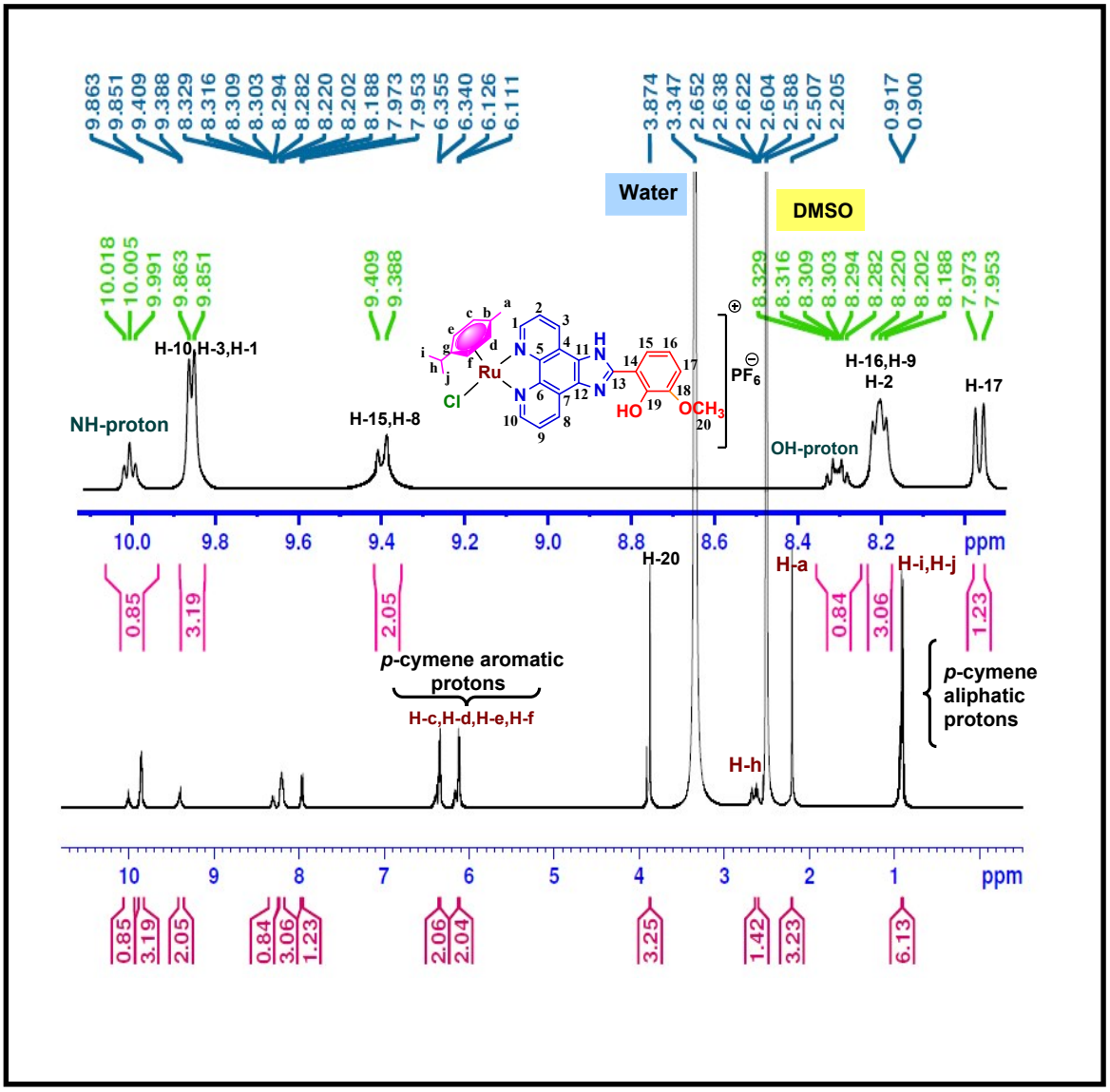

^{13}C NMR of complex RuL2:

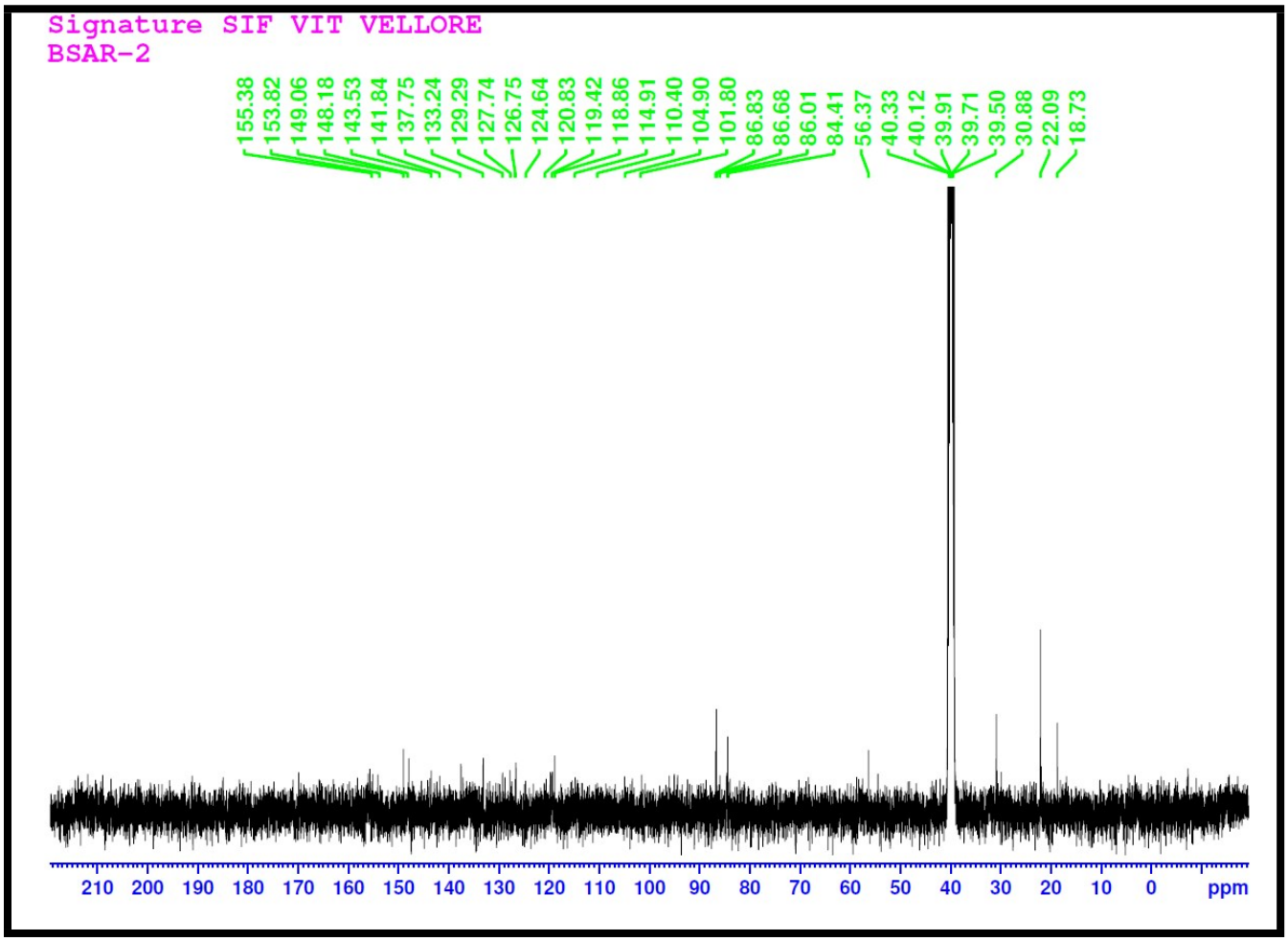

^{19}F NMR of complex RuL2:

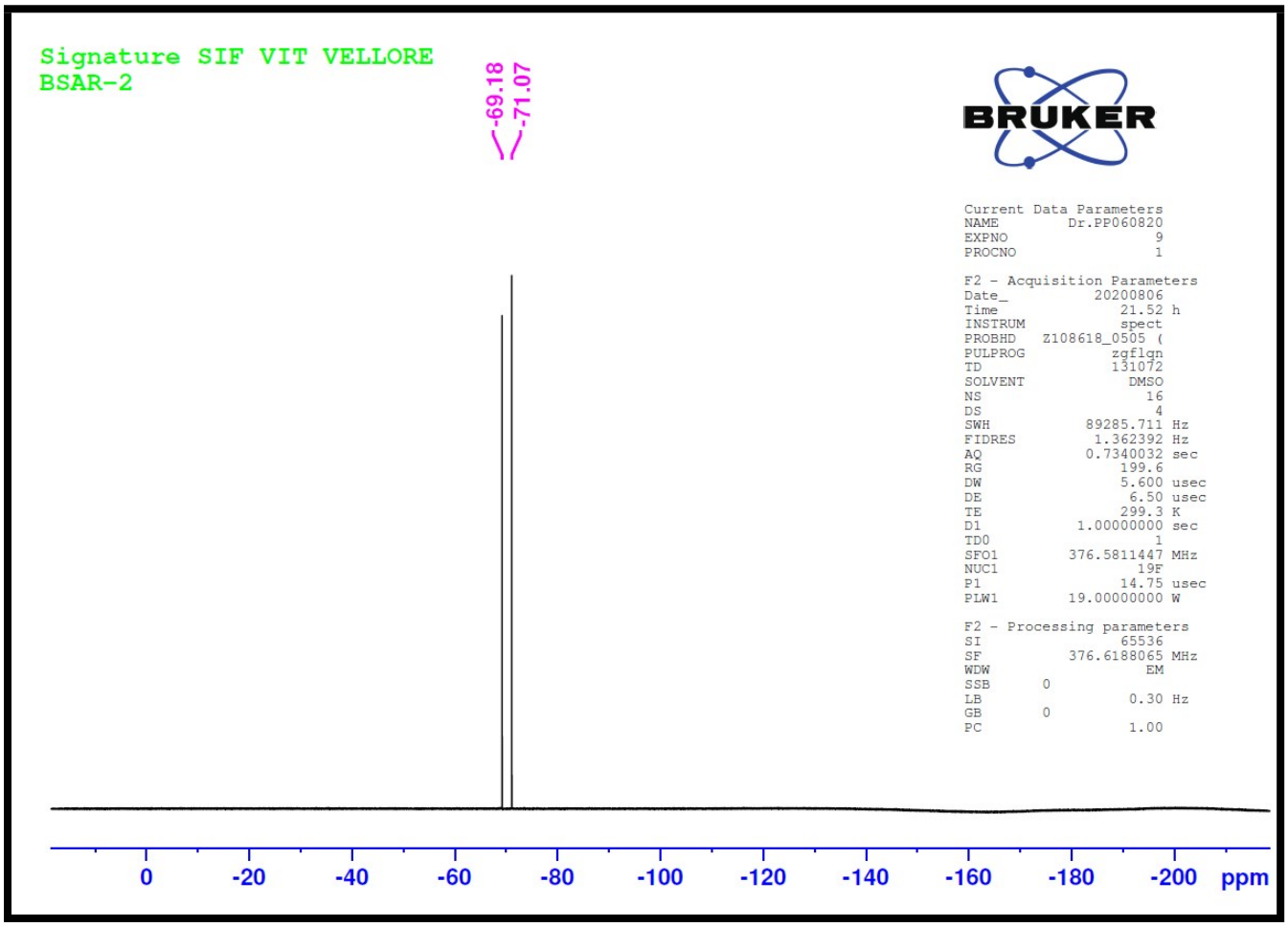

^{31}P NMR of complex RuL2:

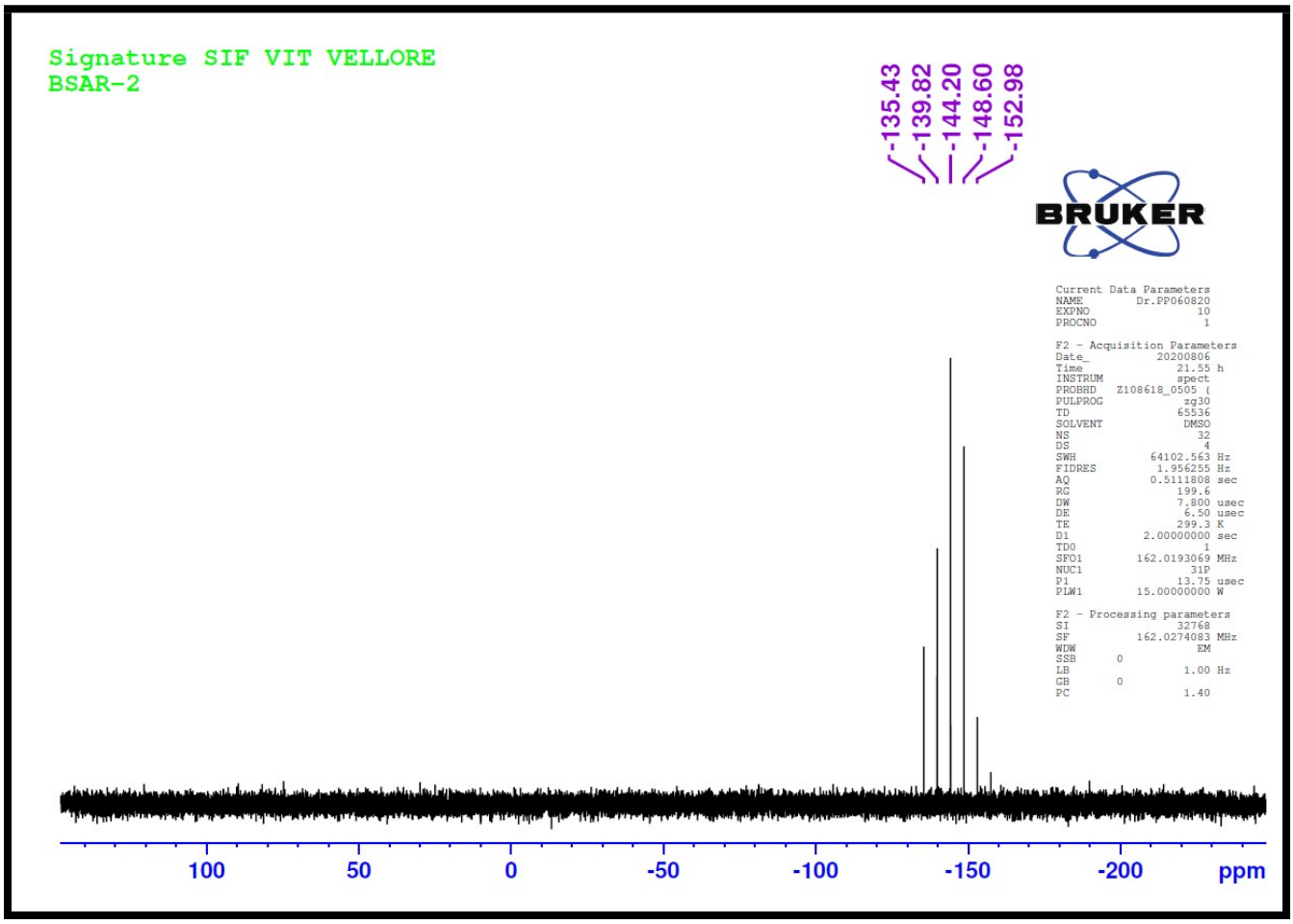

IR spectrum of RuL2

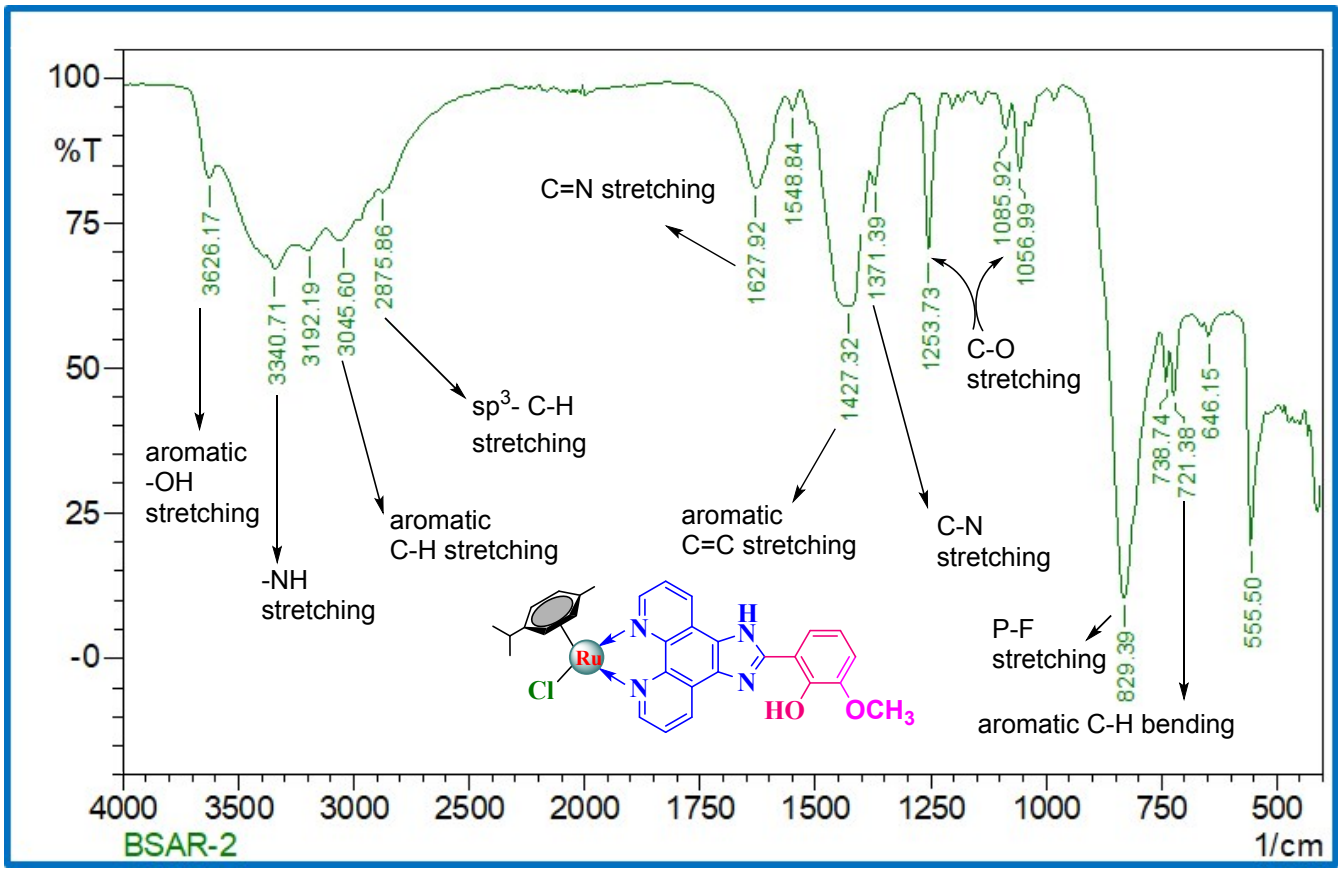

[1]H NMR of complex RuL3:

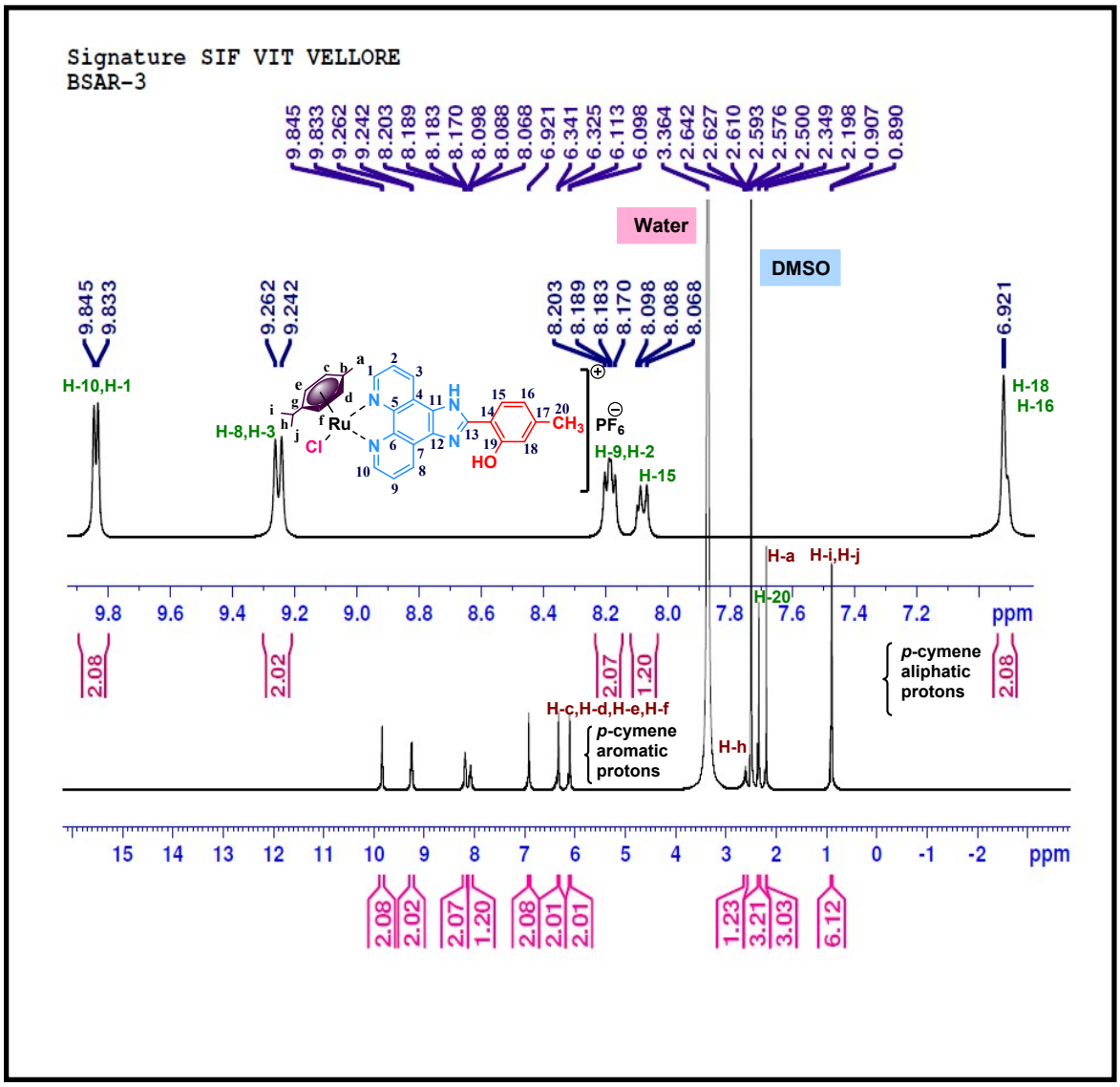

^{13}C NMR of complex RuL3:

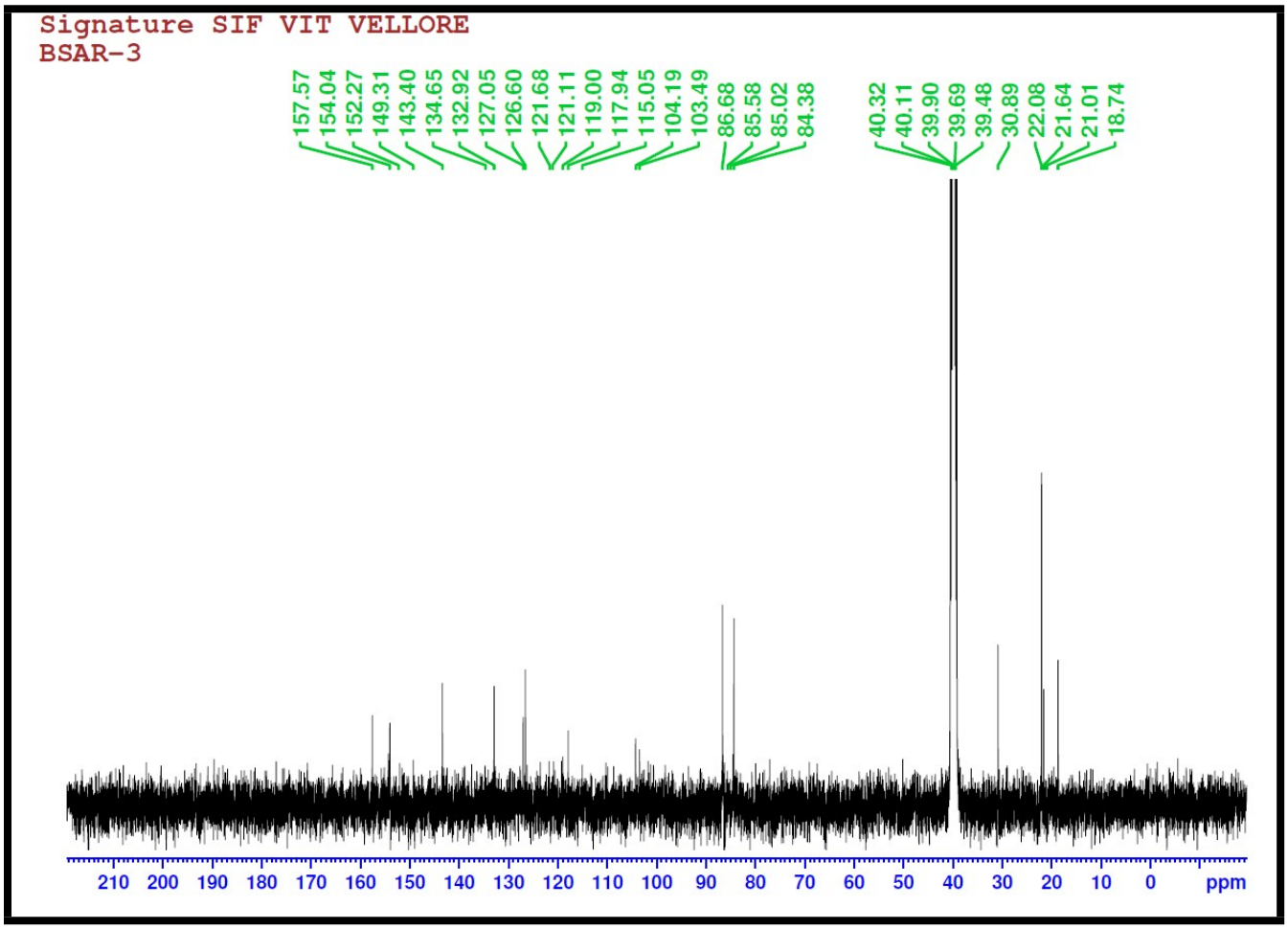

^{19}F NMR of complex RuL3:

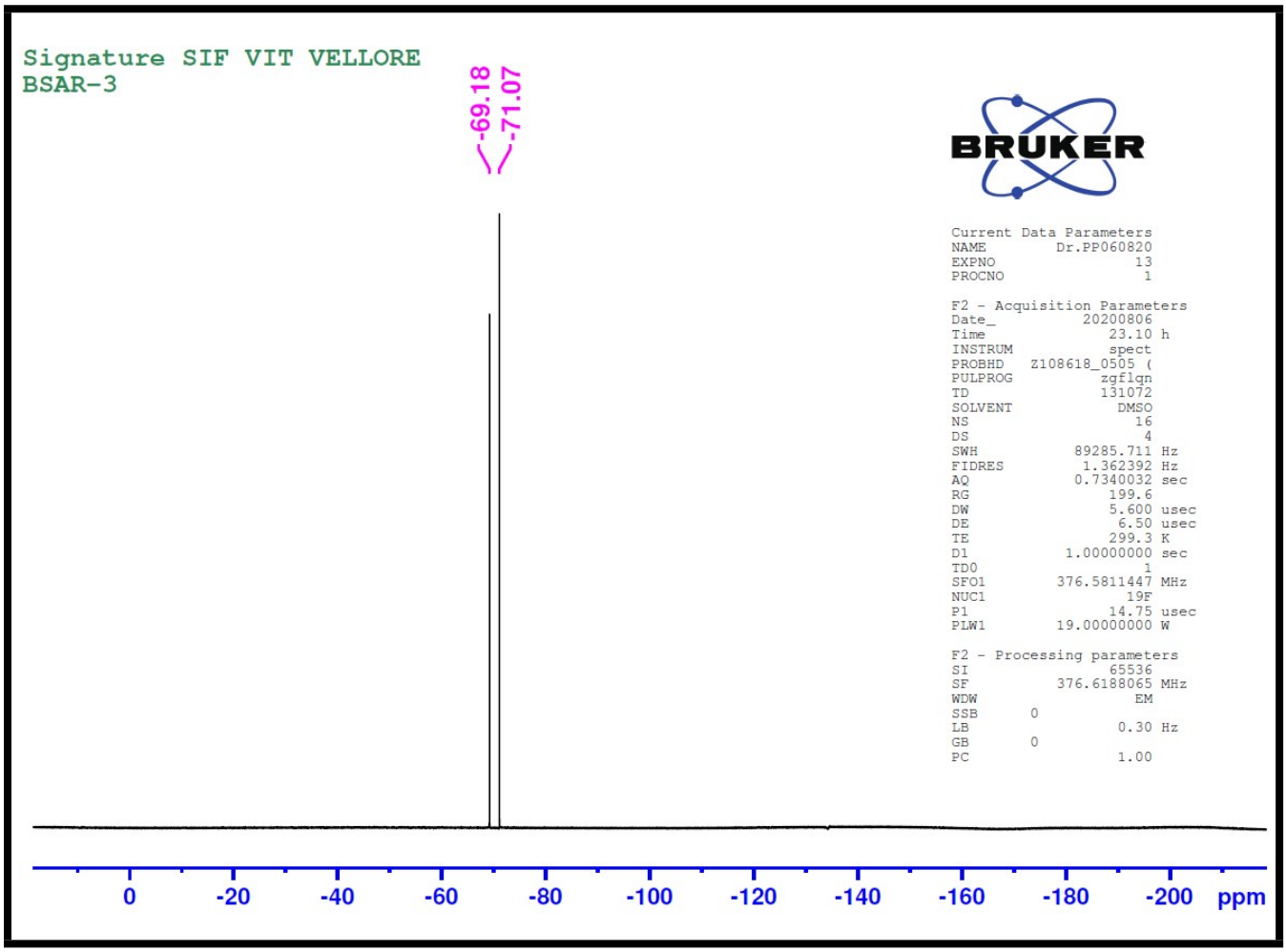

^{31}P NMR of complex RuL3:

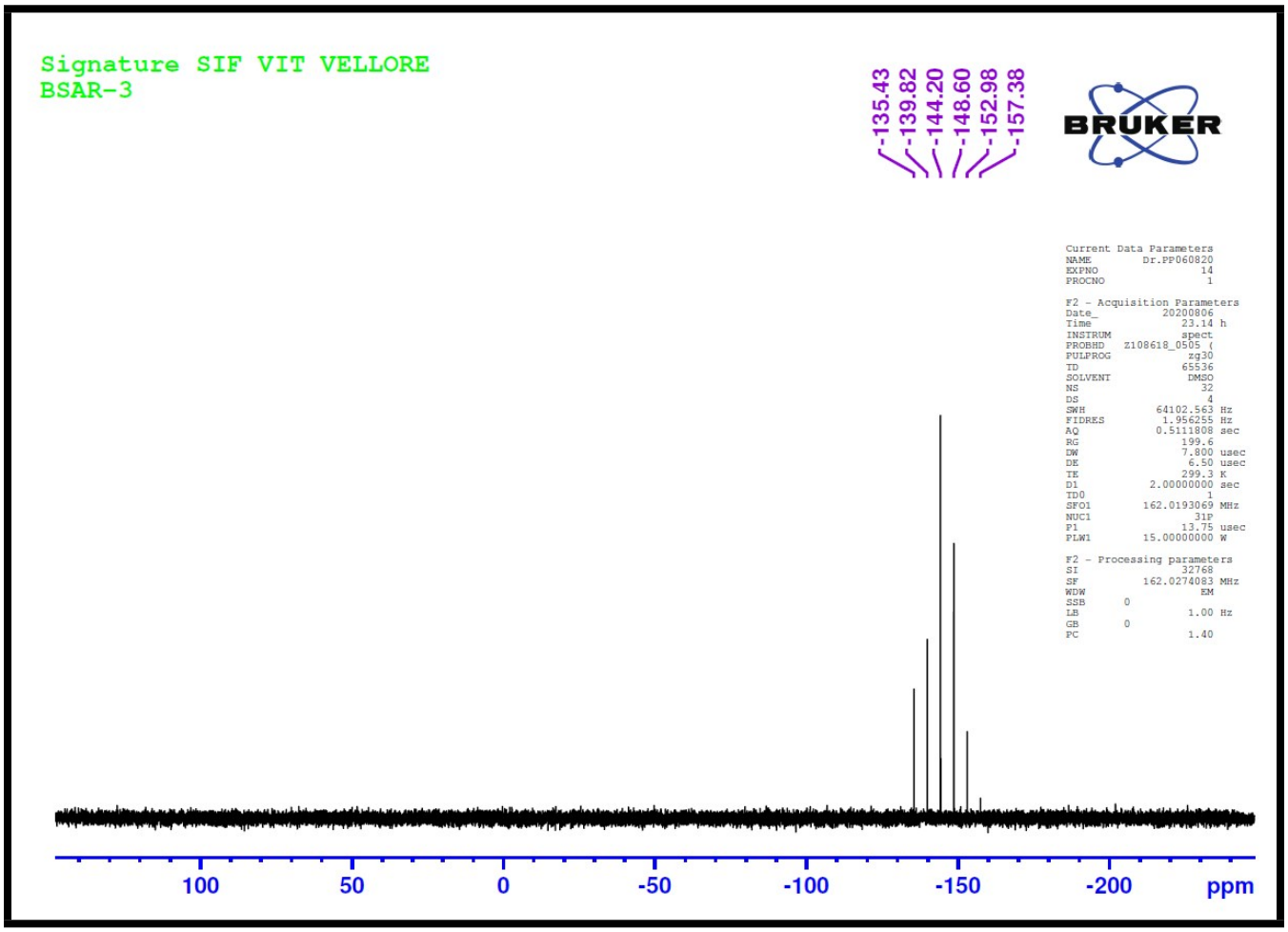

IR spectrum of RuL3

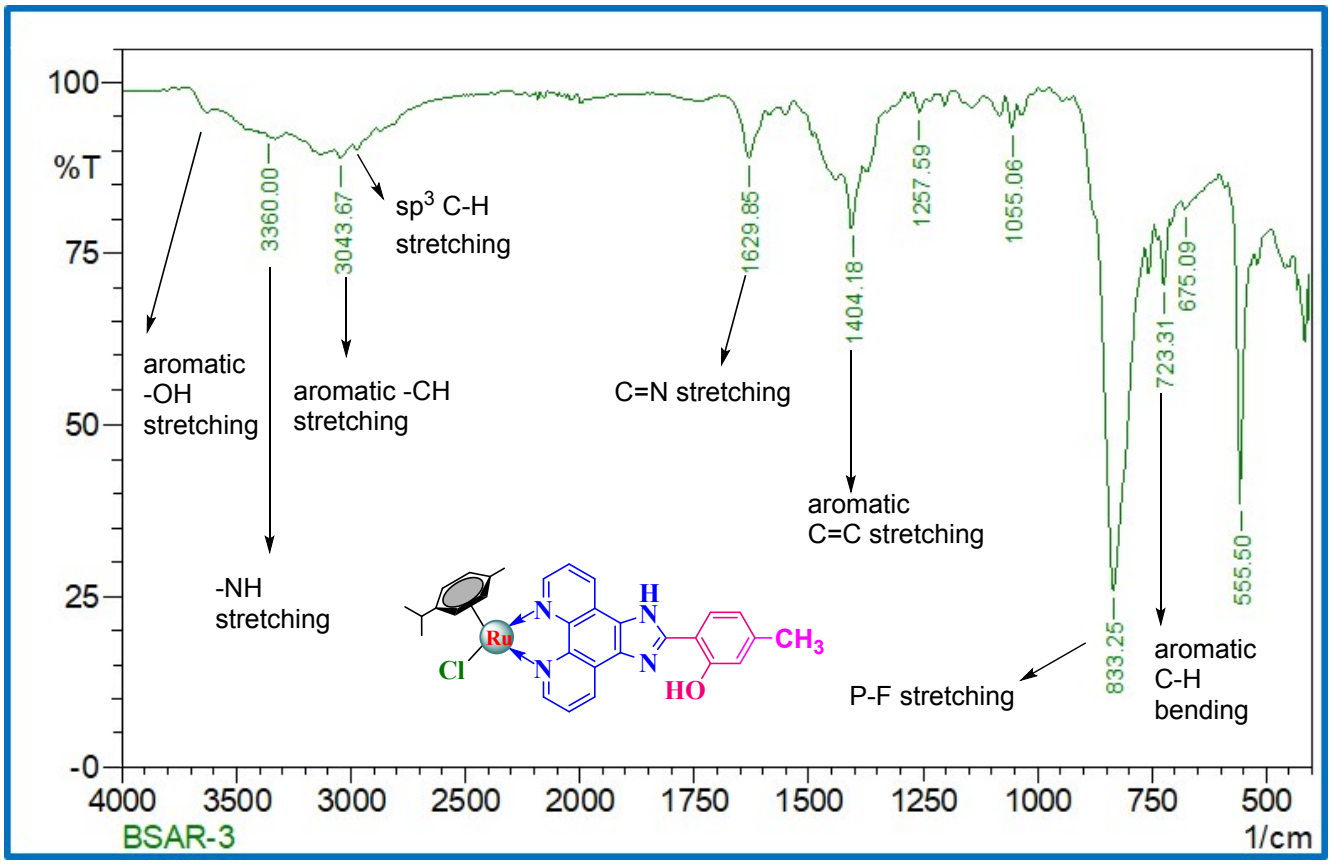

^{1}H NMR of complex RuL4:

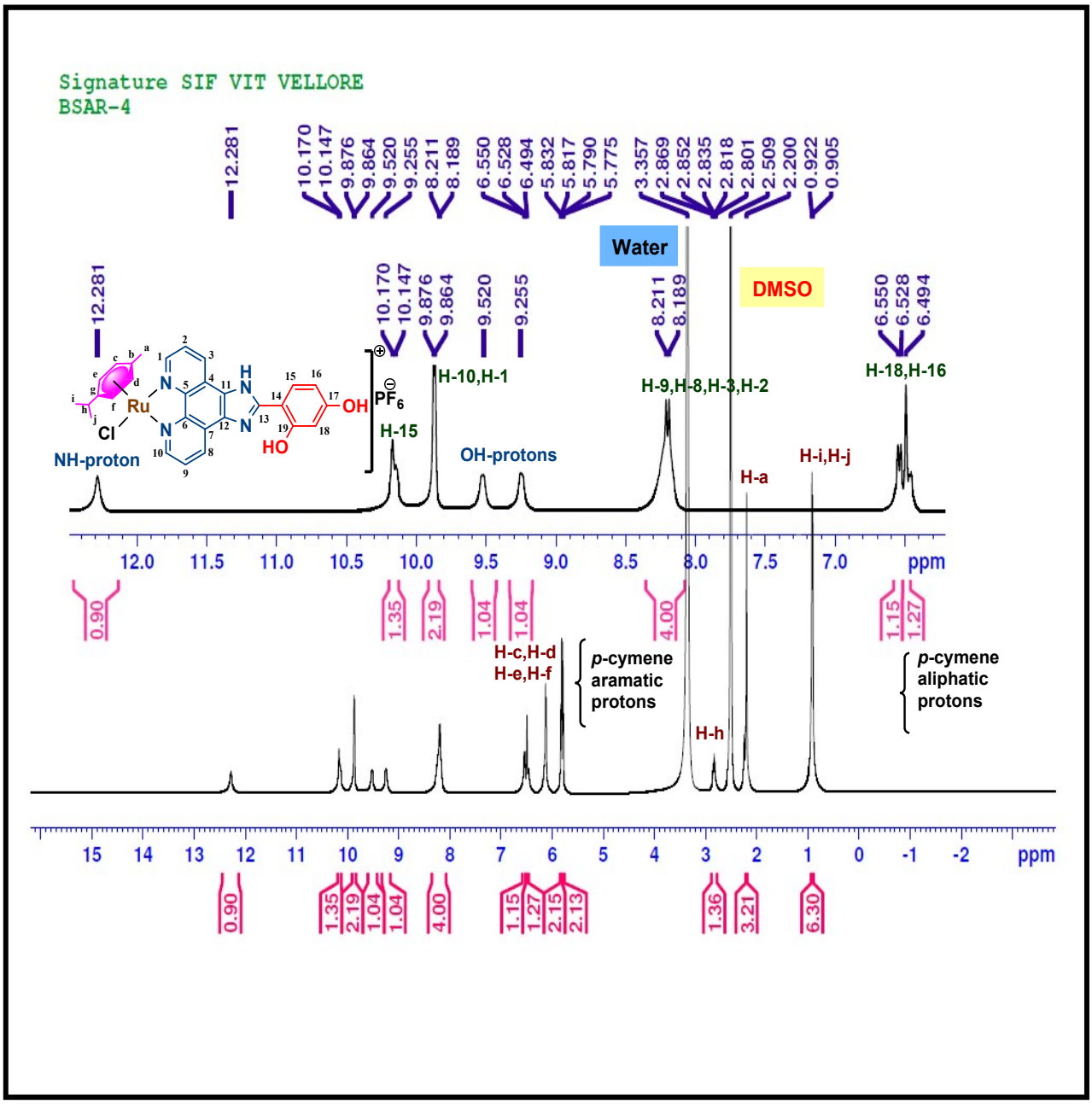

^{13}C NMR of complex RuL4:

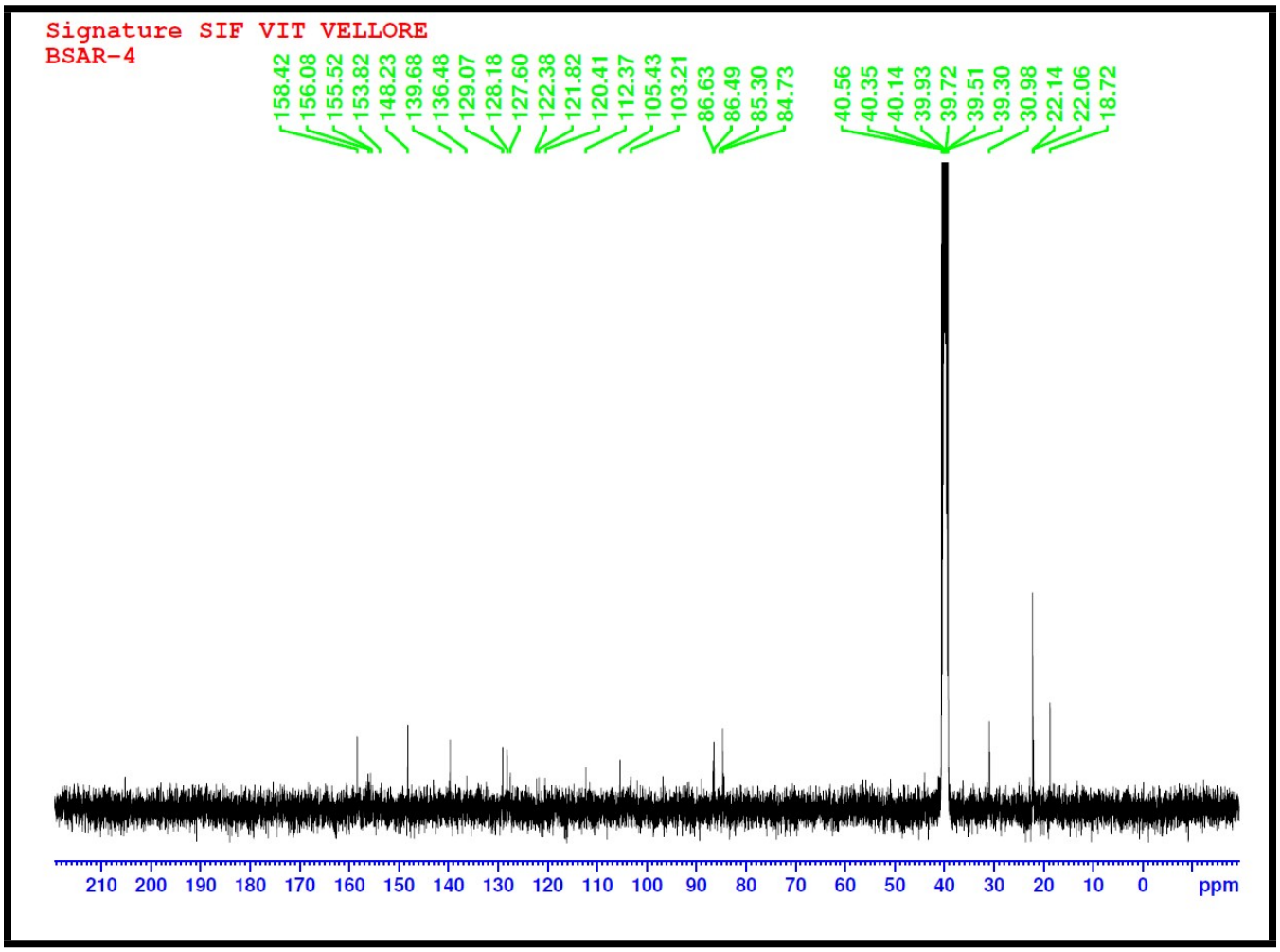

^{19}F NMR of complex RuL4:

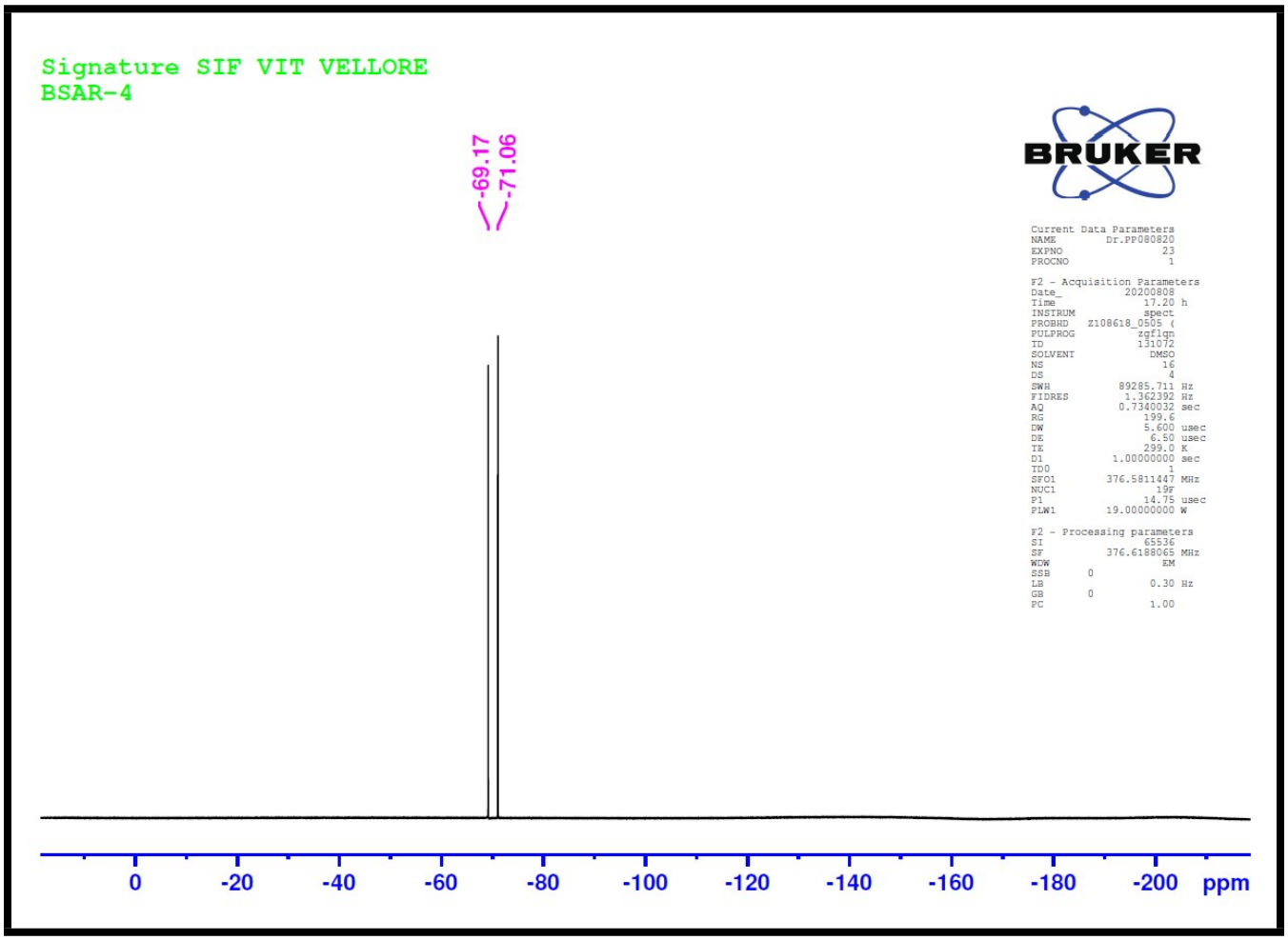

^{31}P NMR of complex RuL4:

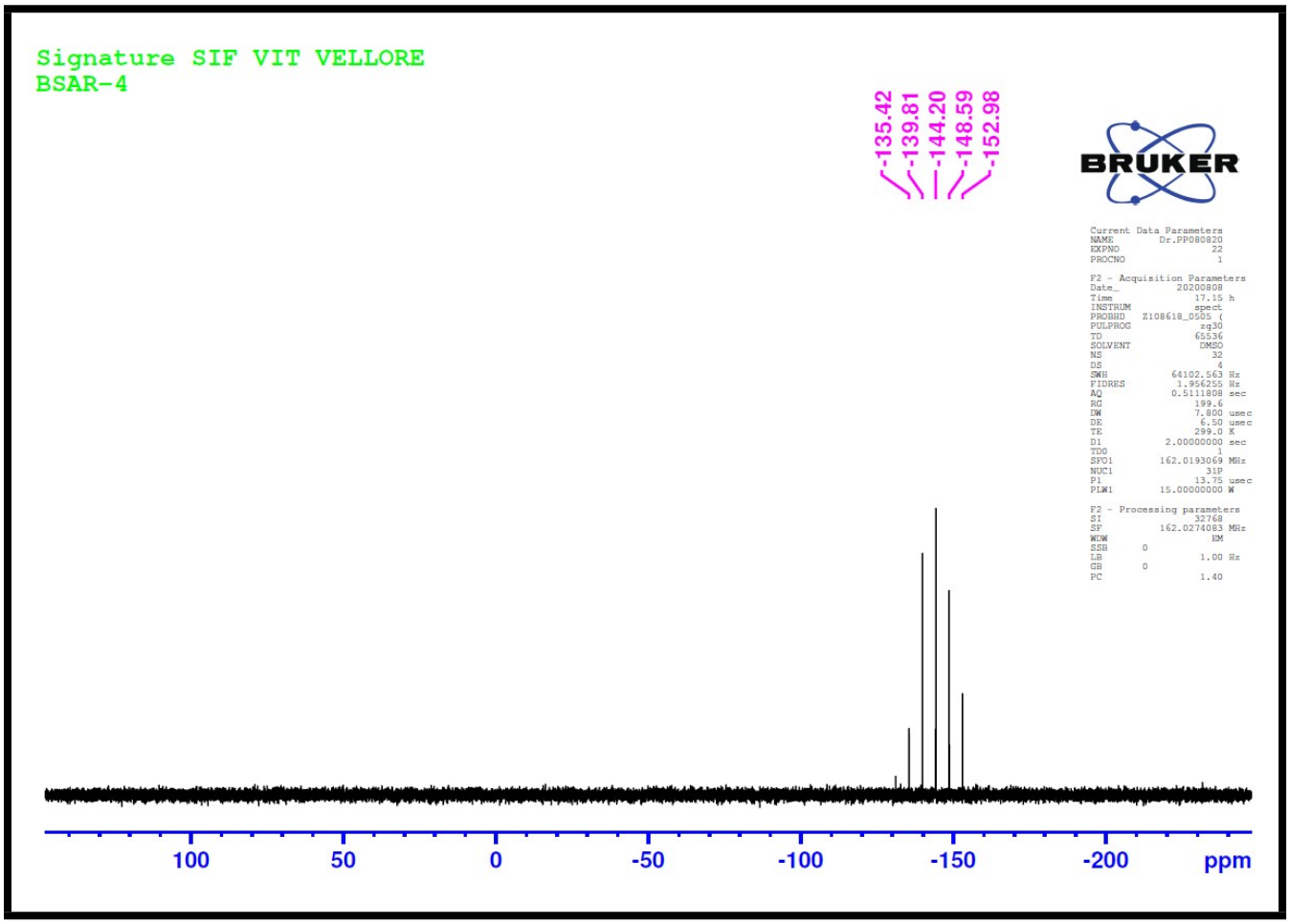

IR spectrum of RuL4

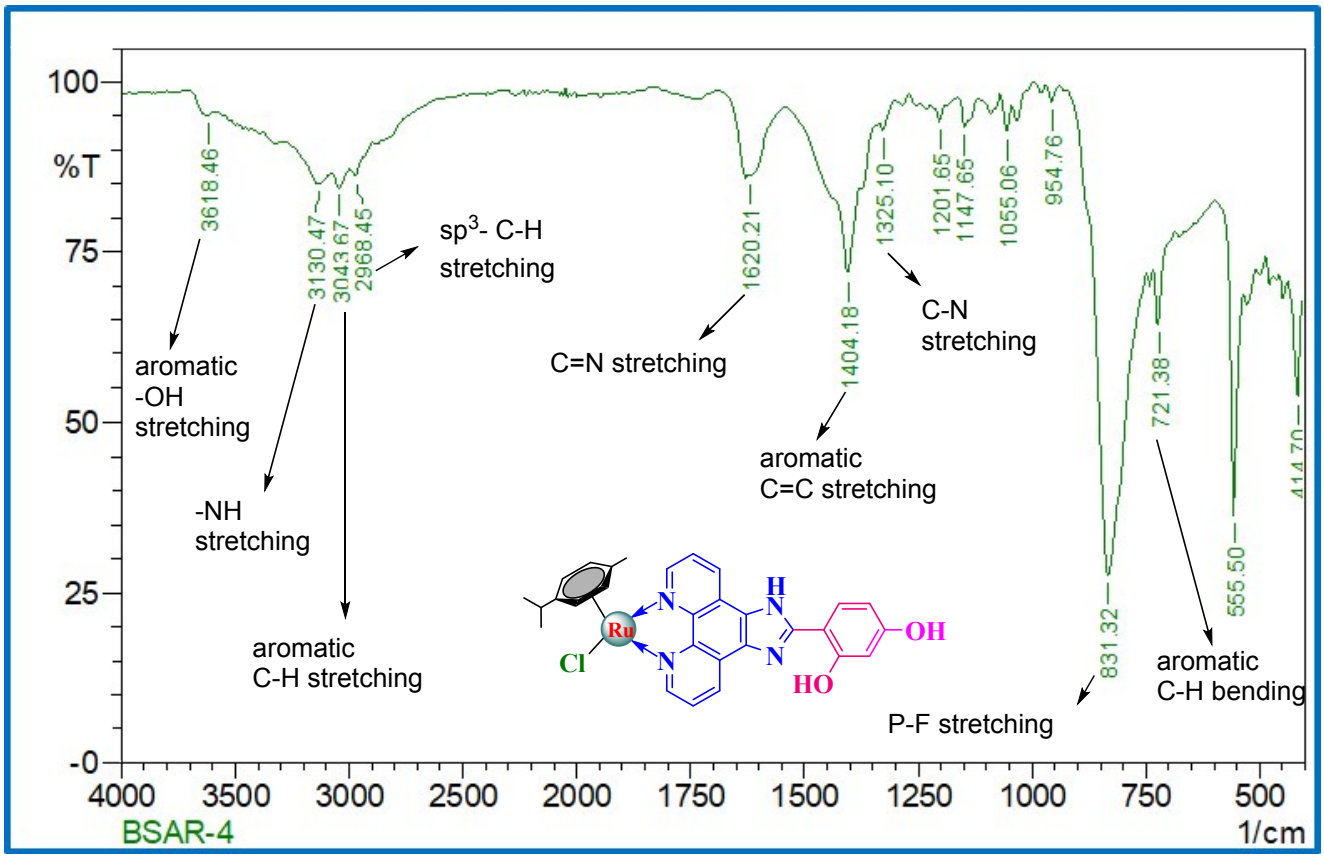

^{1}H NMR of complex RuL5:

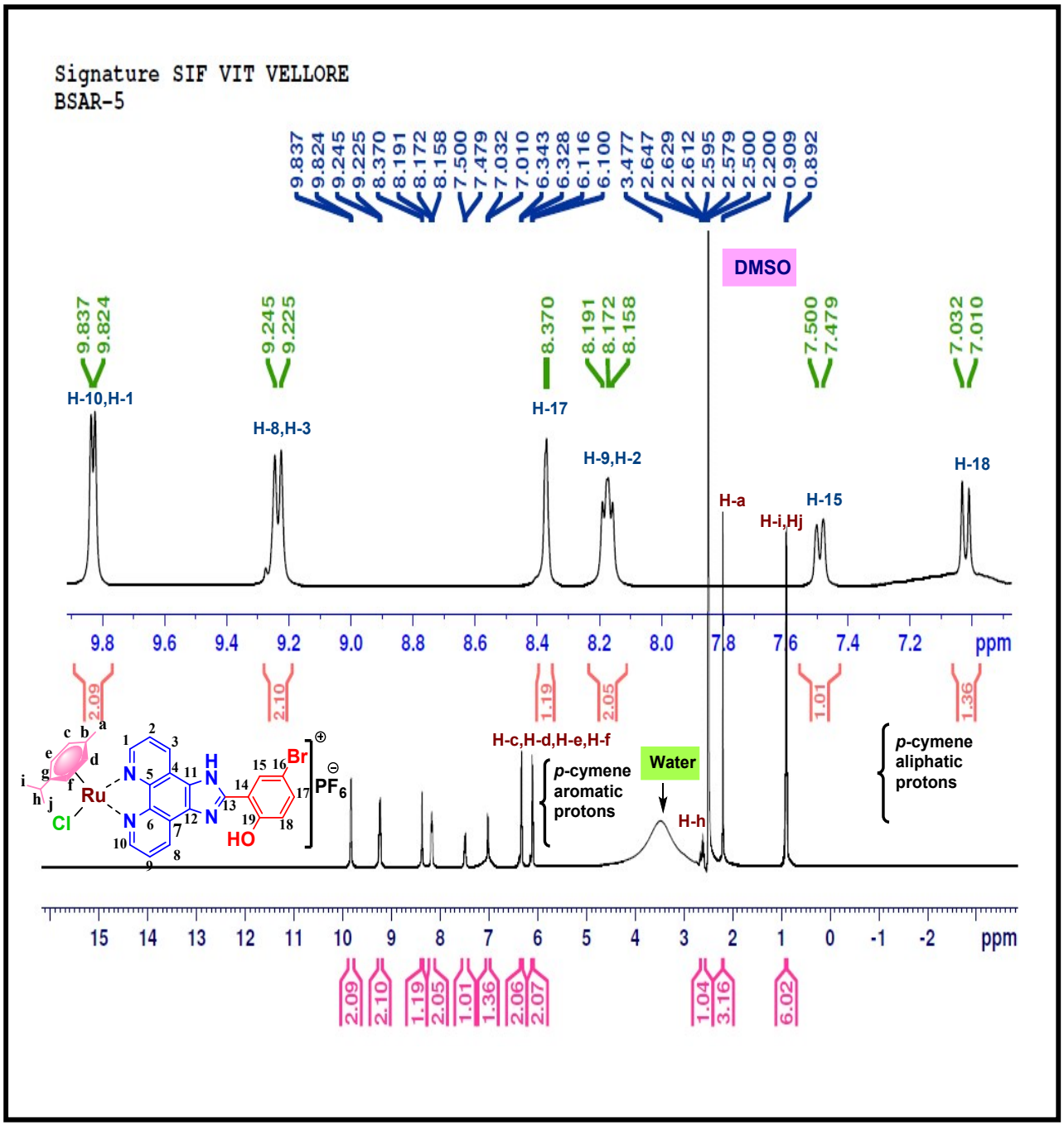

^{13}C NMR of complex RuL5:

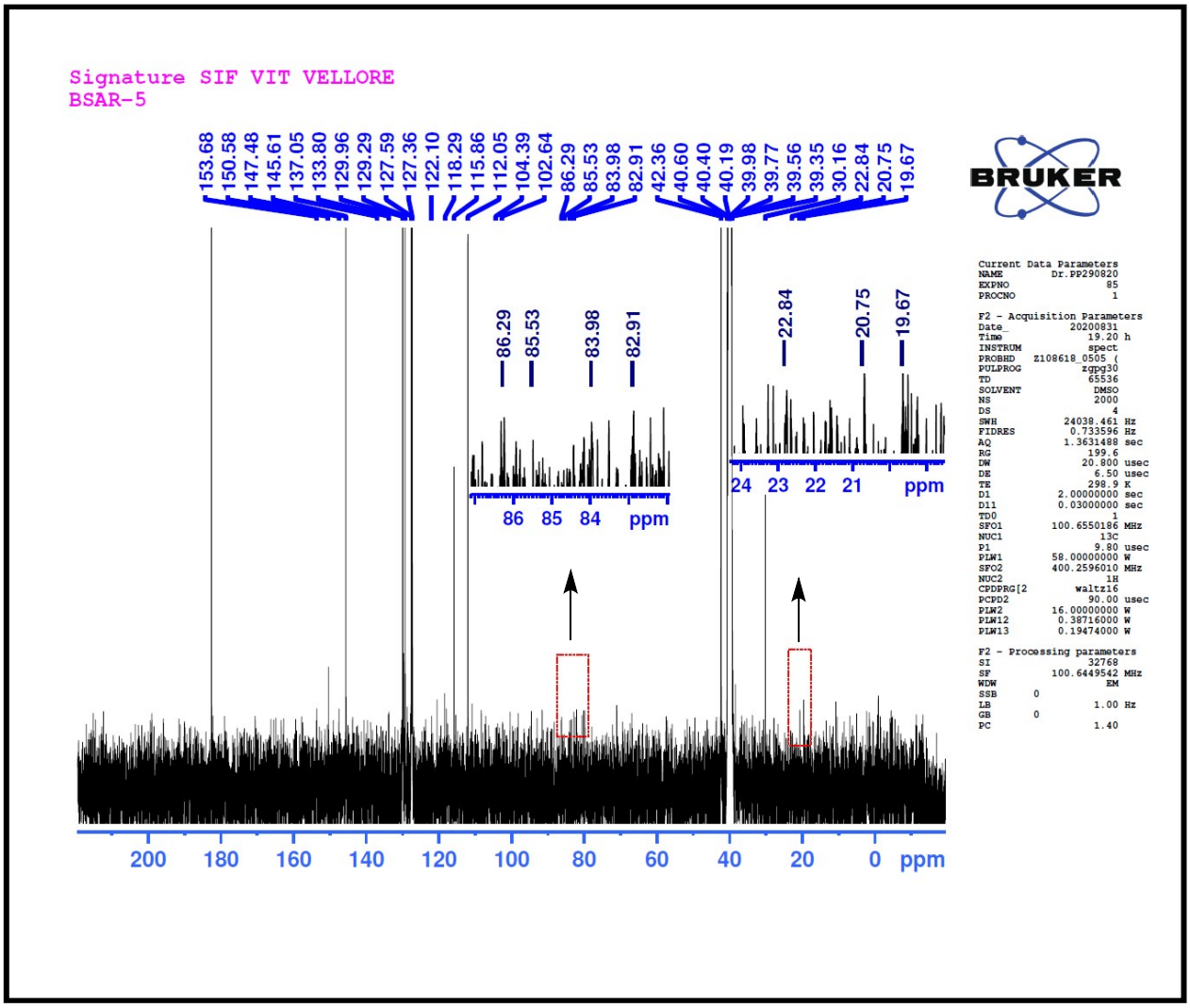

^{19}F NMR of complex RuL5:

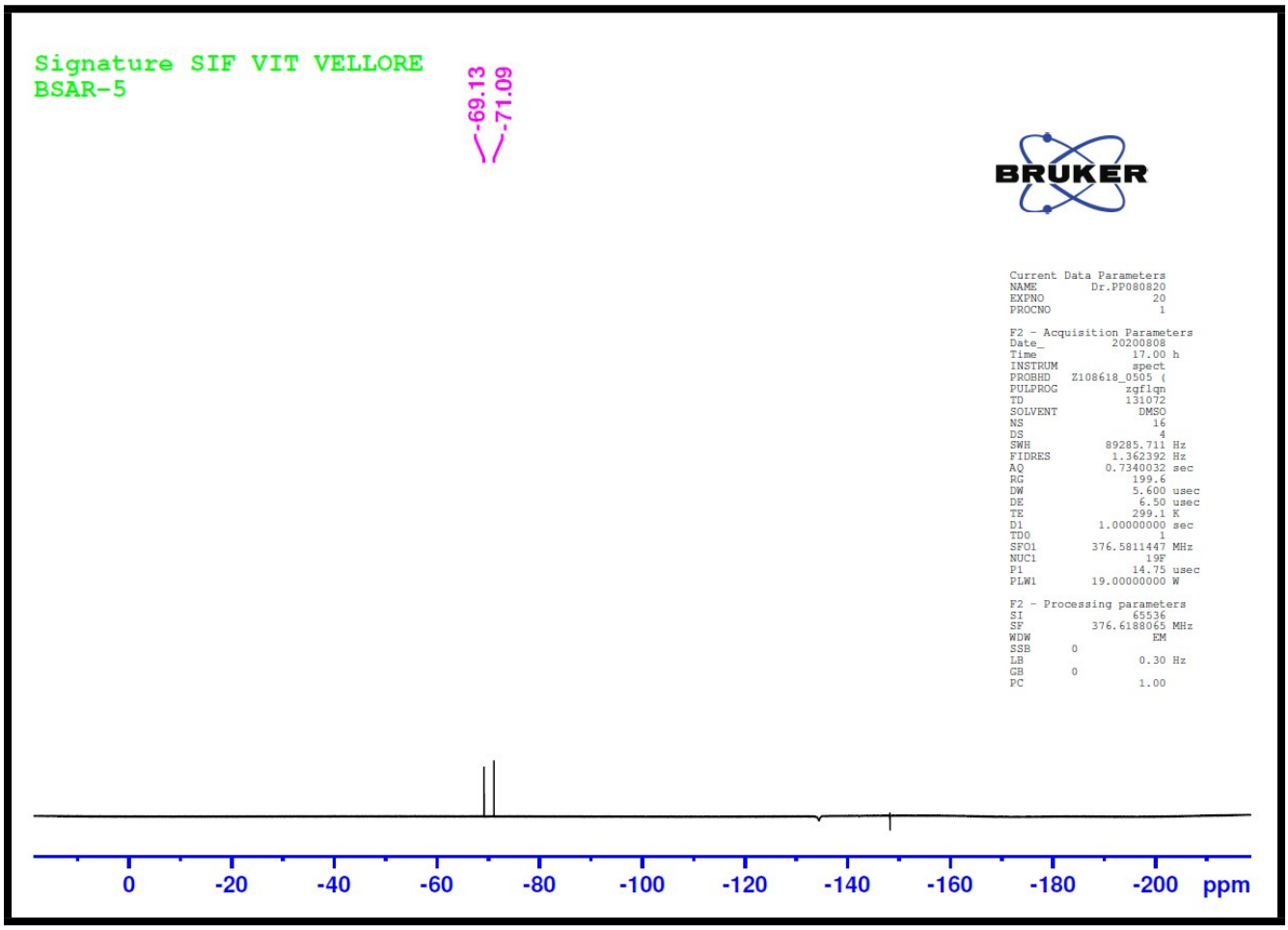

^{31}P NMR of complex RuL5:

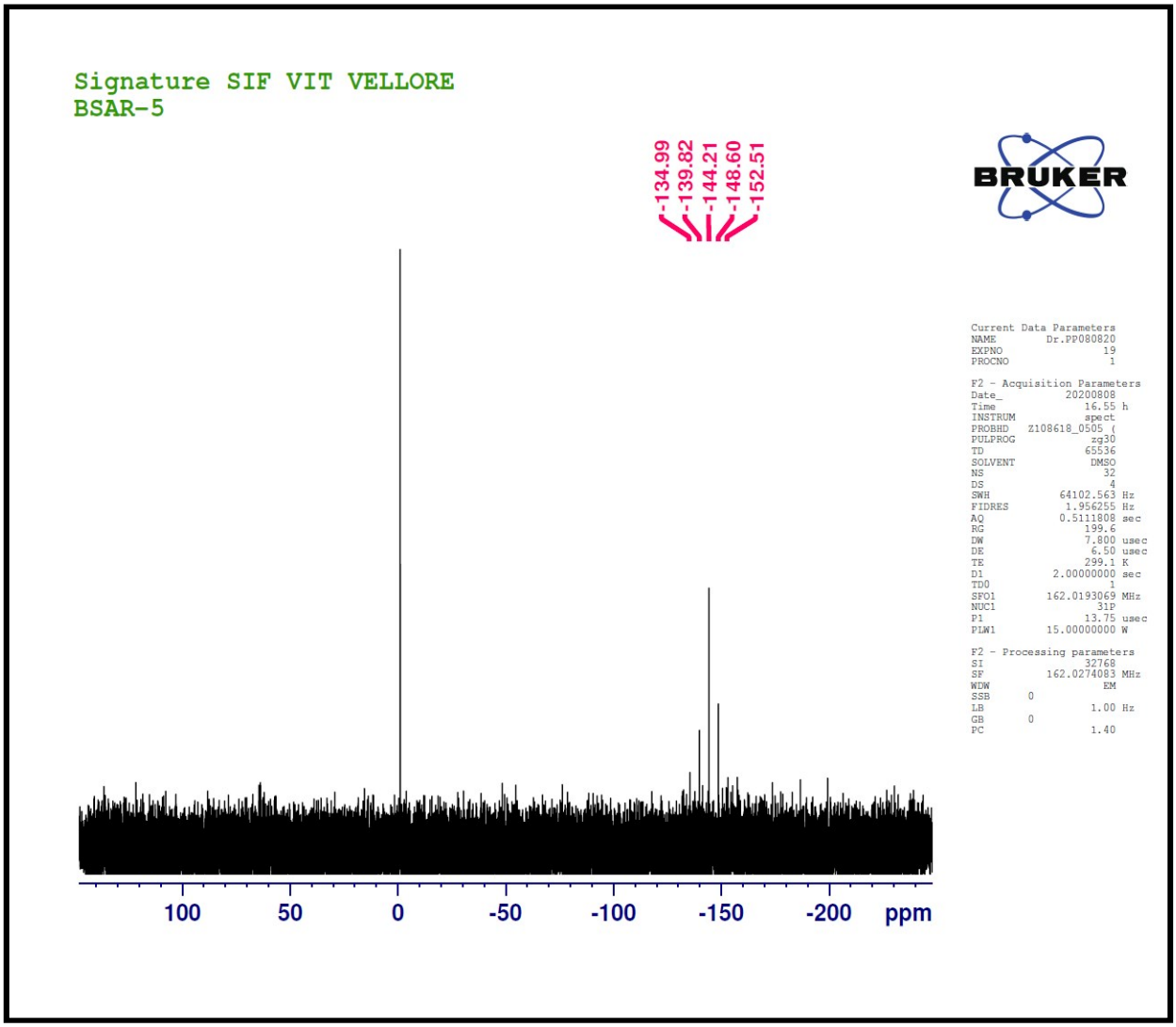

IR spectrum of RuL5

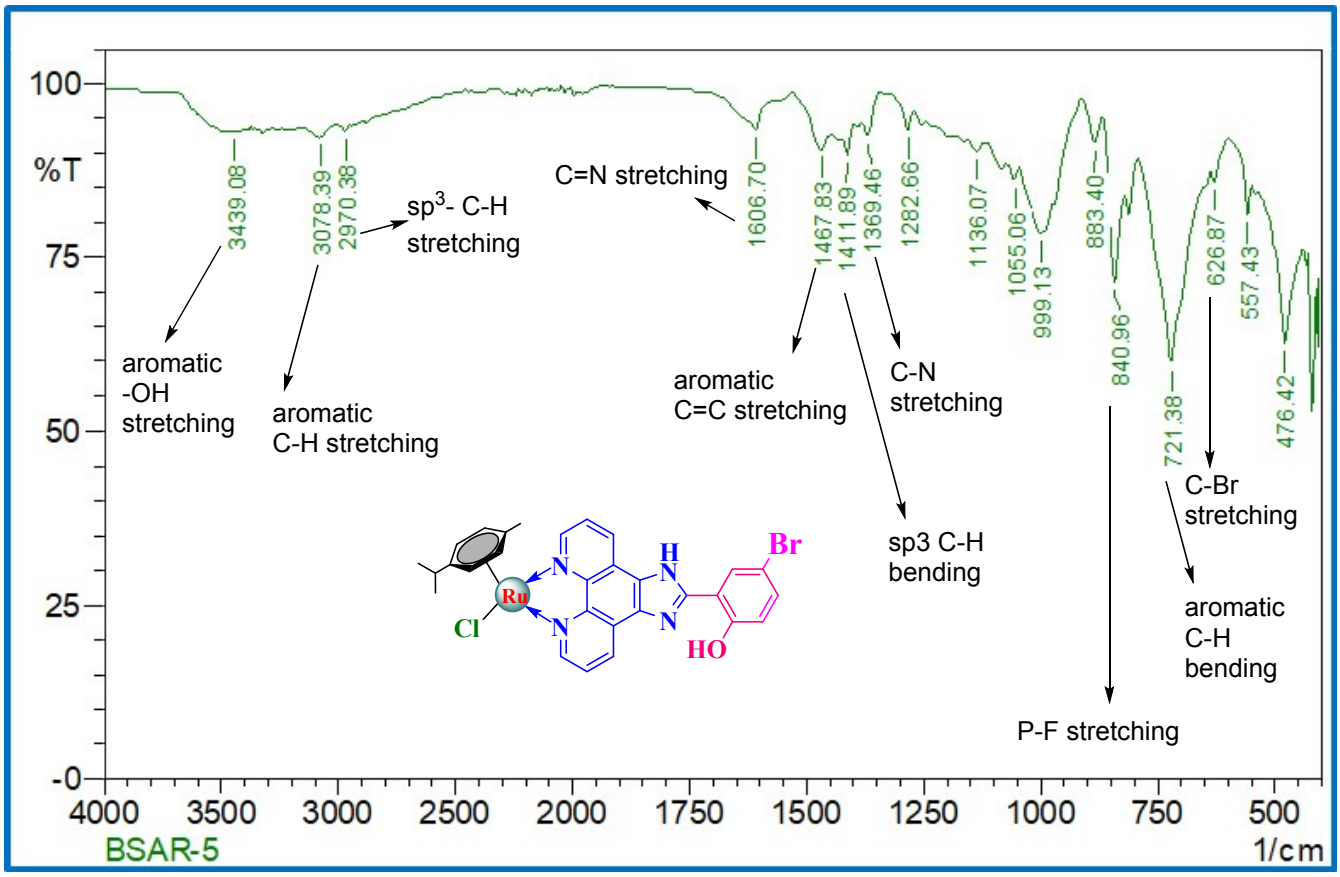

^{1}H NMR of complex RuL6:

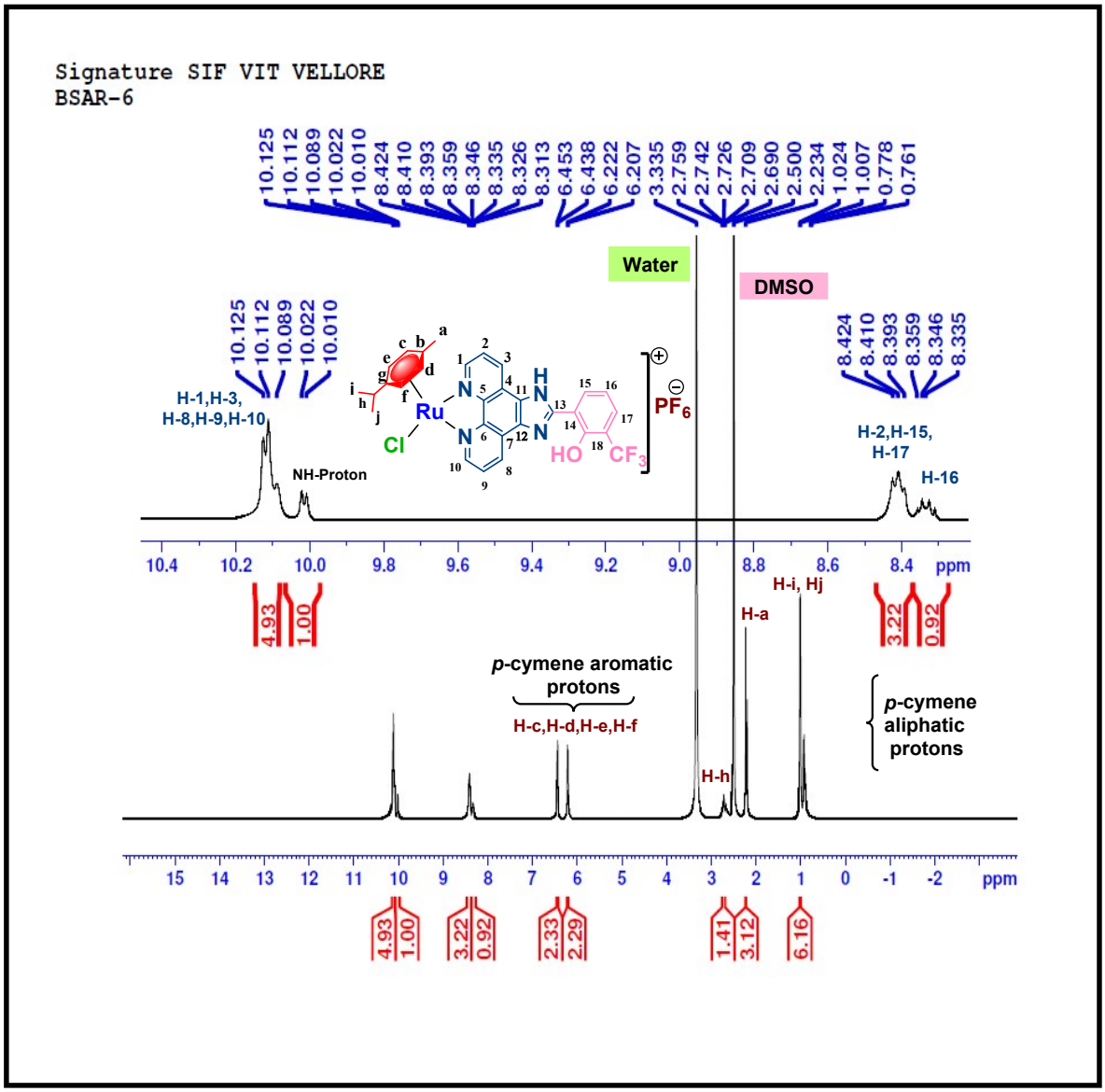

^{13}C NMR of complex RuL6:

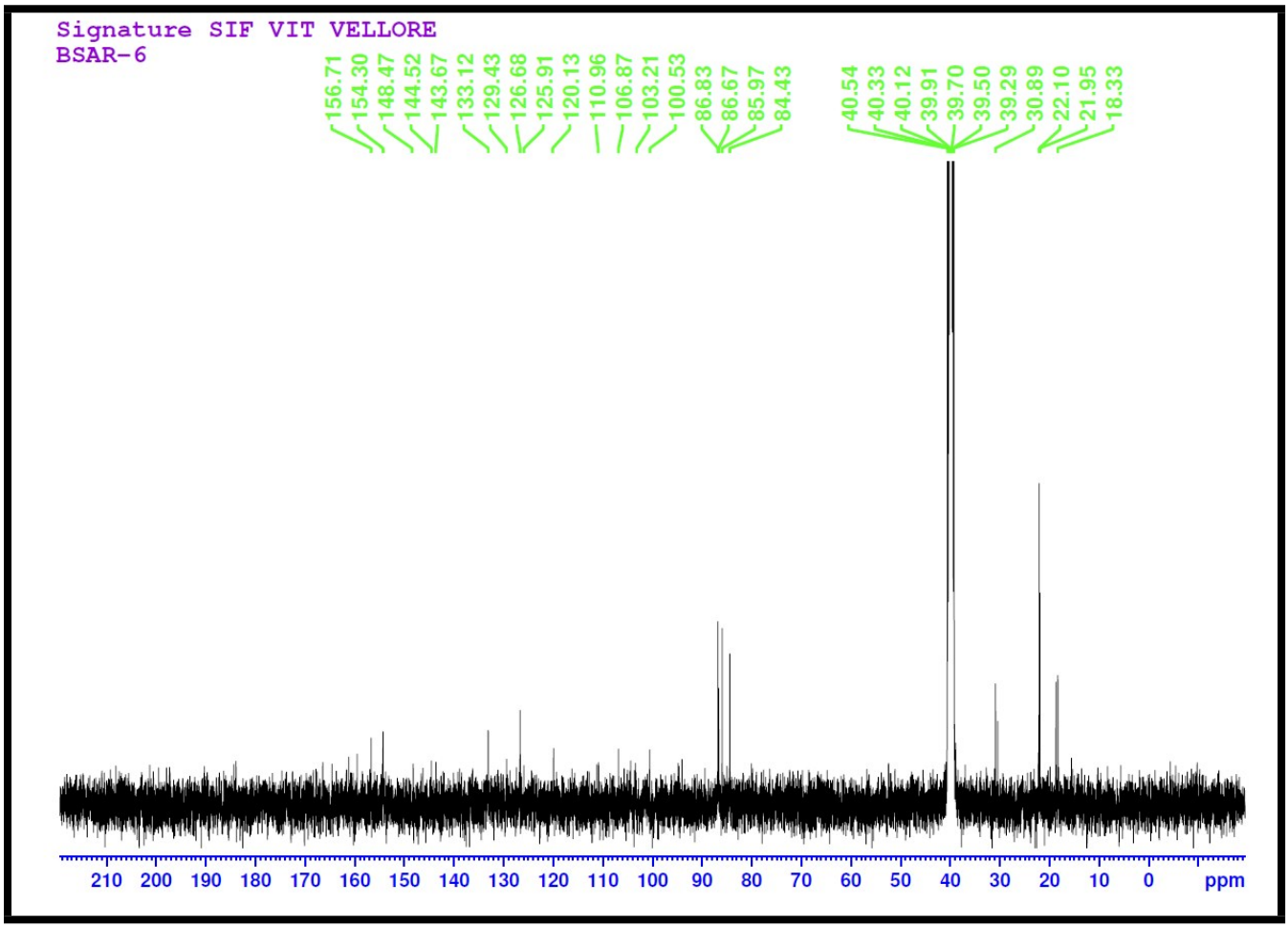

^{19}F NMR of complex RuL6:

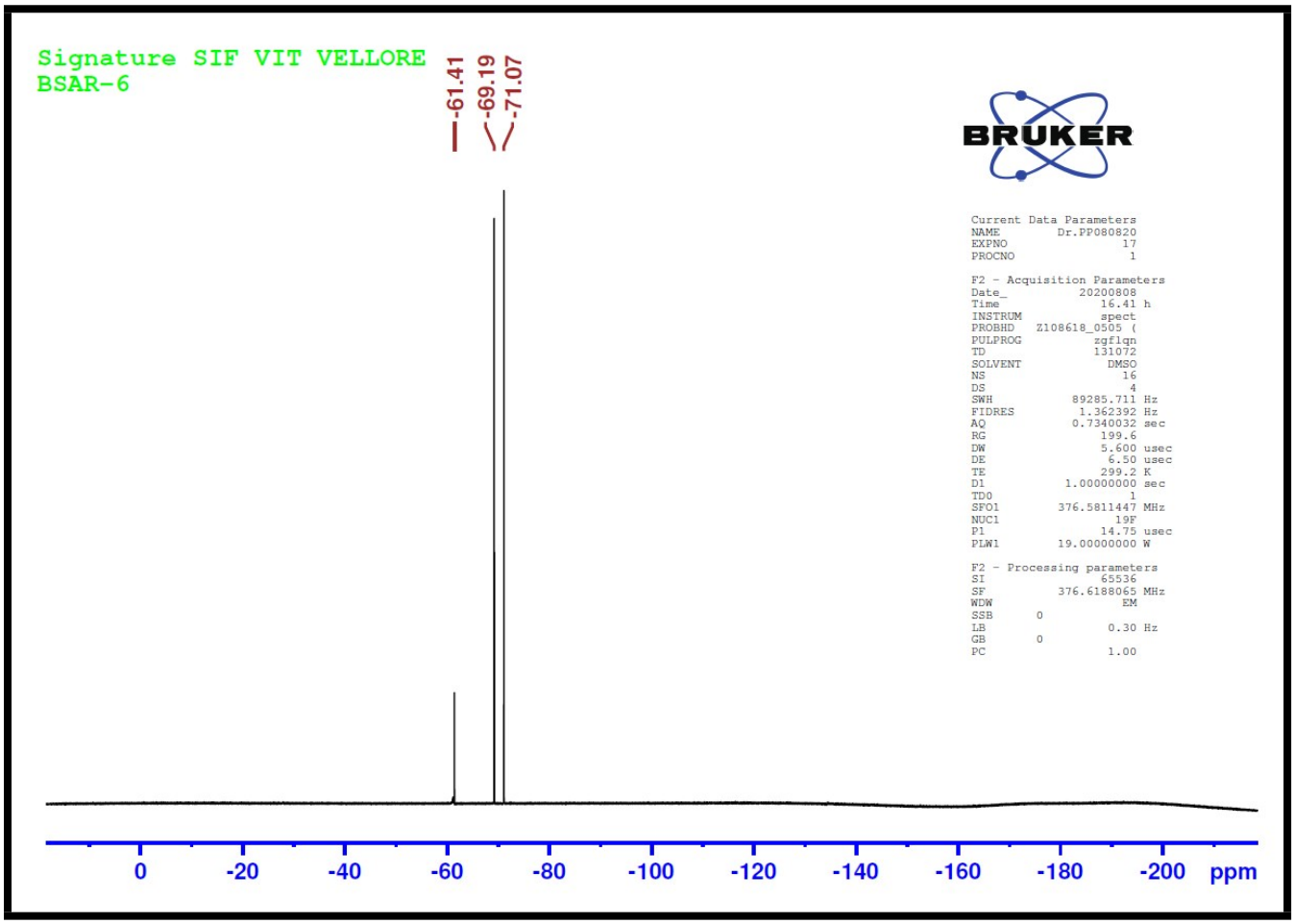

^{31}P NMR of complex RuL6:

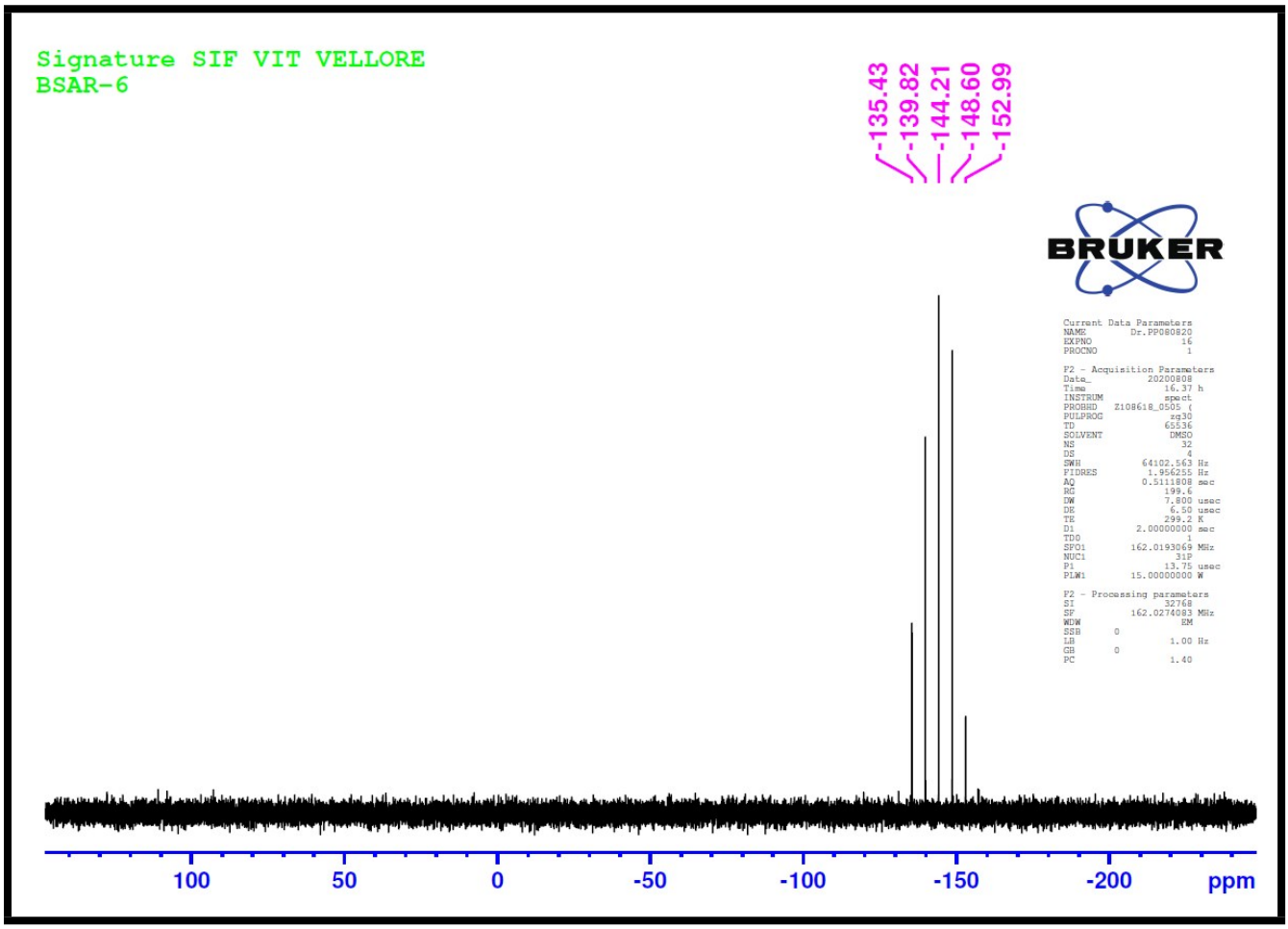

IR spectrum of RuL6

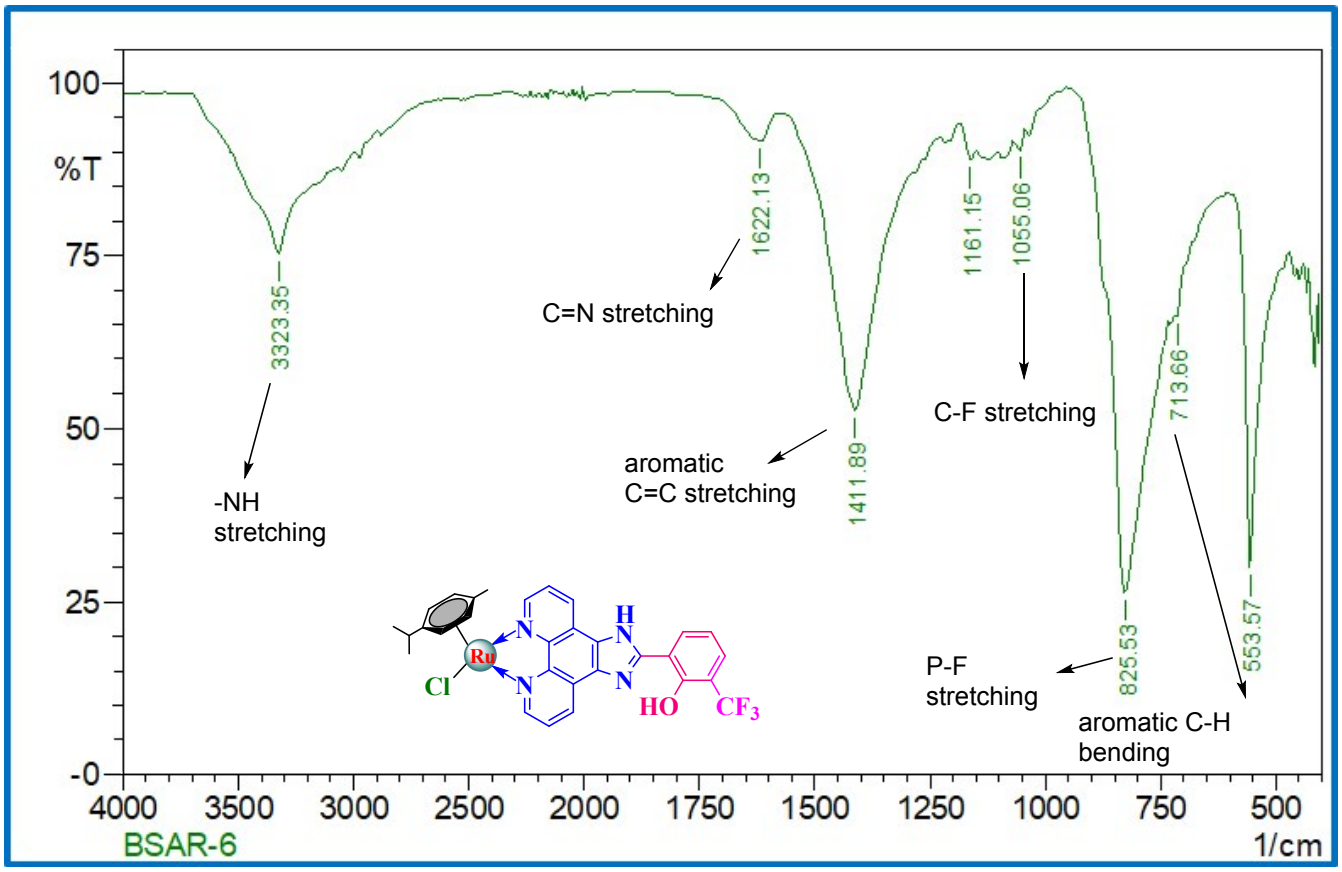

^{1}H NMR of complex RuL7:

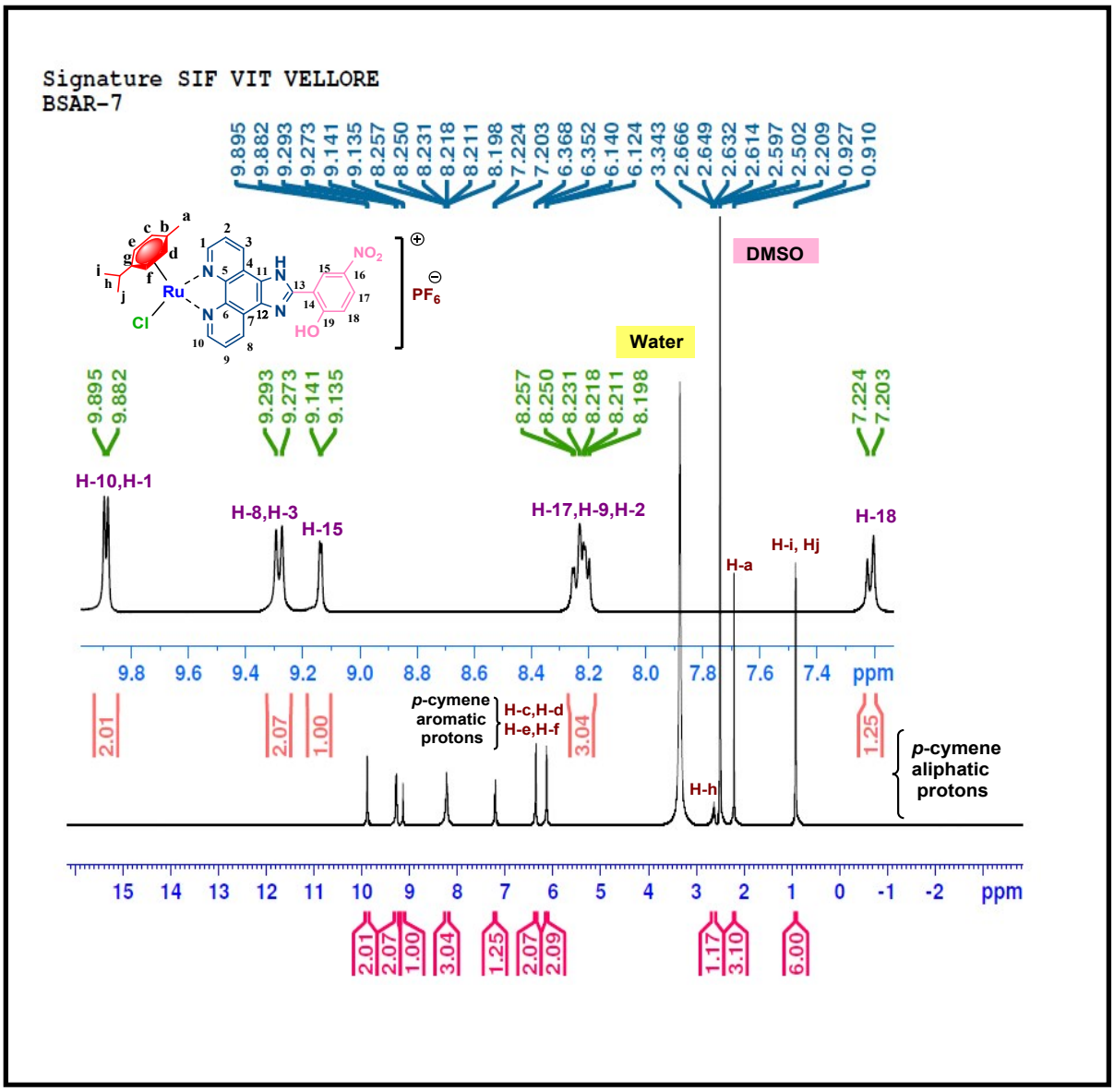

^{13}C NMR of complex RuL7:

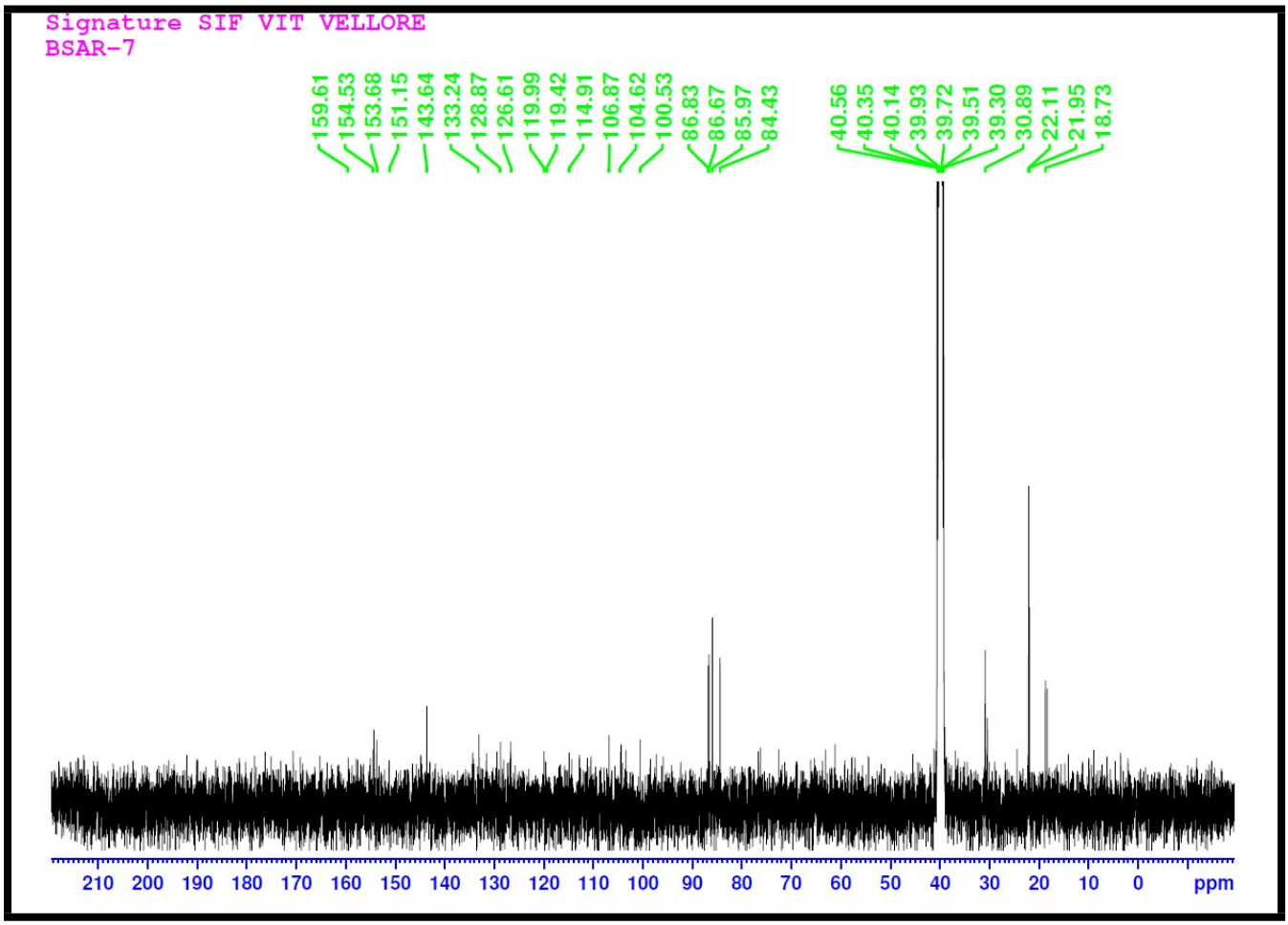

^{19}F NMR of complex RuL7:

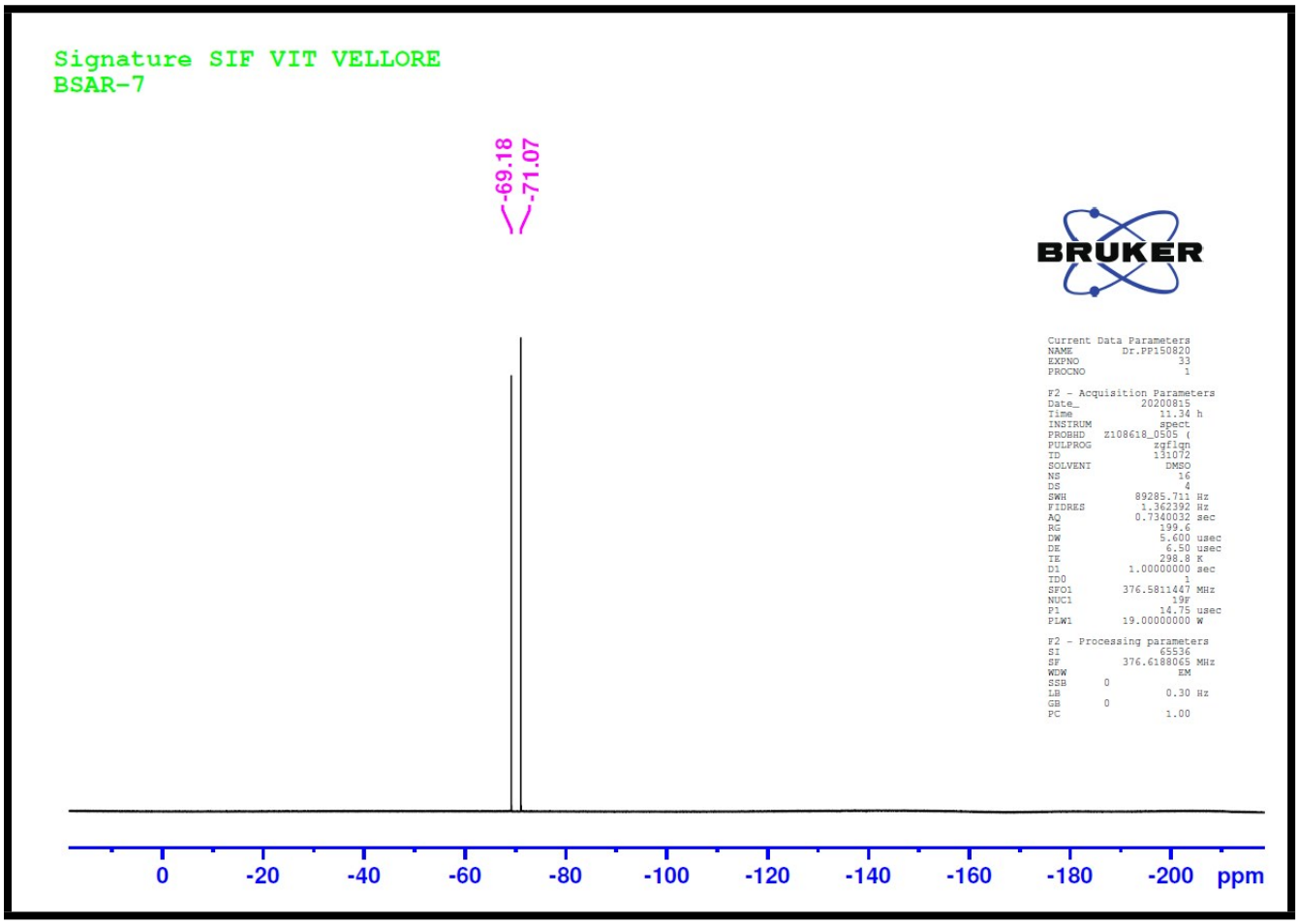

^{31}P NMR of complex RuL7:

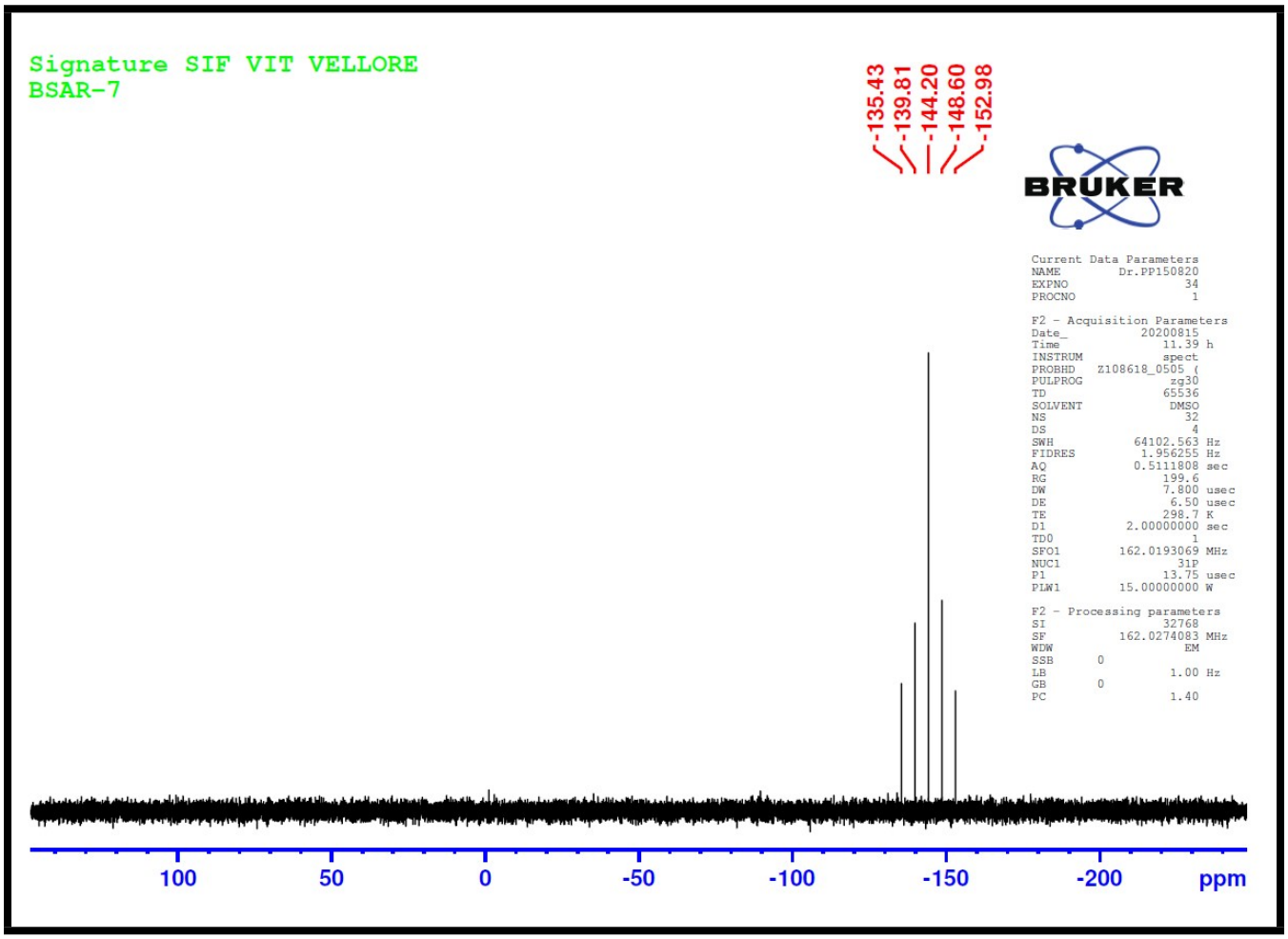

IR spectrum of RuL7

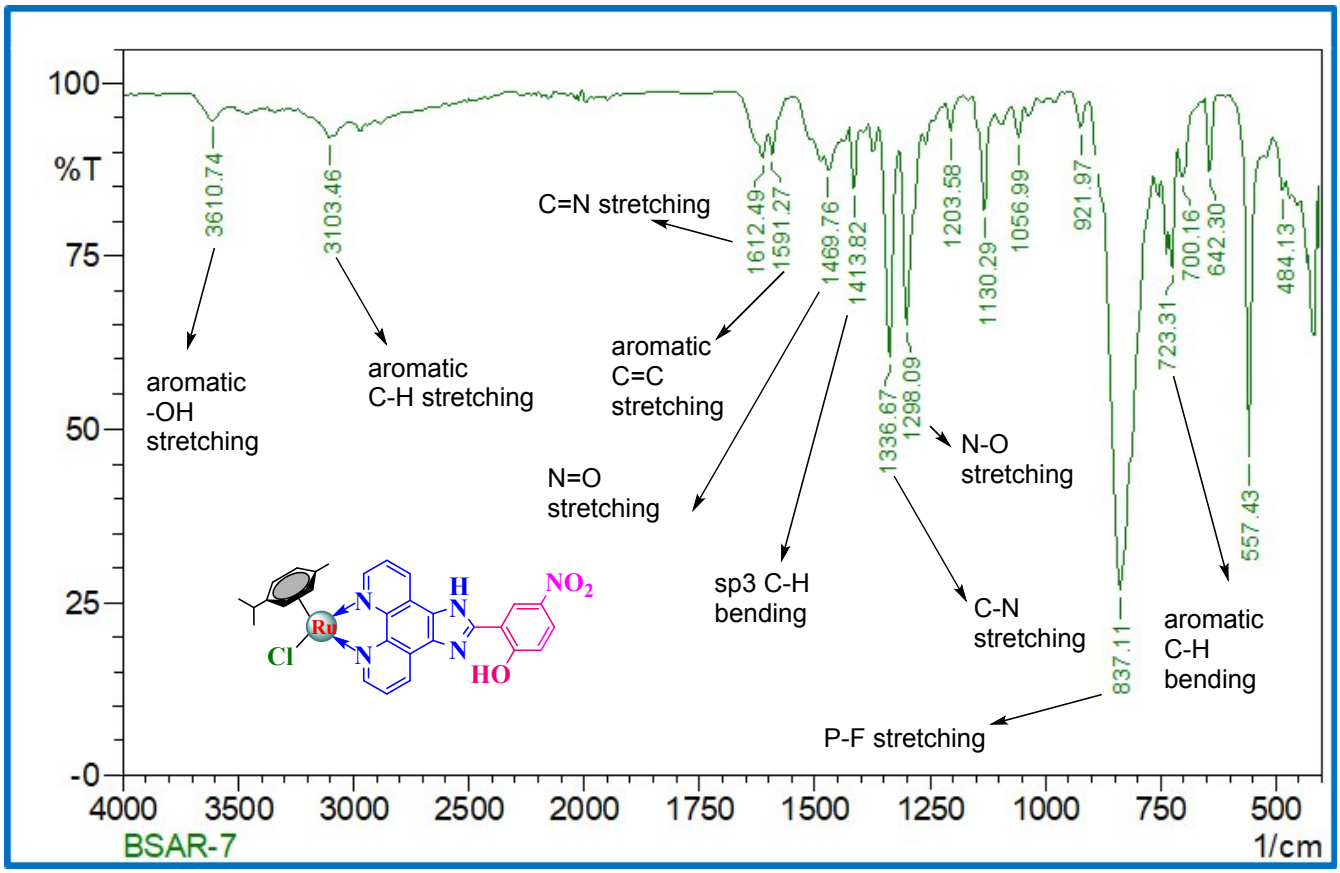

ESI-MS spectrum of complexes (RuL1 - RuL7):

RuL1

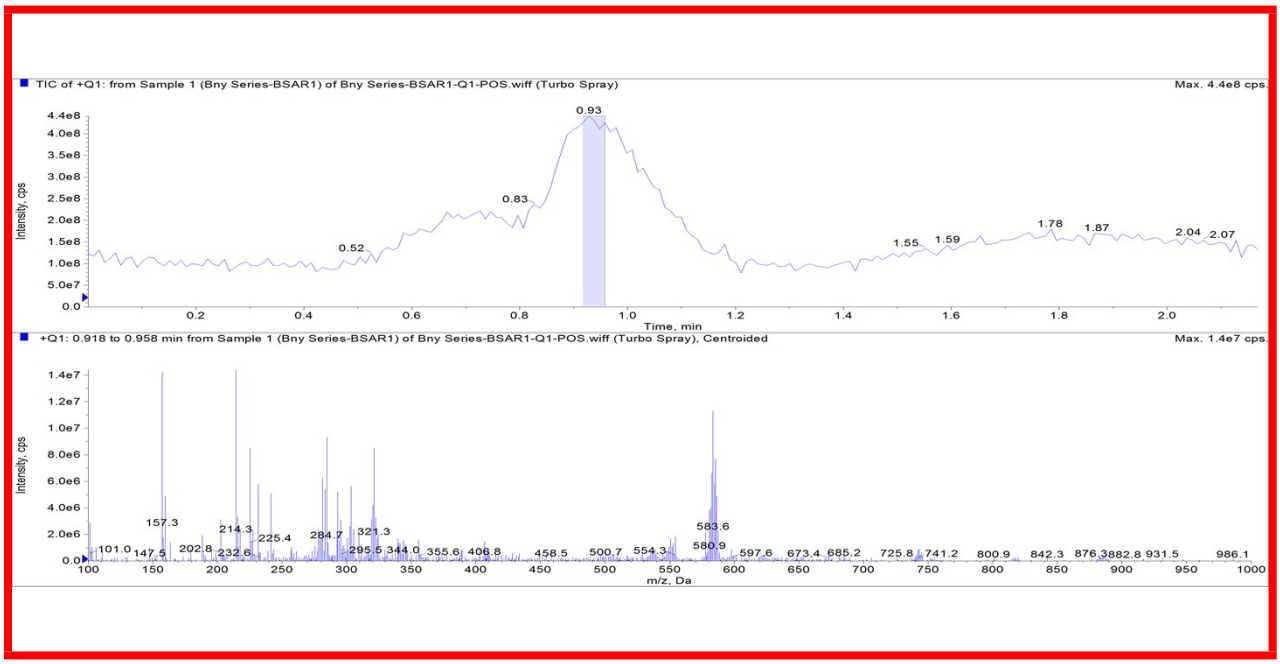

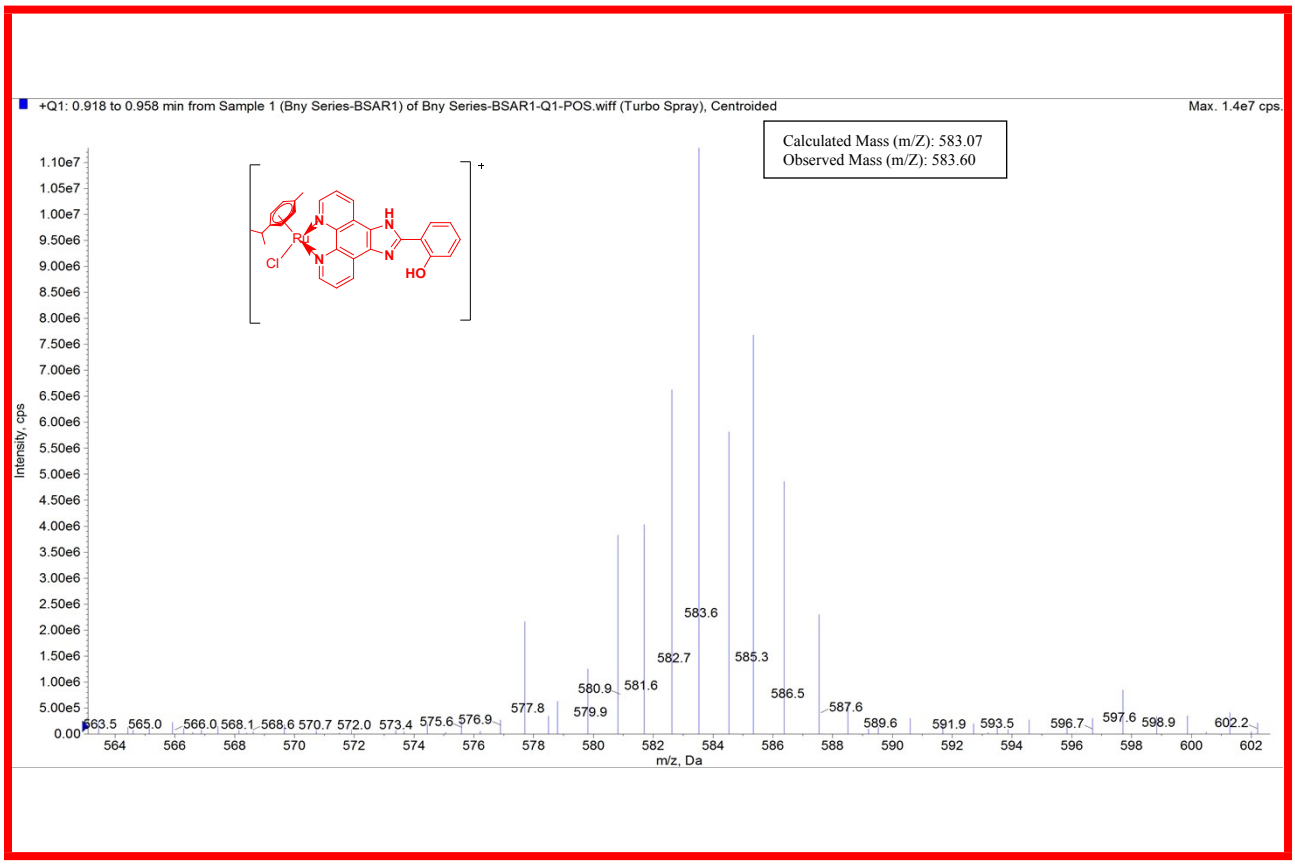

RuL2

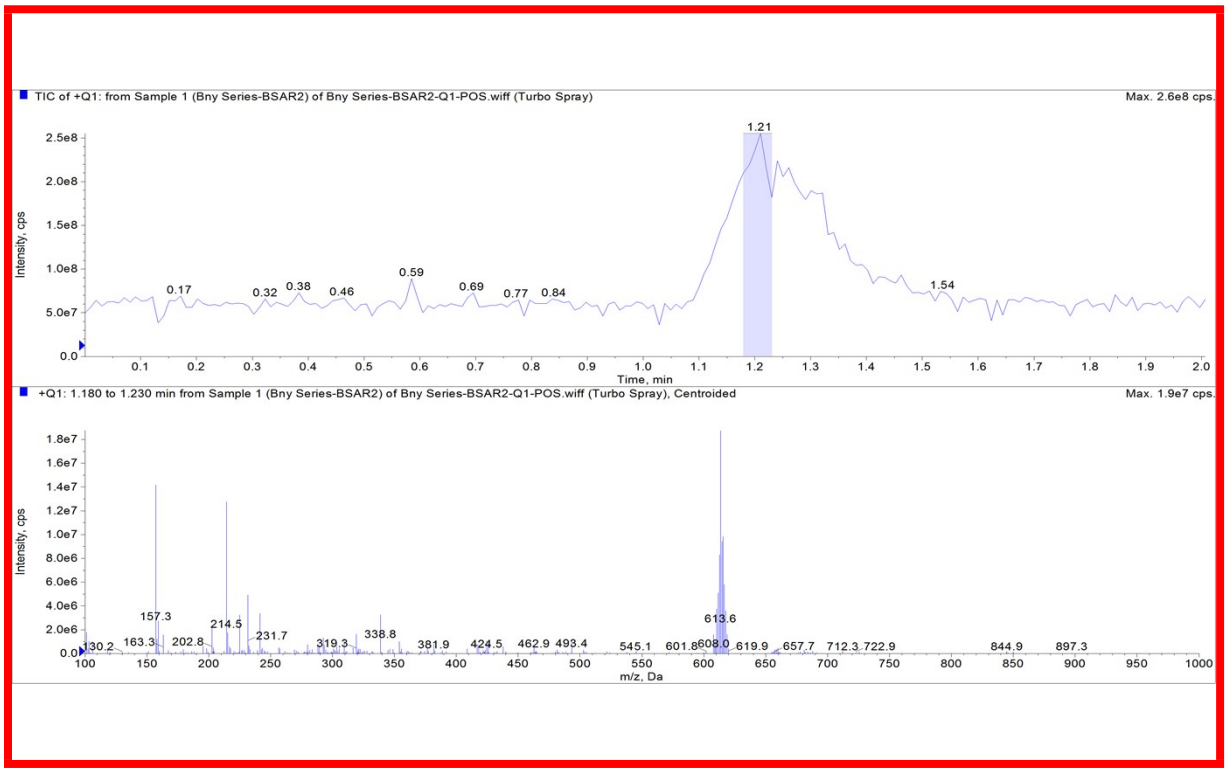
TIC of +Q1: from Sample 1 (Bny Series-BSAR2) of Bny Series-BSAR2-Q1-POS.wiff (Turbo Spray)
Max. 2.6e8 cps.
Intensity, cps
Time, min
+Q1: 1.180 to 1.230 min from Sample 1 (Bny Series-BSAR2) of Bny Series-BSAR2-Q1-POS.wiff (Turbo Spray), Centroided
Max. 1.9e7 cps.
m/z, Da

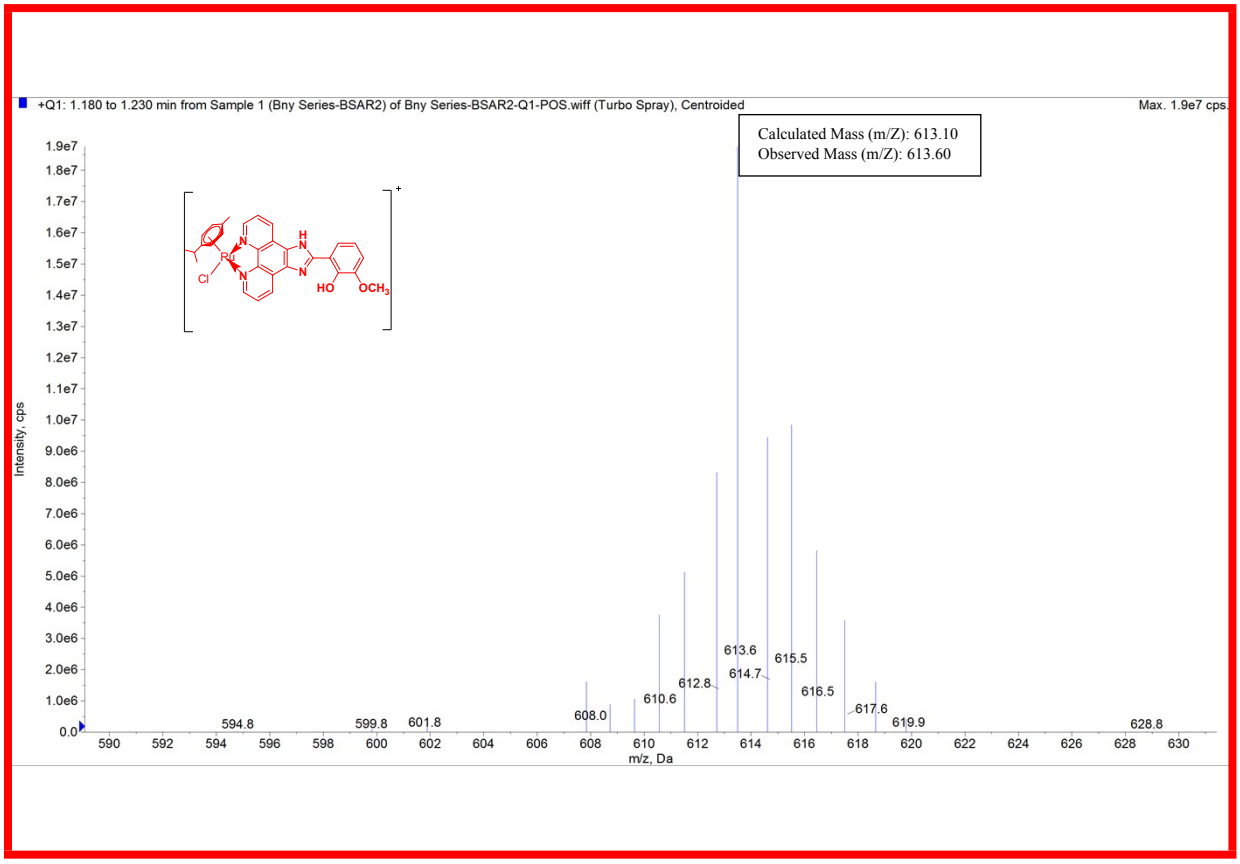
+Q1: 1.180 to 1.230 min from Sample 1 (Bny Series-BSAR2) of Bny Series-BSAR2-Q1-POS.wiff (Turbo Spray), Centroided
Max. 1.9e7 cps.
Calculated Mass (m/Z): 613.10
Observed Mass (m/Z): 613.60
Intensity, cps
m/z, Da

RuL3

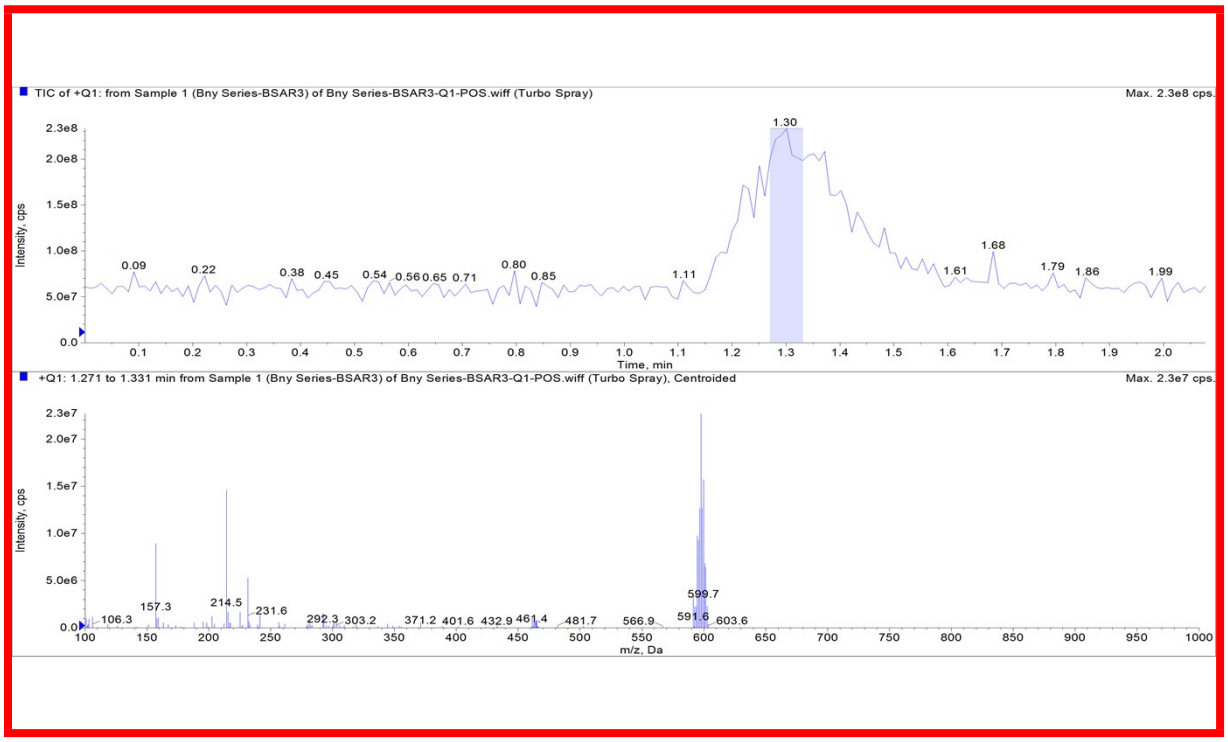
TIC of +Q1: from Sample 1 (Bny Series-BSAR3) of Bny Series-BSAR3-Q1-POS.wiff (Turbo Spray)
Max. 2.3e8 cps.
Intensity, cps
Time, min
+Q1: 1.271 to 1.331 min from Sample 1 (Bny Series-BSAR3) of Bny Series-BSAR3-Q1-POS.wiff (Turbo Spray), Centroided
Max. 2.3e7 cps.
m/z, Da

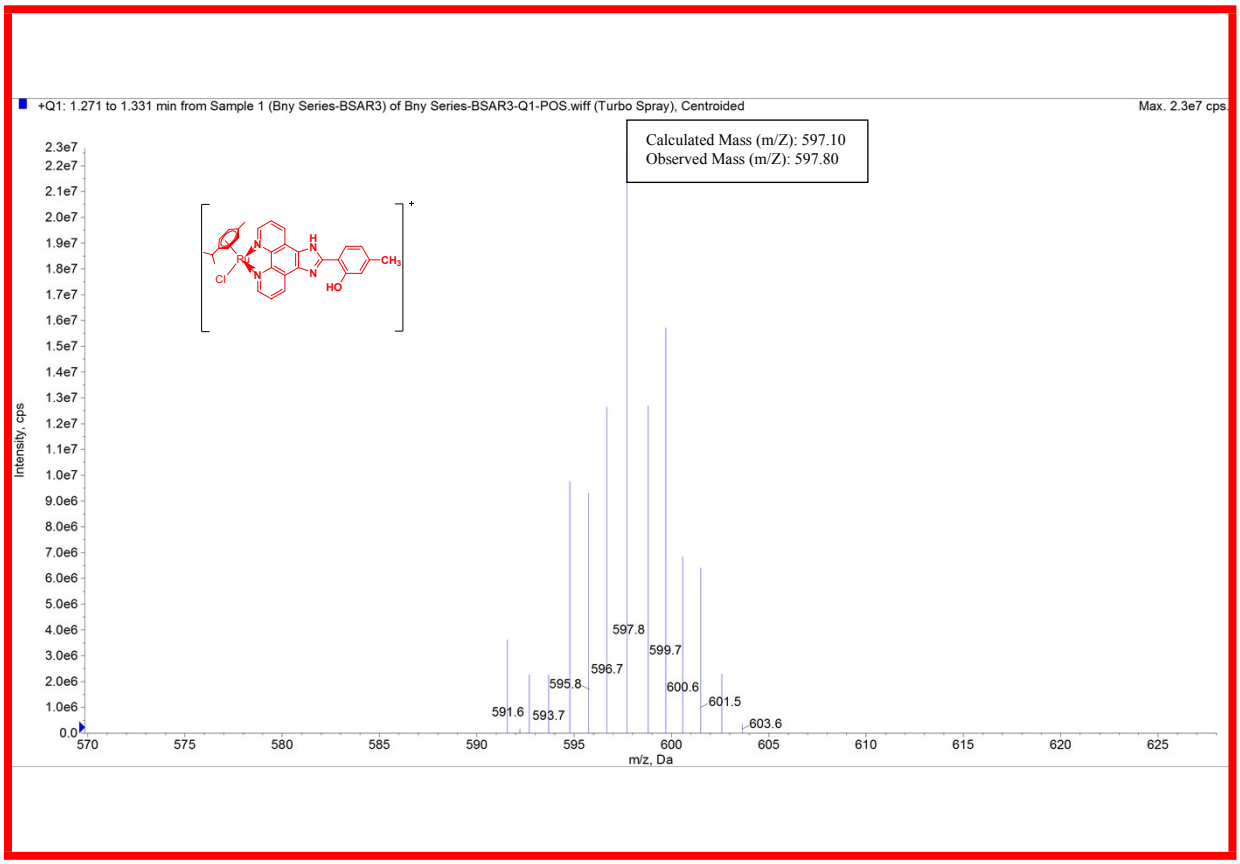
+Q1: 1.271 to 1.331 min from Sample 1 (Bny Series-BSAR3) of Bny Series-BSAR3-Q1-POS.wiff (Turbo Spray), Centroided
Max. 2.3e7 cps.
Calculated Mass (m/Z): 597.10
Observed Mass (m/Z): 597.80
Intensity, cps
m/z, Da

RuL4

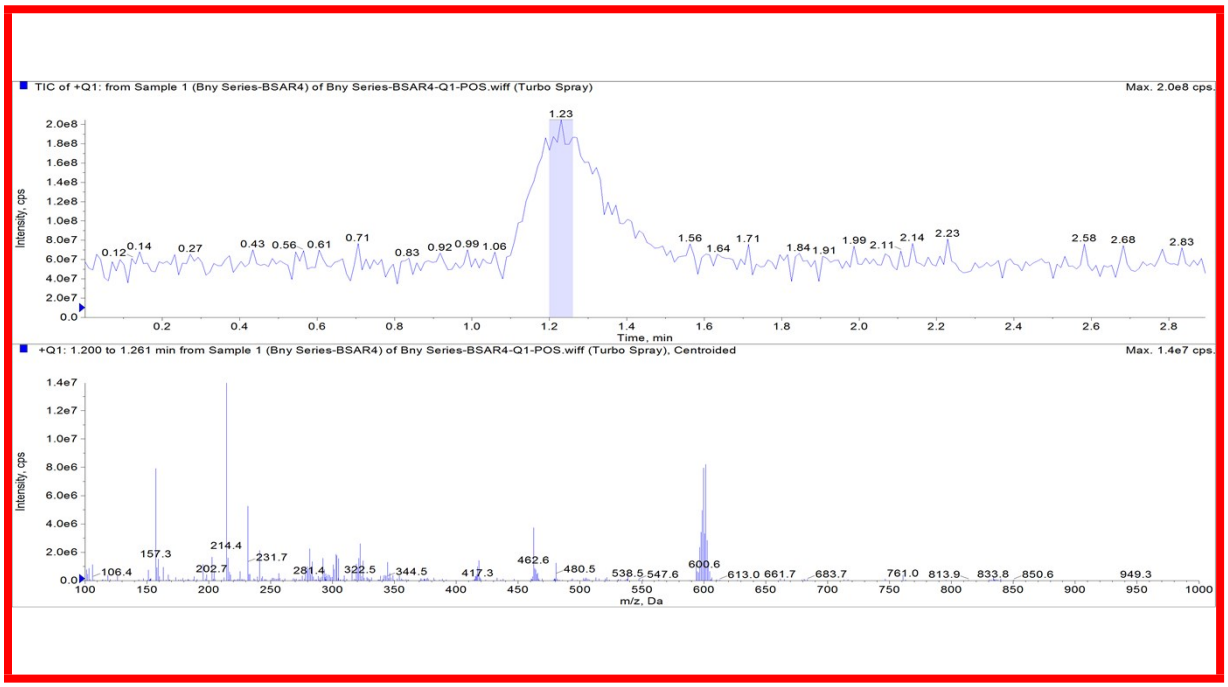
TIC of +Q1: from Sample 1 (Bny Series-BSAR4) of Bny Series-BSAR4-Q1-POS.wiff (Turbo Spray)
Max. 2.0e8 cps.
Intensity, cps
Time, min
+Q1: 1.200 to 1.261 min from Sample 1 (Bny Series-BSAR4) of Bny Series-BSAR4-Q1-POS.wiff (Turbo Spray), Centroided
Max. 1.4e7 cps.
Intensity, cps
m/z, Da

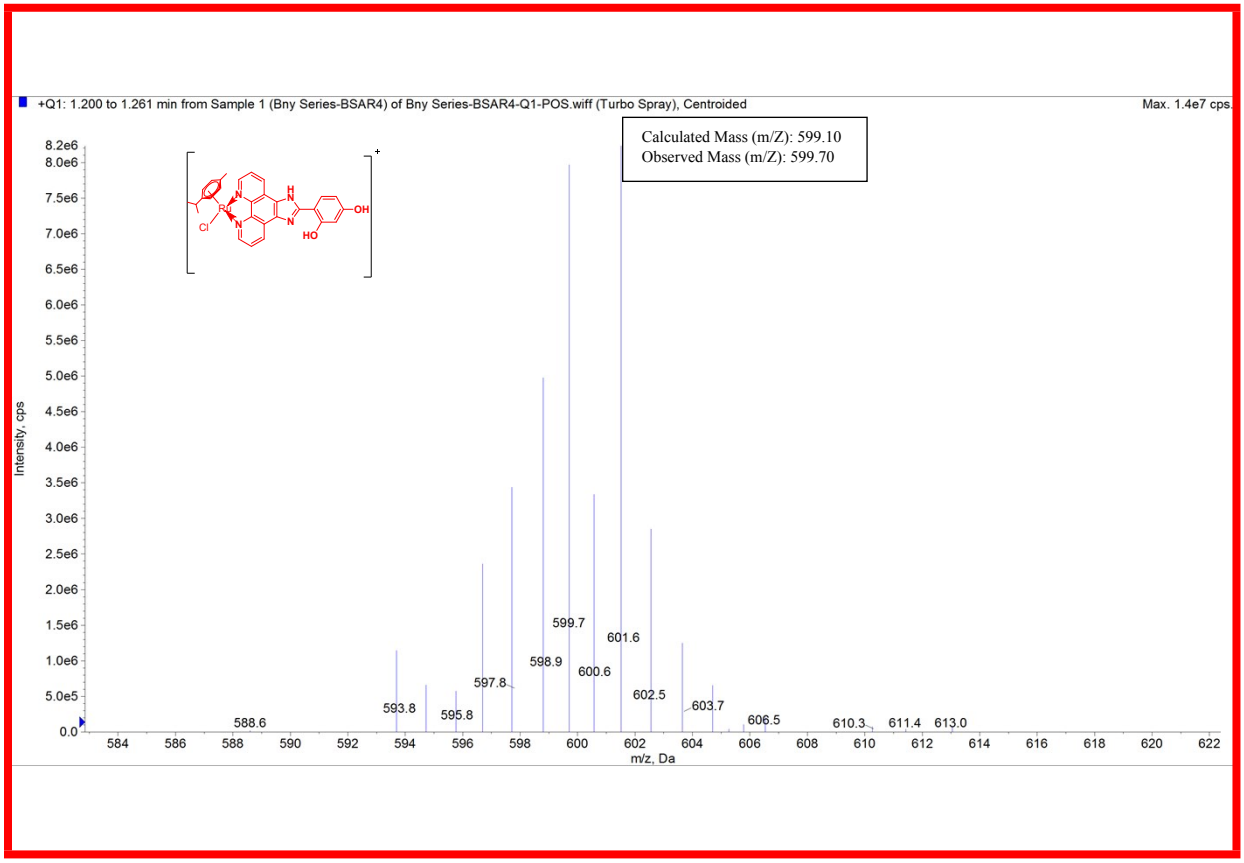
+Q1: 1.200 to 1.261 min from Sample 1 (Bny Series-BSAR4) of Bny Series-BSAR4-Q1-POS.wiff (Turbo Spray), Centroided
Max. 1.4e7 cps.
Calculated Mass (m/Z): 599.10
Observed Mass (m/Z): 599.70
Intensity, cps
m/z, Da

RuL5

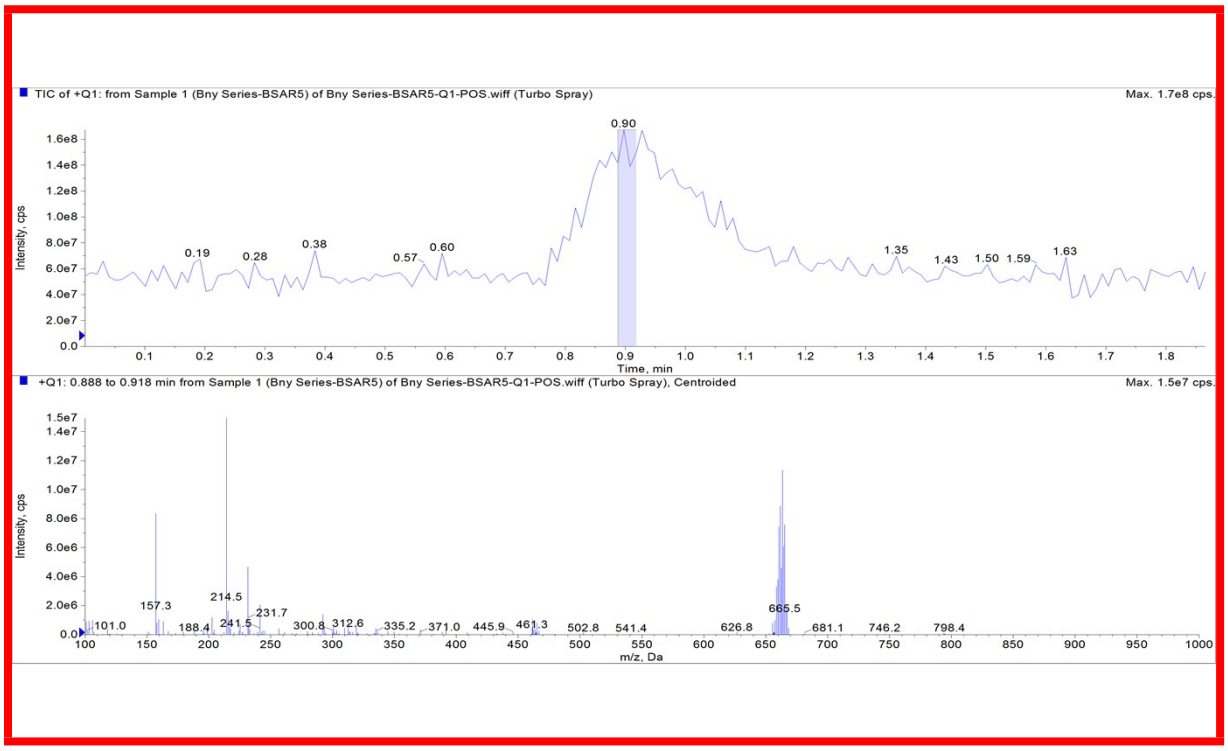
TIC of +Q1: from Sample 1 (Bny Series-BSAR5) of Bny Series-BSAR5-Q1-POS.wiff (Turbo Spray)
Max. 1.7e8 cps.
Intensity, cps
Time, min
+Q1: 0.888 to 0.918 min from Sample 1 (Bny Series-BSAR5) of Bny Series-BSAR5-Q1-POS.wiff (Turbo Spray), Centroided
Max. 1.5e7 cps.
Intensity, cps
m/z, Da

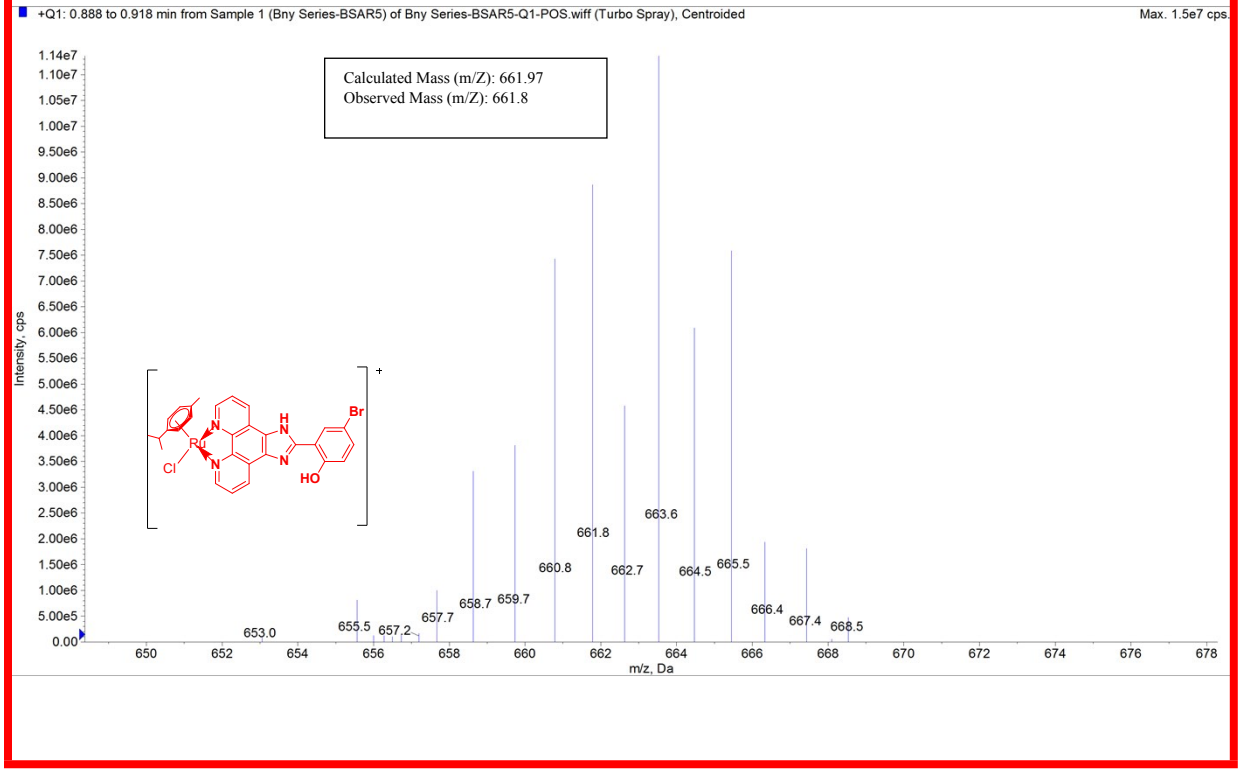
+Q1: 0.888 to 0.918 min from Sample 1 (Bny Series-BSAR5) of Bny Series-BSAR5-Q1-POS.wiff (Turbo Spray), Centroided
Max. 1.5e7 cps.
Calculated Mass (m/Z): 661.97
Observed Mass (m/Z): 661.8
Intensity, cps
m/z, Da

RuL6

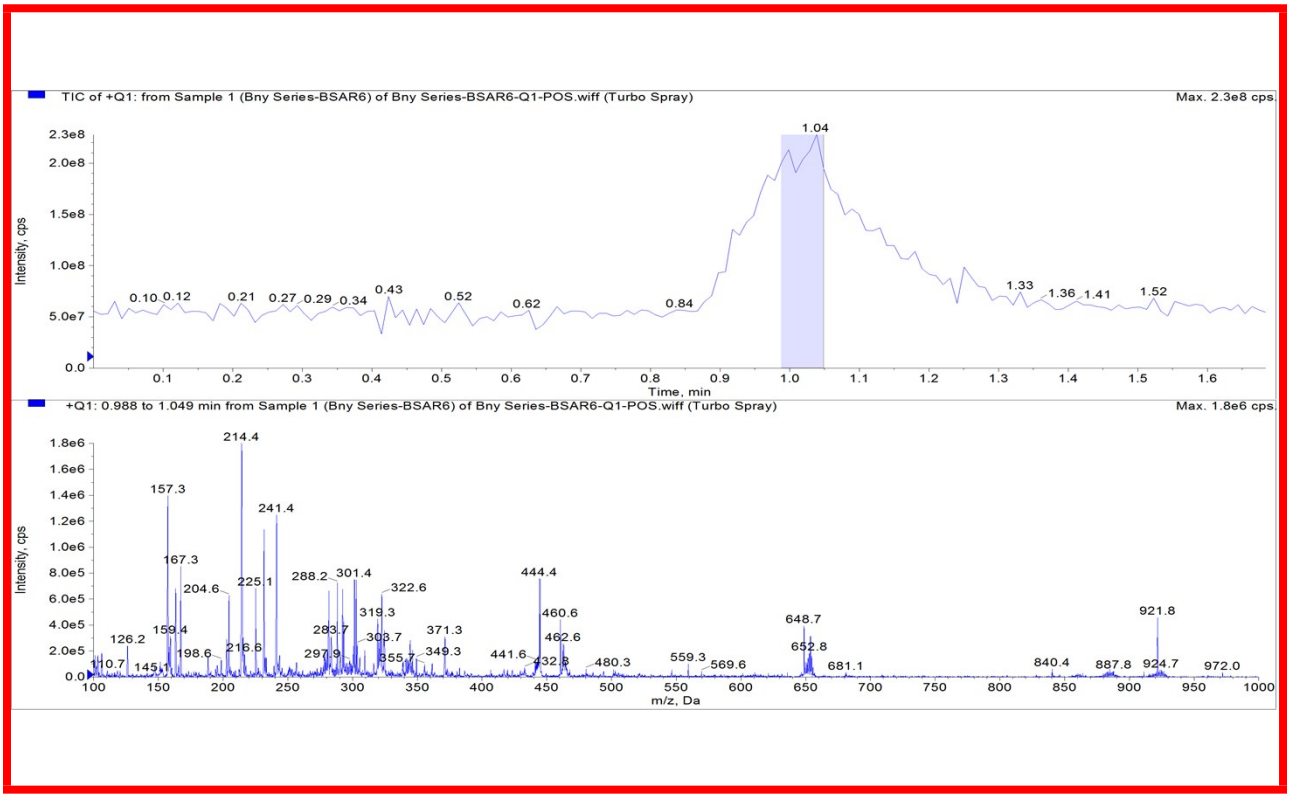
TIC of +Q1: from Sample 1 (Bny Series-BSAR6) of Bny Series-BSAR6-Q1-POS.wiff (Turbo Spray)
Max. 2.3e8 cps.
Intensity, cps
Time, min
+Q1: 0.988 to 1.049 min from Sample 1 (Bny Series-BSAR6) of Bny Series-BSAR6-Q1-POS.wiff (Turbo Spray)
Max. 1.8e6 cps.
Intensity, cps
m/z, Da

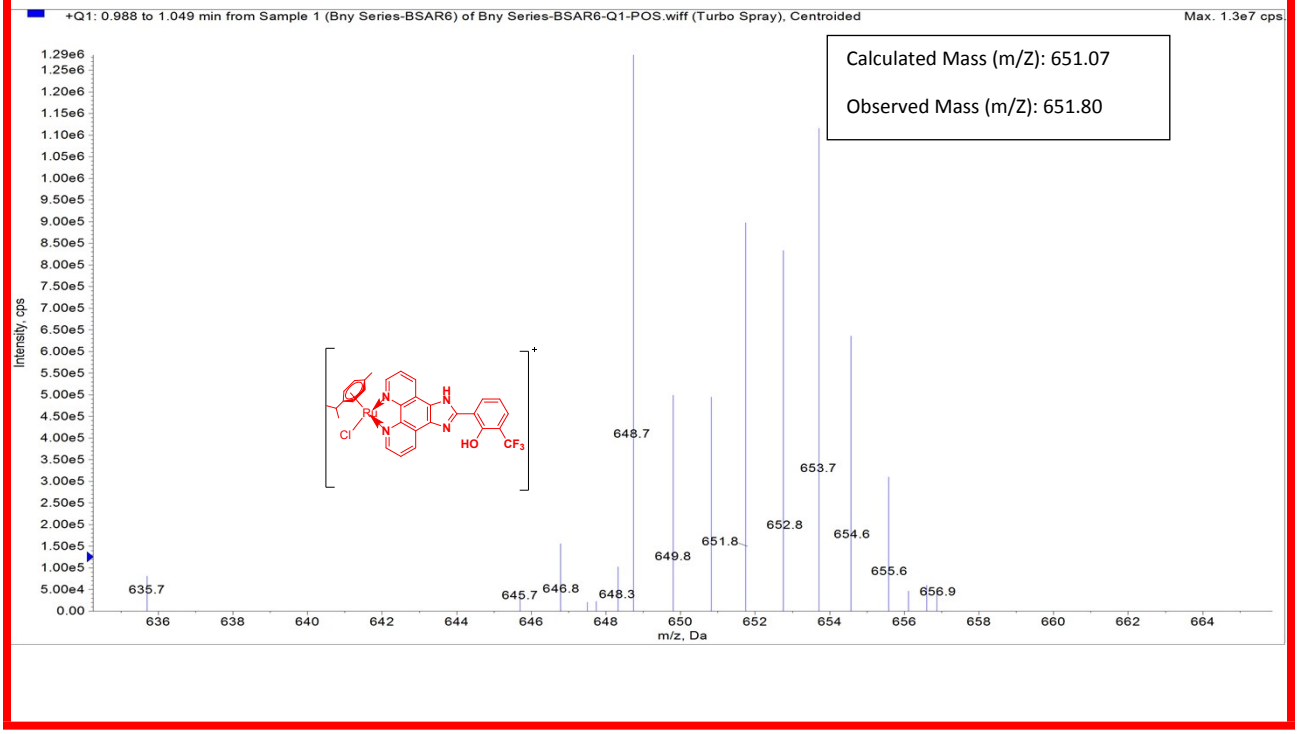
+Q1: 0.988 to 1.049 min from Sample 1 (Bny Series-BSAR6) of Bny Series-BSAR6-Q1-POS.wiff (Turbo Spray), Centroided
Max. 1.3e7 cps.
Calculated Mass (m/Z): 651.07
Observed Mass (m/Z): 651.80
Intensity, cps
m/z, Da

RuL7

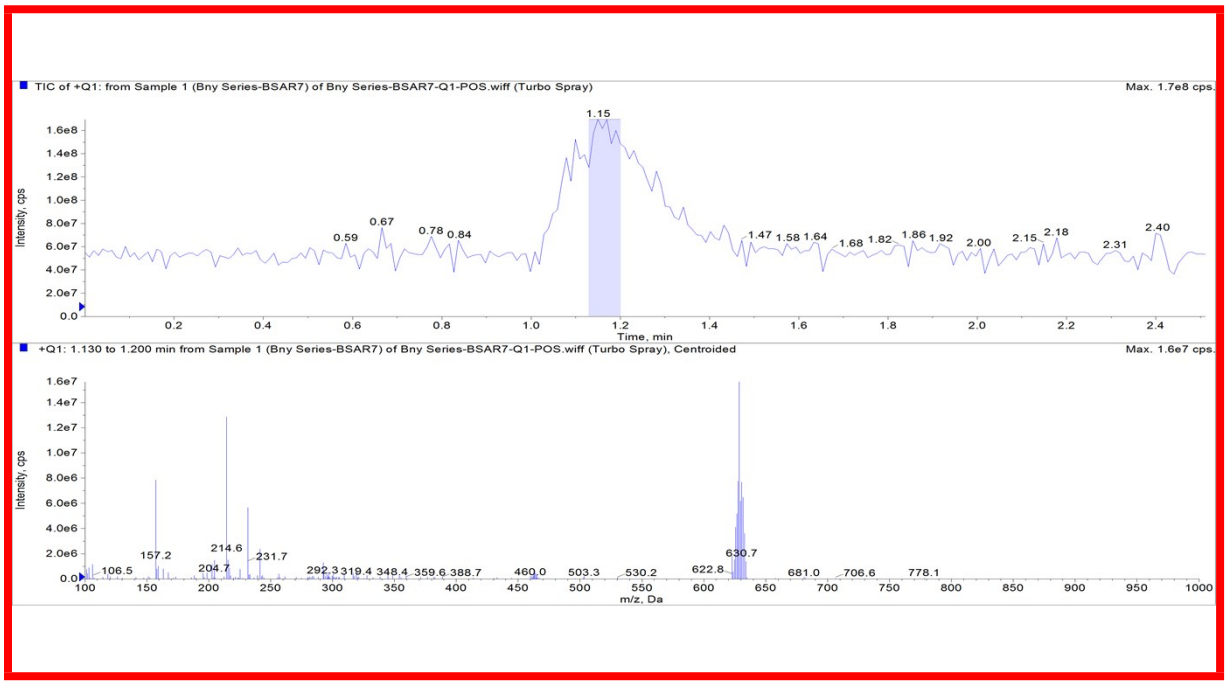
TIC of +Q1: from Sample 1 (Bny Series-BSAR7) of Bny Series-BSAR7-Q1-POS.wiff (Turbo Spray)
Max. 1.7e8 cps.
Intensity, cps
Time, min
+Q1: 1.130 to 1.200 min from Sample 1 (Bny Series-BSAR7) of Bny Series-BSAR7-Q1-POS.wiff (Turbo Spray), Centroided
Max. 1.6e7 cps.
Intensity, cps
m/z, Da

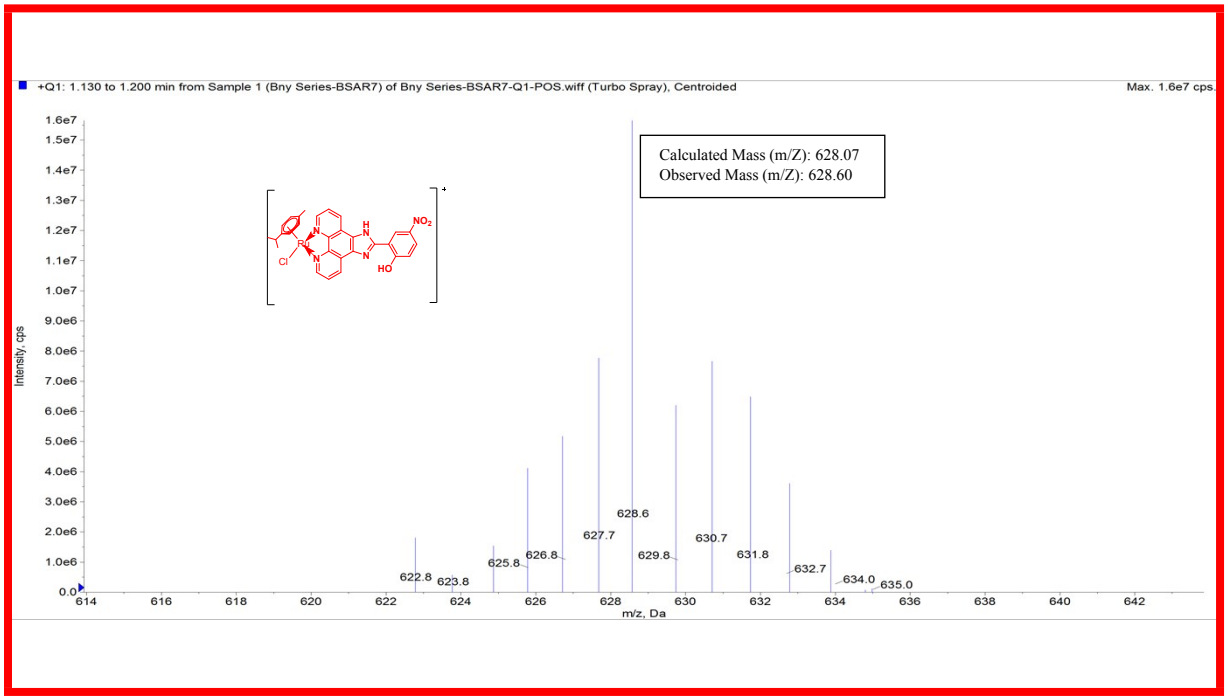
+Q1: 1.130 to 1.200 min from Sample 1 (Bny Series-BSAR7) of Bny Series-BSAR7-Q1-POS.wiff (Turbo Spray), Centroided
Max. 1.6e7 cps.
Calculated Mass (m/Z): 628.07
Observed Mass (m/Z): 628.60
Intensity, cps
m/z, Da

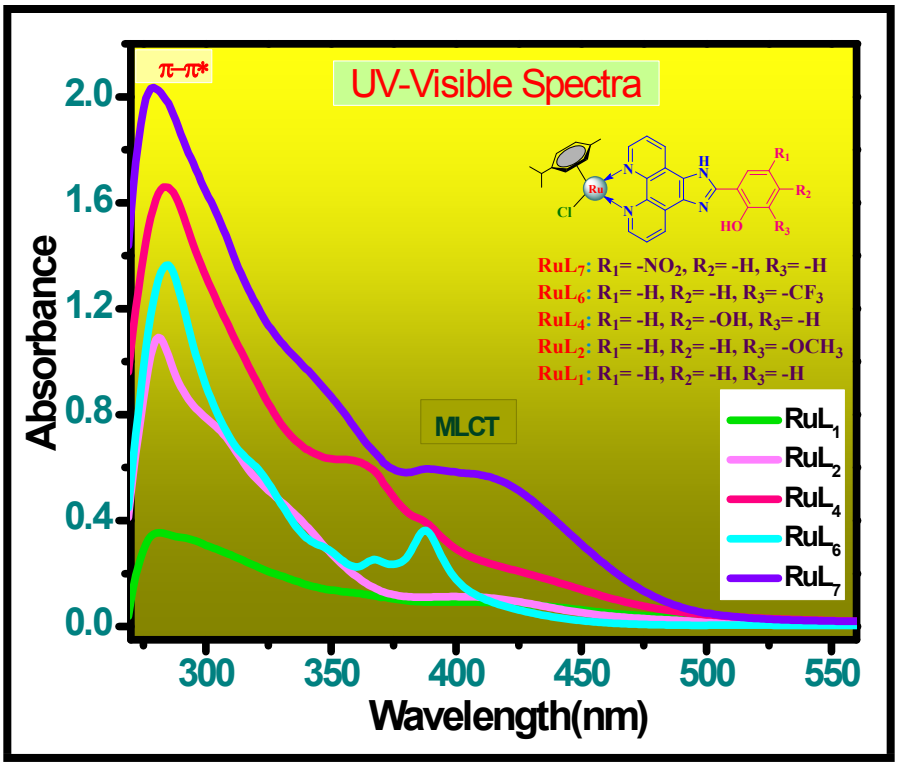
UV-Visible Spectra
π–π*
MLCT
RuL7: R1= -NO2, R2= -H, R3= -H
RuL6: R1= -H, R2= -H, R3= -CF3
RuL4: R1= -H, R2= -OH, R3= -H
RuL2: R1= -H, R2= -H, R3= -OCH3
RuL1: R1= -H, R2= -H, R3= -H
RuL1
RuL2
RuL4
RuL6
RuL7
Absorbance
Wavelength(nm)
2.0
1.6
1.2
0.8
0.4
0.0
300
350
400
450
500
550

(a)

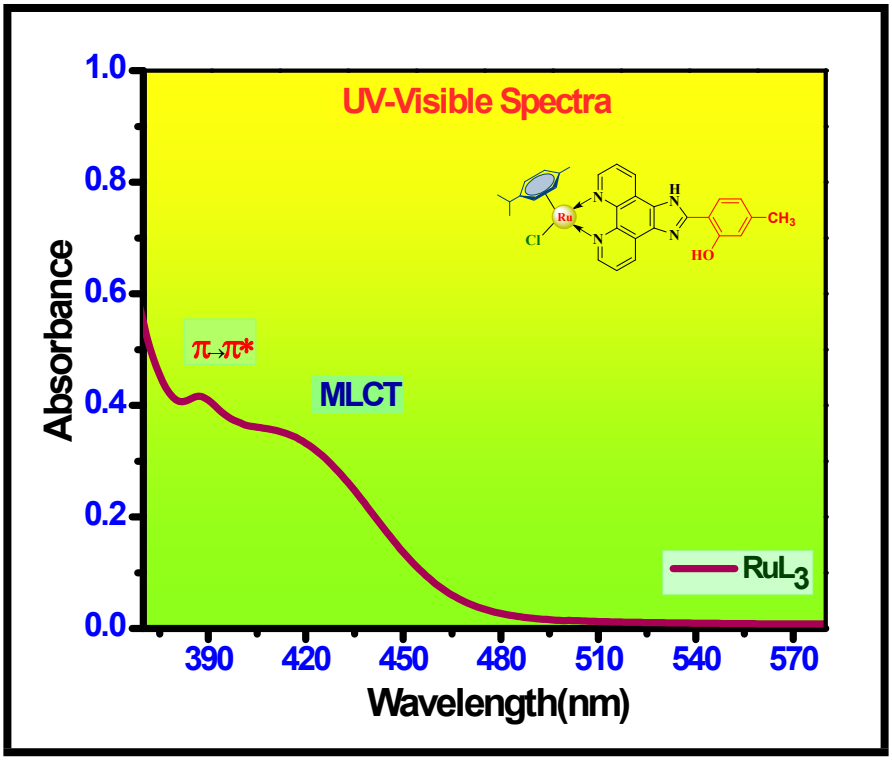
UV-Visible Spectra
π→π*
MLCT
RuL3
Absorbance
Wavelength(nm)
1.0
0.8
0.6
0.4
0.2
0.0
390
420
450
480
510
540
570

(b)

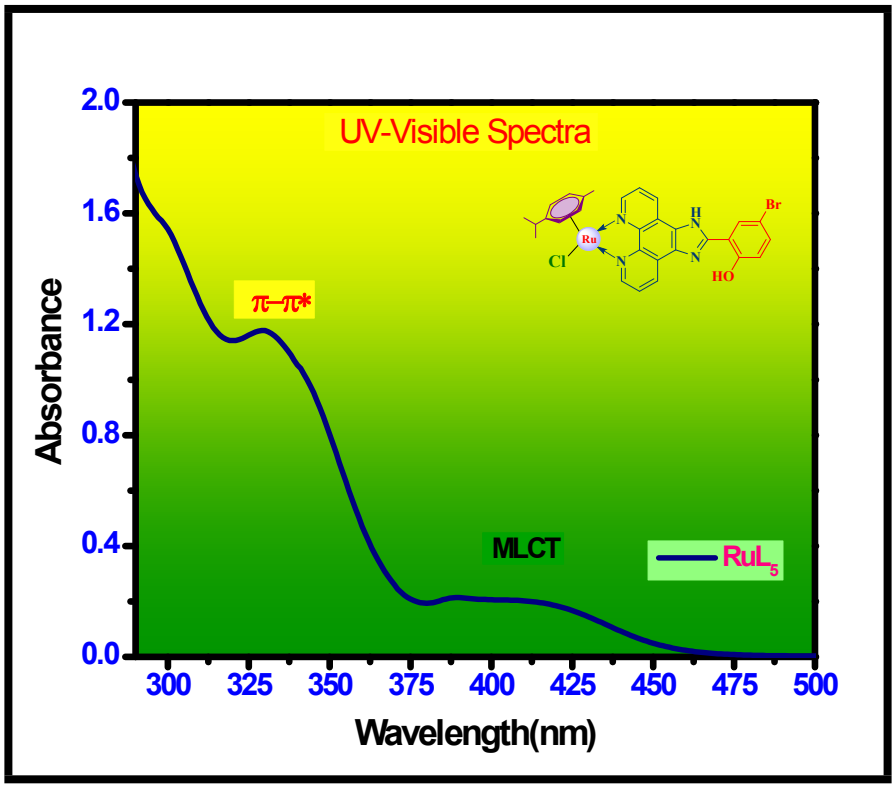

(c)

Fig. S1: UV-Vis spectra of (a) complex RuL1, RuL2, RuL4, RuL6 and RuL7 (b) complex RuL3 (c) complex RuL5

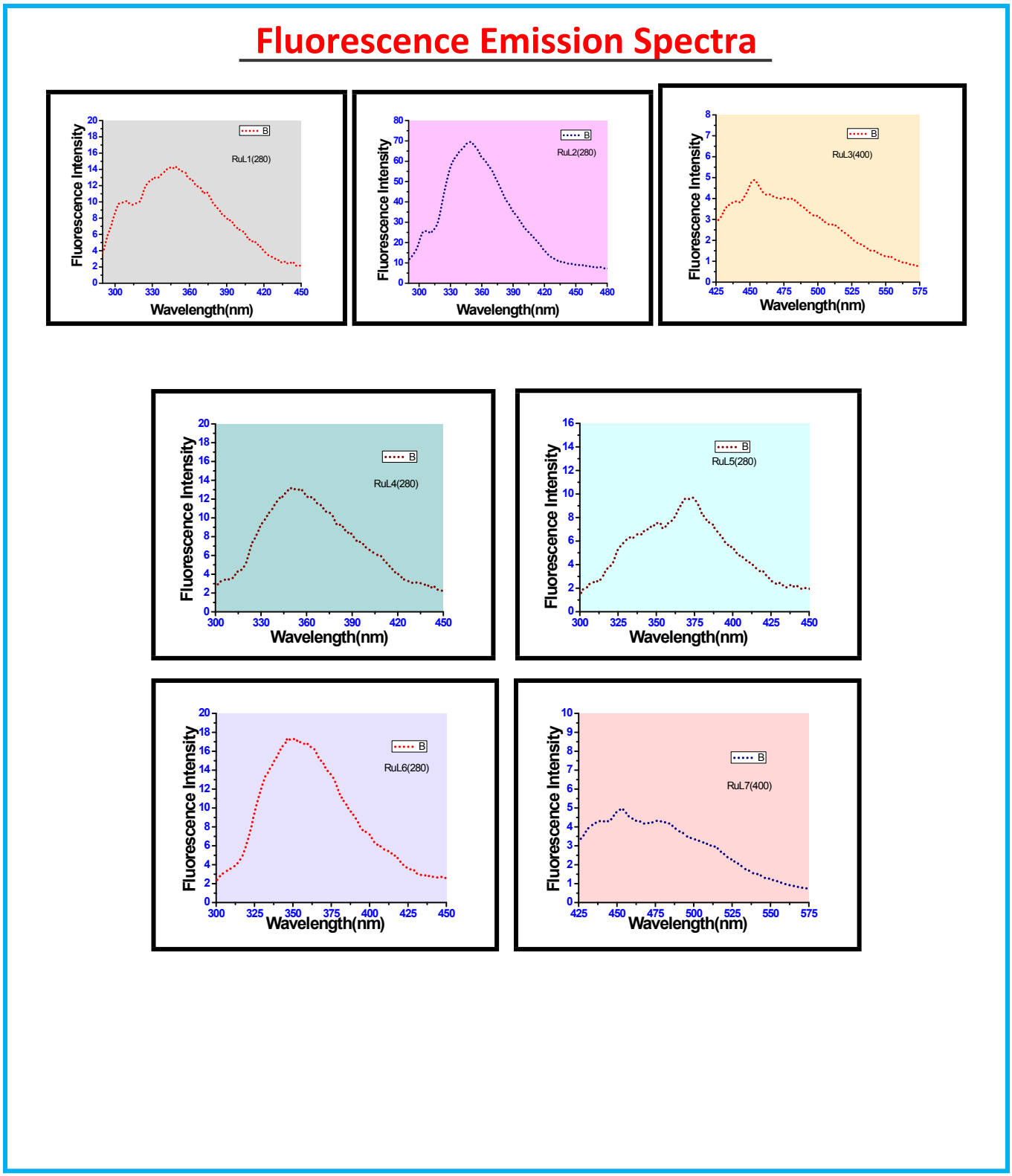

Fig. S2: Emission spectra of complexes RuL1–RuL7 in 10% DMSO-water solvent system at room temperature, λexc = 280-400 nm.

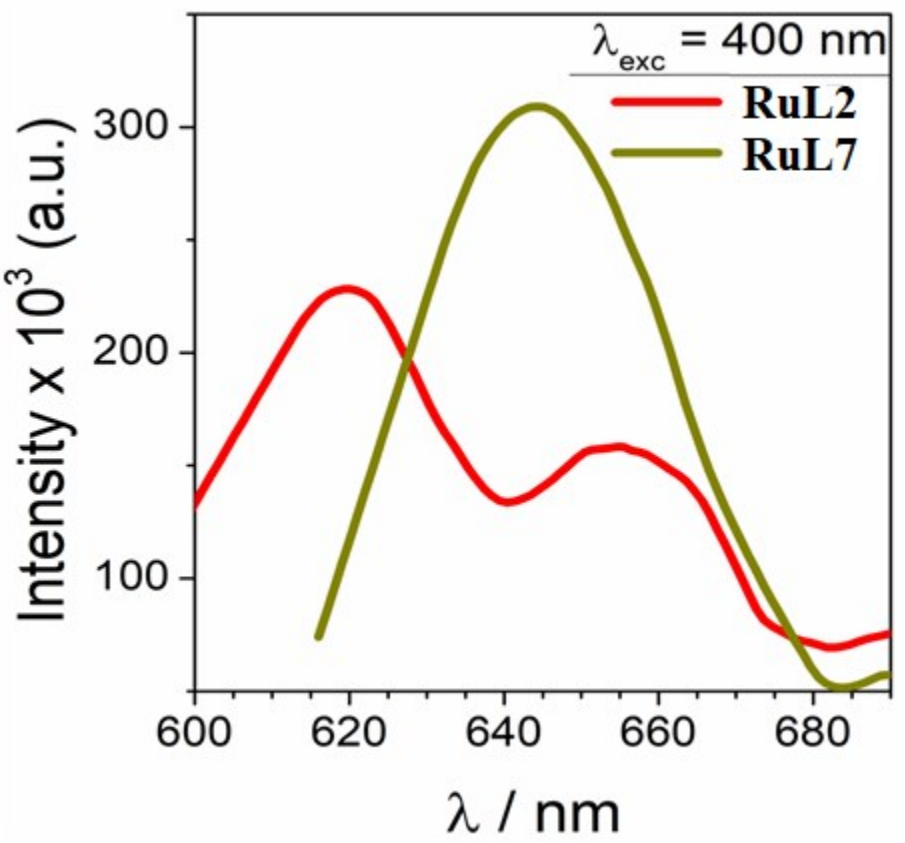

Fig. S3: Emission spectra of complexes RuL2 and RuL7 in 100% DMSO at room temperature, λexc = 400 nm. ** All other complexes except these two did not show any fluorescence in 100% DMSO at room temperature when excited at 400 nm**

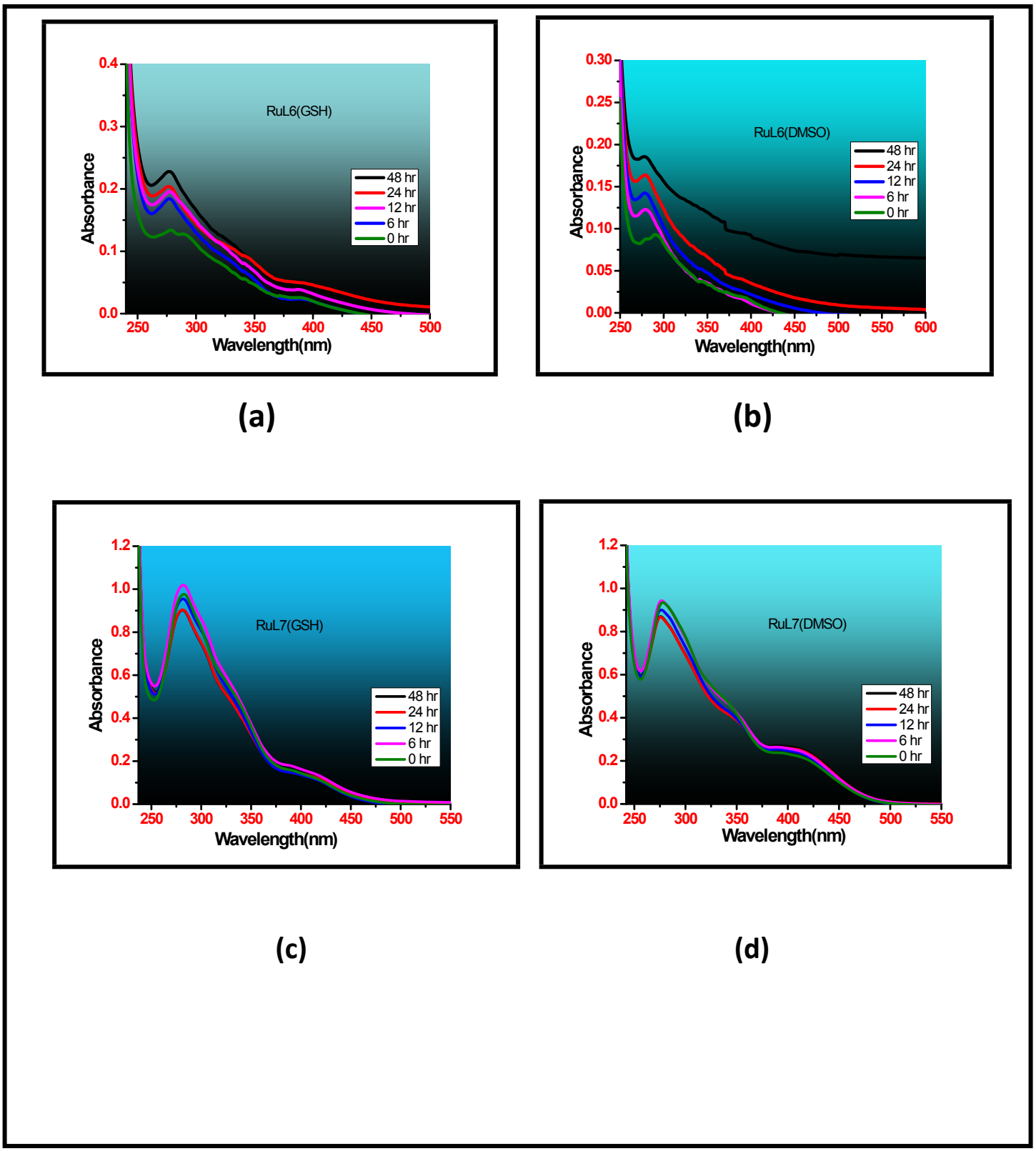

Fig. S4: Stability of selected Ru(II) complexes (RuL6 and RuL7) in aqueous GSH media [(a) and (c)] and also in 10% DMSO media [(b) and (d)]

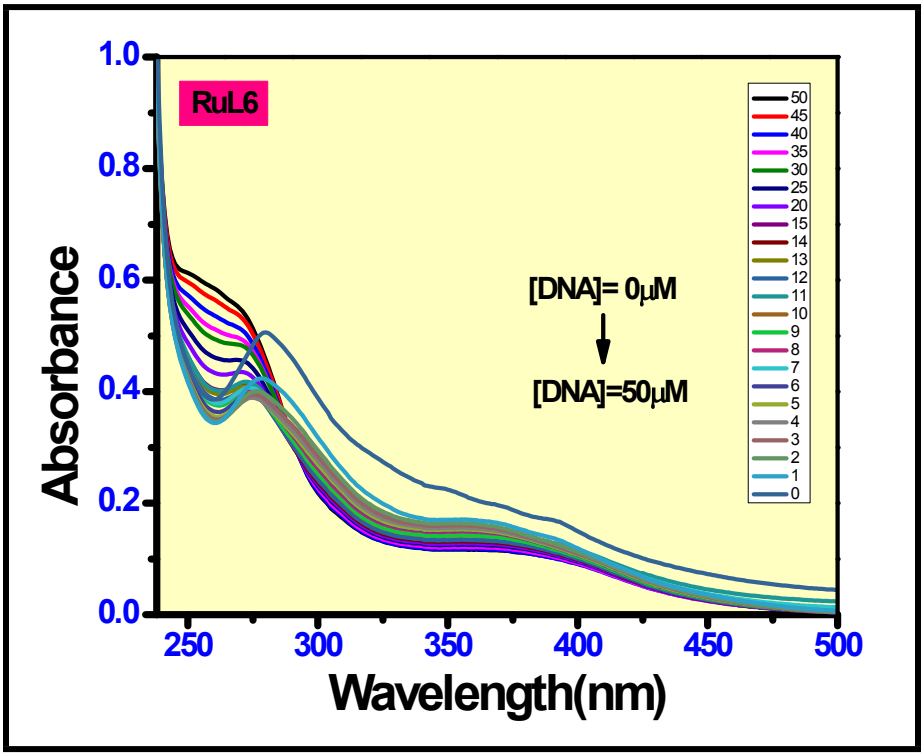
RuL6
[DNA]= 0μM
[DNA]=50μM
Absorbance
Wavelength(nm)
1.0
0.8
0.6
0.4
0.2
0.0
250
300
350
400
450
500
50
45
40
35
30
25
20
15
14
13
12
11
10
9
8
7
6
5
4
3
2
1
0

(a)

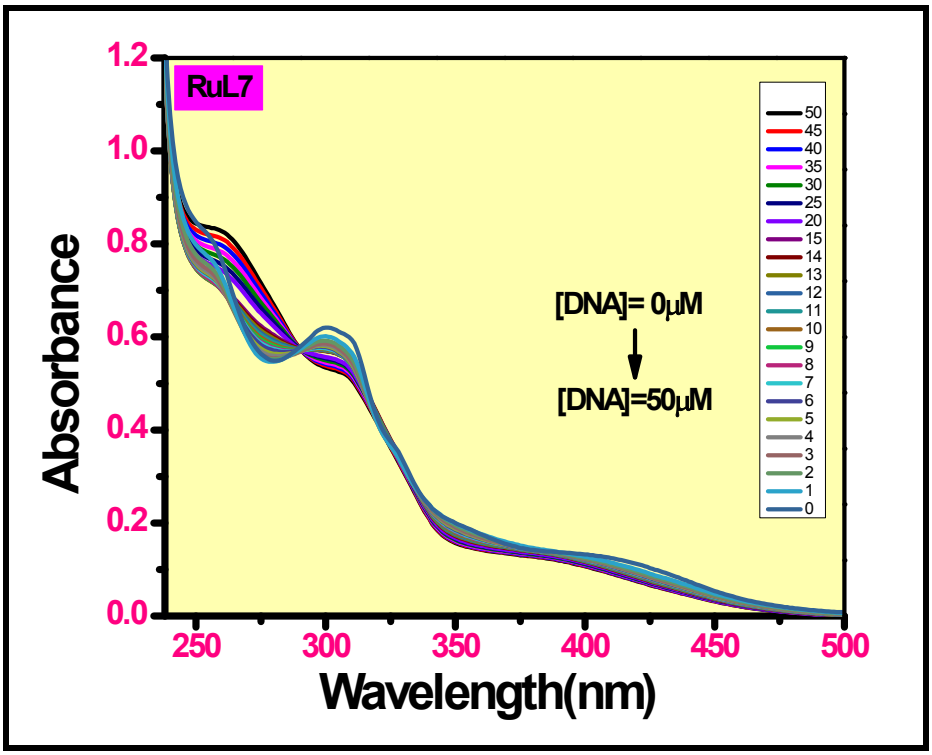

(b)

Fig. S5: DNA binding plots of (a) complex RuL6 and (b) complex RuL7

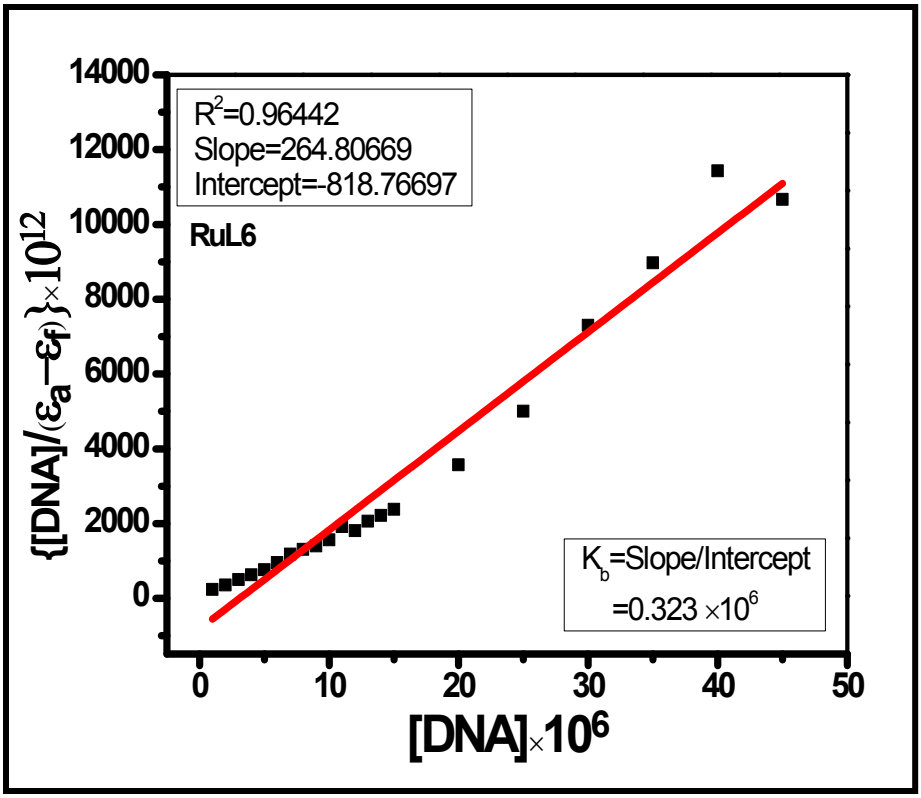
R²=0.96442
Slope=264.80669
Intercept=-818.76697
RuL6
K_b=Slope/Intercept
=0.323 ×10^6
{[DNA]/(ε_a−ε_f)}×10^12
[DNA]×10^6
14000
12000
10000
8000
6000
4000
2000
0
0
10
20
30
40
50

(a)

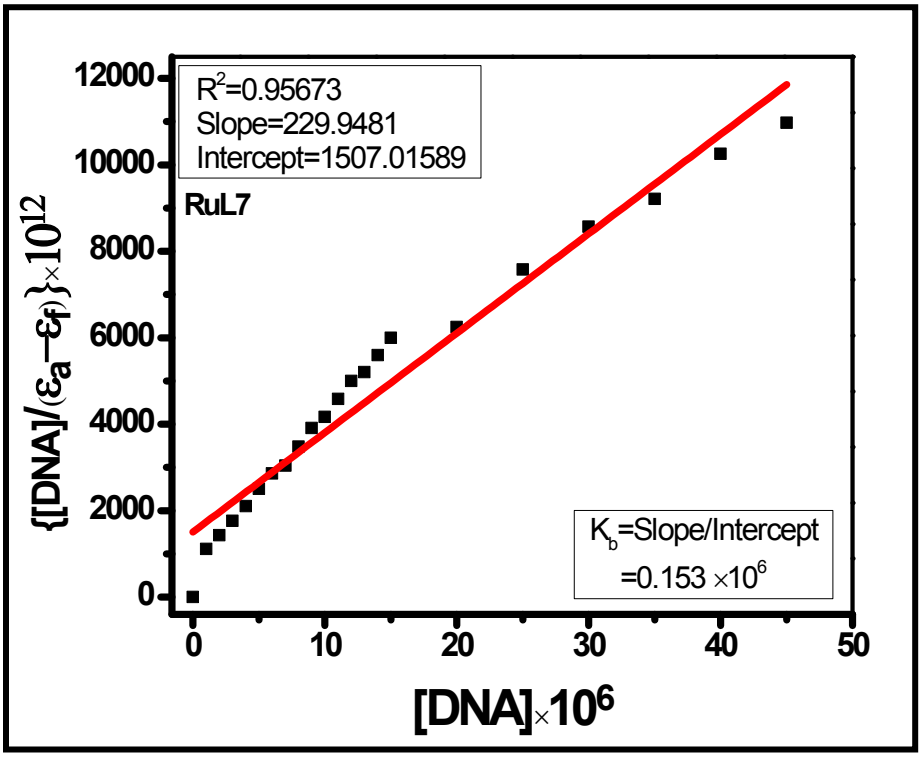
R²=0.95673
Slope=229.9481
Intercept=1507.01589
RuL7
K_b=Slope/Intercept
=0.153 ×10^6
{[DNA]/(ε_a−ε_f)}×10^12
[DNA]×10^6
12000
10000
8000
6000
4000
2000
0
0
10
20
30
40
50

(b)

Fig. S6: [DNA]/(ε_a-ε_f) vs. [DNA] linear plots of complex (a) RuL6 and (b) RuL7

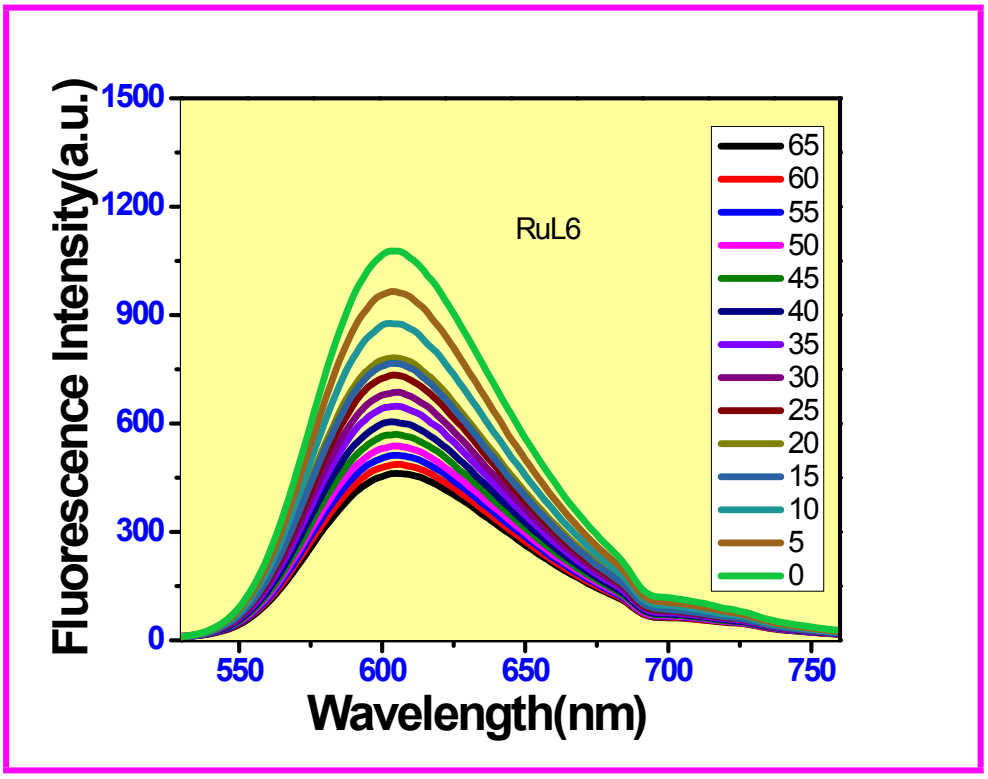
Fluorescence Intensity(a.u.)
1500
1200
900
600
300
0
550
600
650
700
750
Wavelength(nm)
RuL6
65
60
55
50
45
40
35
30
25
20
15
10
5
0

(a)

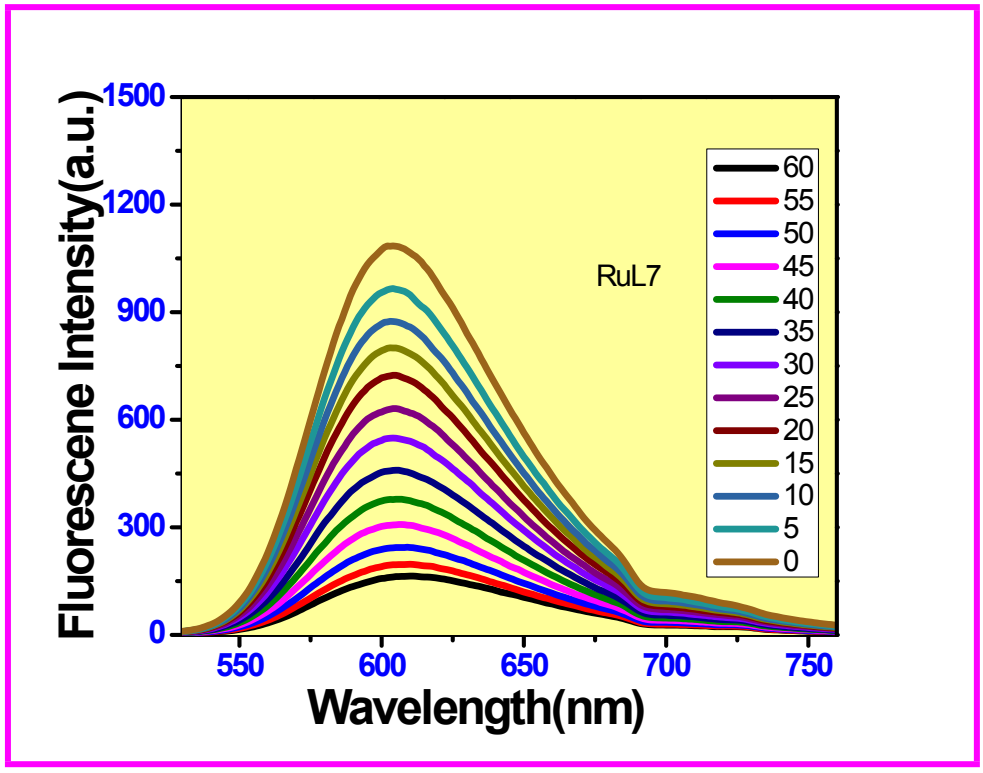
Fluorescene Intensity(a.u.)
1500
1200
900
600
300
0
550
600
650
700
750
Wavelength(nm)
RuL7
60
55
50
45
40
35
30
25
20
15
10
5
0

(b)

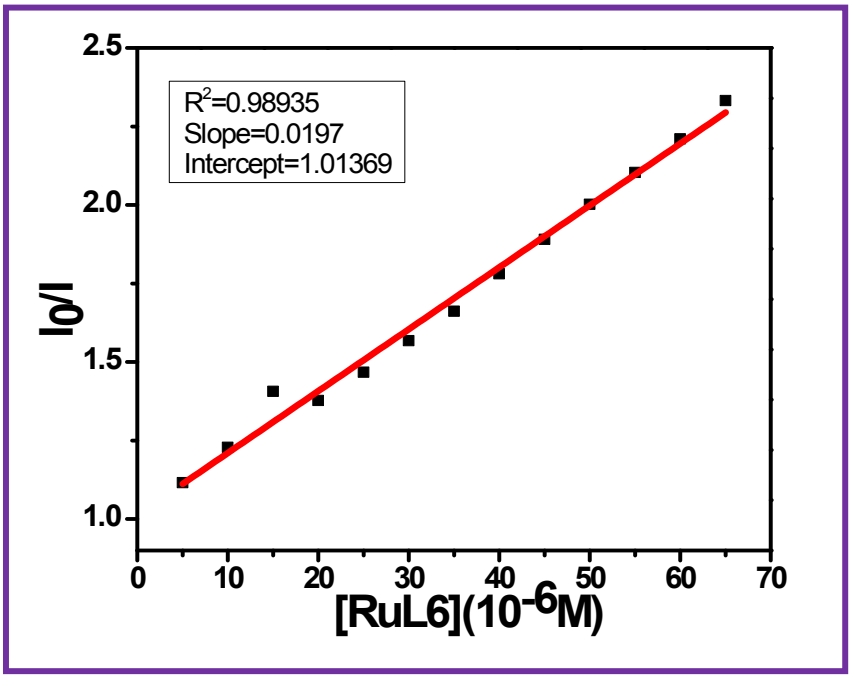
R2=0.98935
Slope=0.0197
Intercept=1.01369
I0/I
[RuL6](10-6M)

(c)

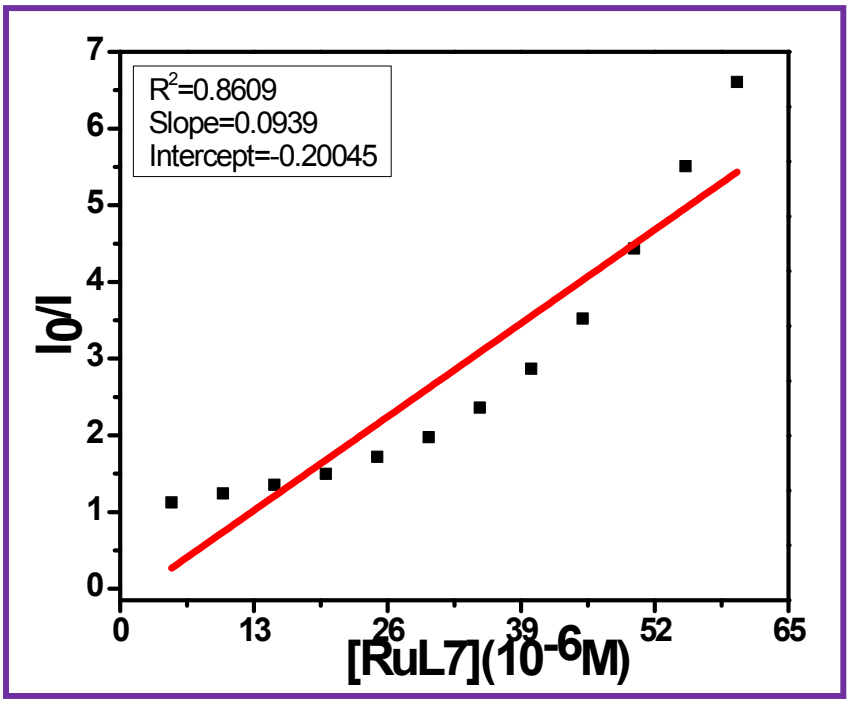
R2=0.8609
Slope=0.0939
Intercept=-0.20045
I0/I
[RuL7](10-6M)

(d)

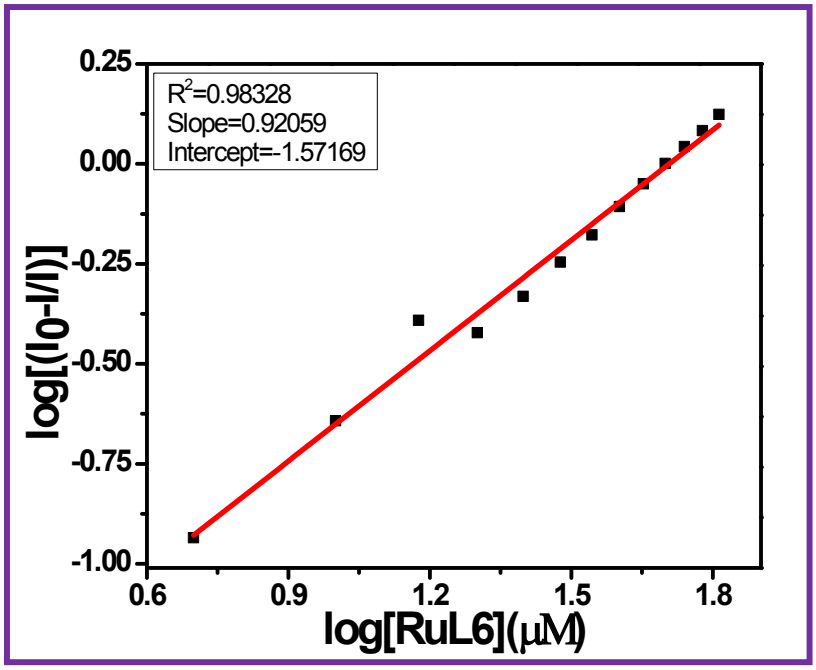

(e)

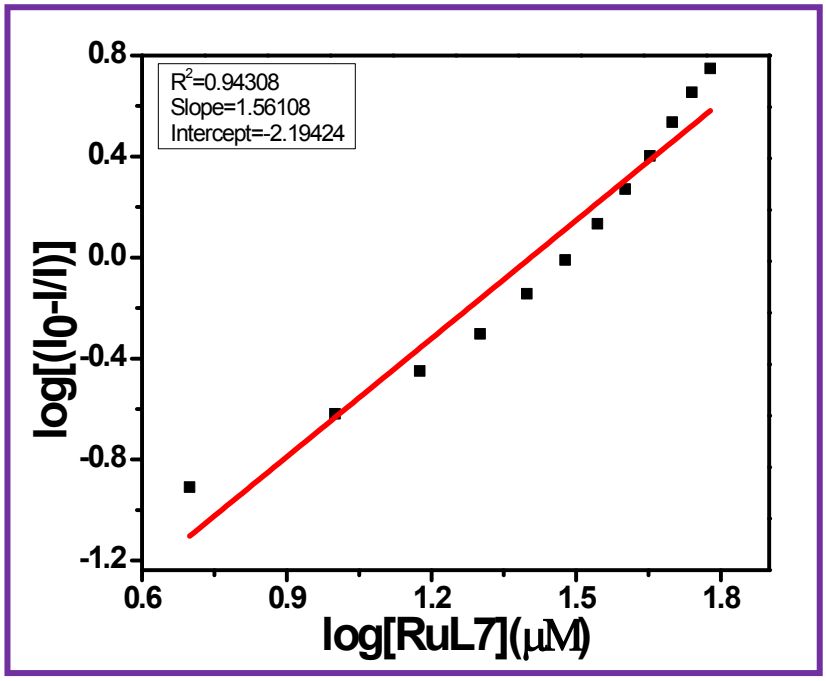

(f)

Fig. S7: Interaction of complexes (a) RuL6 and (b) RuL7 with EtBr. Stern-Volmer Plot of I_0/I vs. concentration of complex (c) RuL6 (d) RuL7. Scatchard Plot of log($[I_0-I]/I$) vs. log[Complex] for EtBr in the presence of complex (e) RuL6 (f) RuL7.

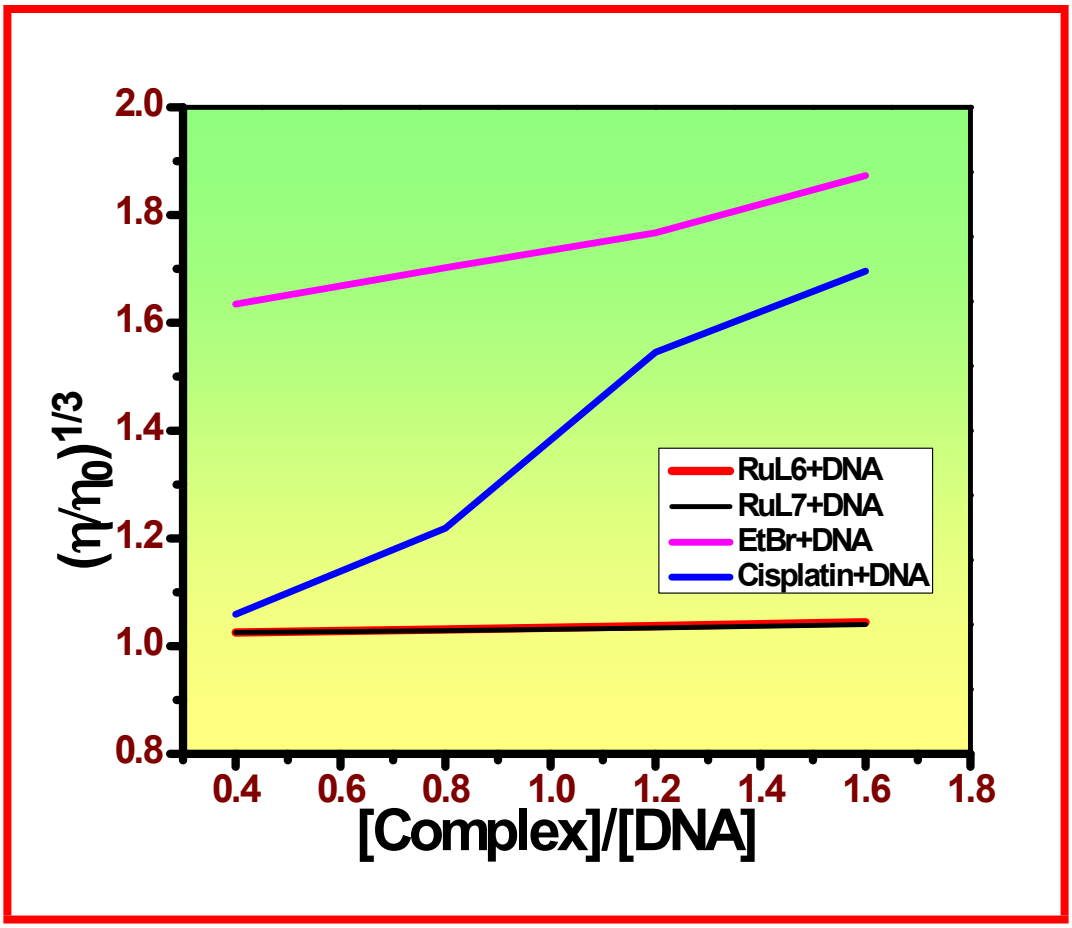

Fig. S8: Viscosity plot of complexes RuL6, RuL7 and EtBr with Ct-DNA

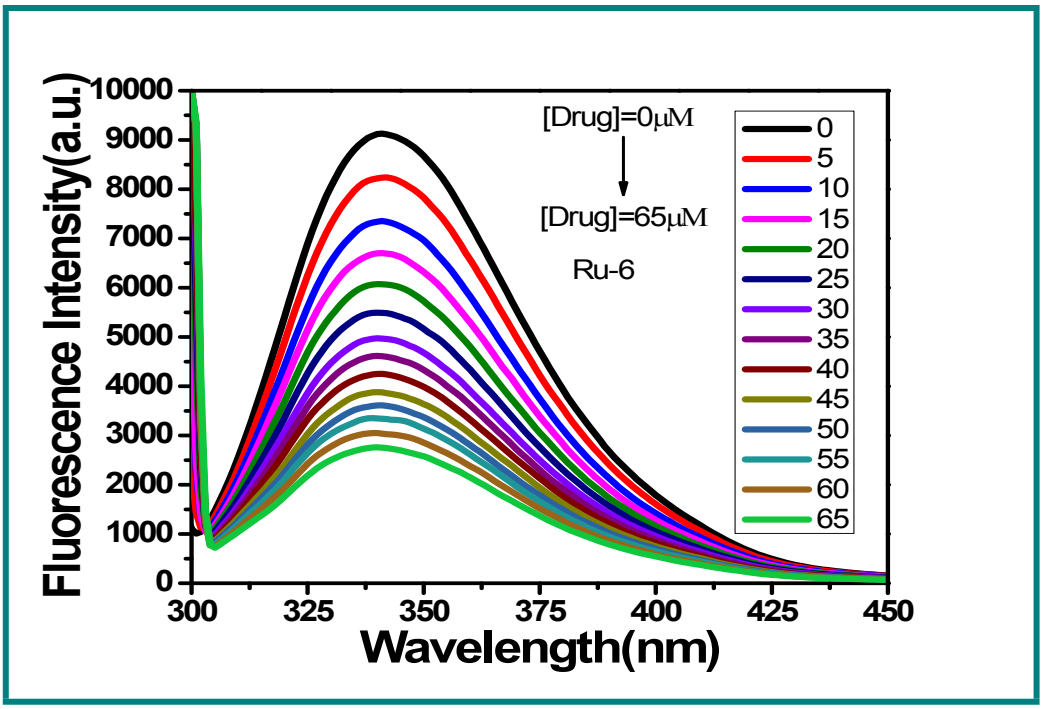
Fluorescence Intensity(a.u.)
Wavelength(nm)
[Drug]=0μM
[Drug]=65μM
Ru-6
0
5
10
15
20
25
30
35
40
45
50
55
60
65

(a)

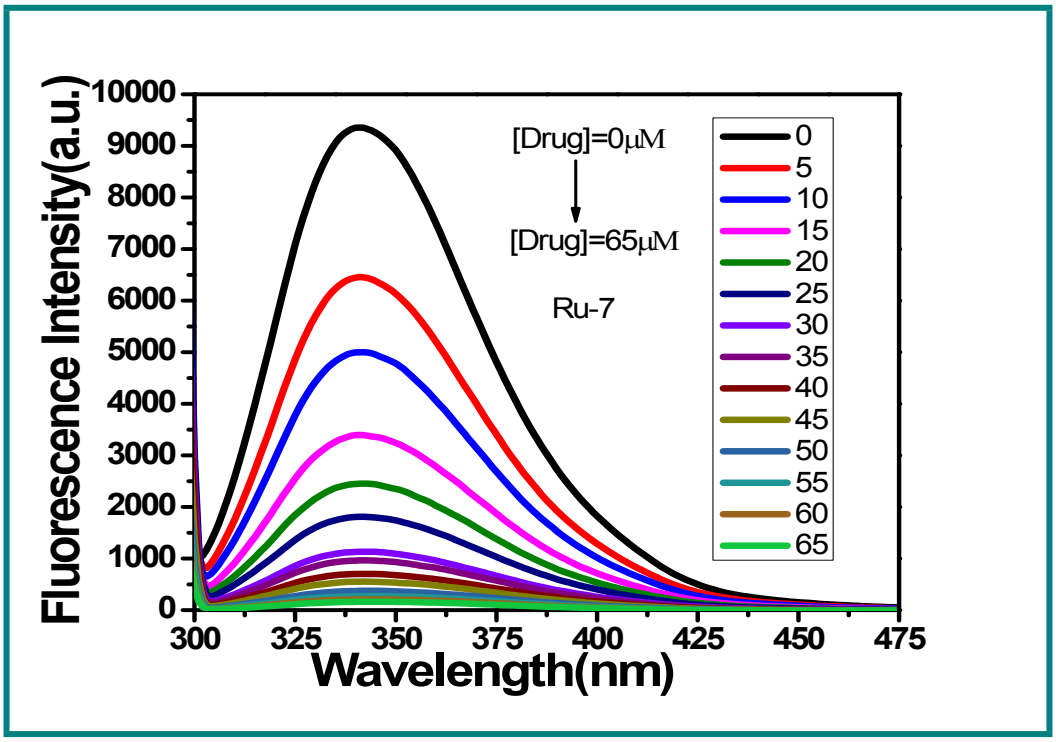
Fluorescence Intensity(a.u.)
Wavelength(nm)
[Drug]=0μM
[Drug]=65μM
Ru-7
0
5
10
15
20
25
30
35
40
45
50
55
60
65

(b)

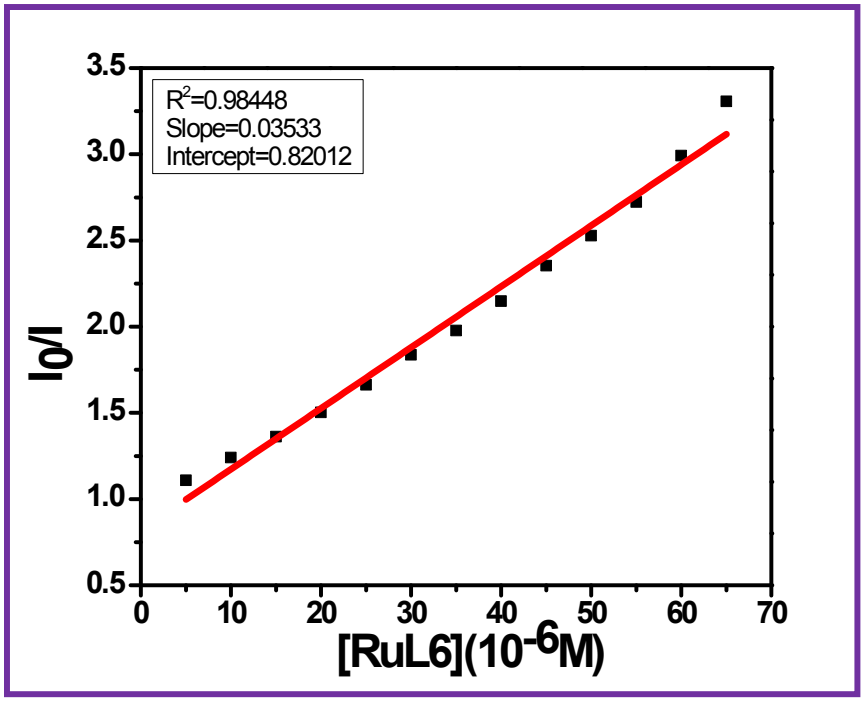
R2=0.98448
Slope=0.03533
Intercept=0.82012
I0/I
[RuL6](10-6M)

(c)

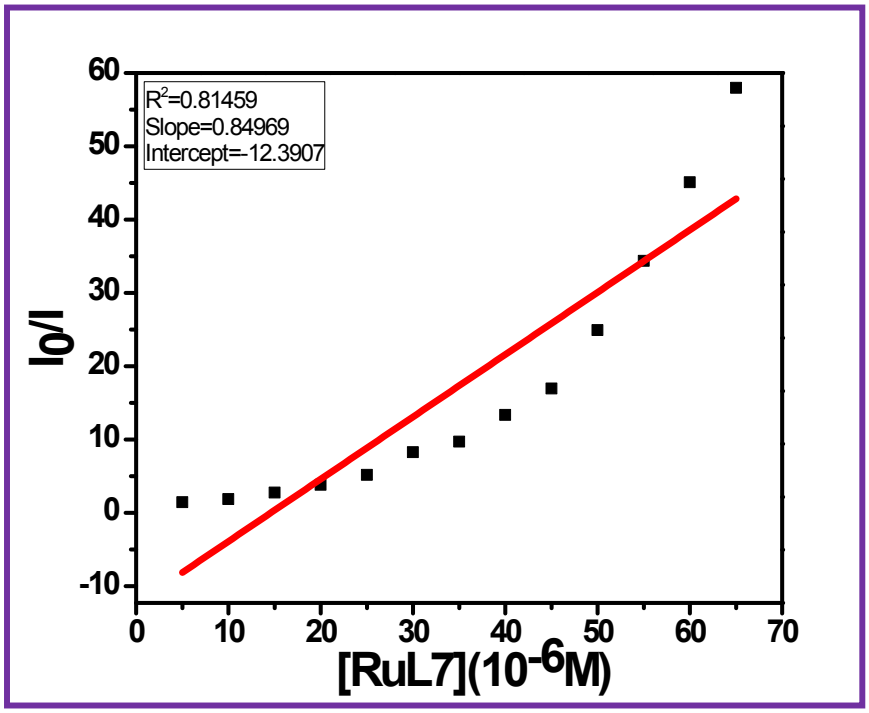
R2=0.81459
Slope=0.84969
Intercept=-12.3907
I0/I
[RuL7](10-6M)

(d)

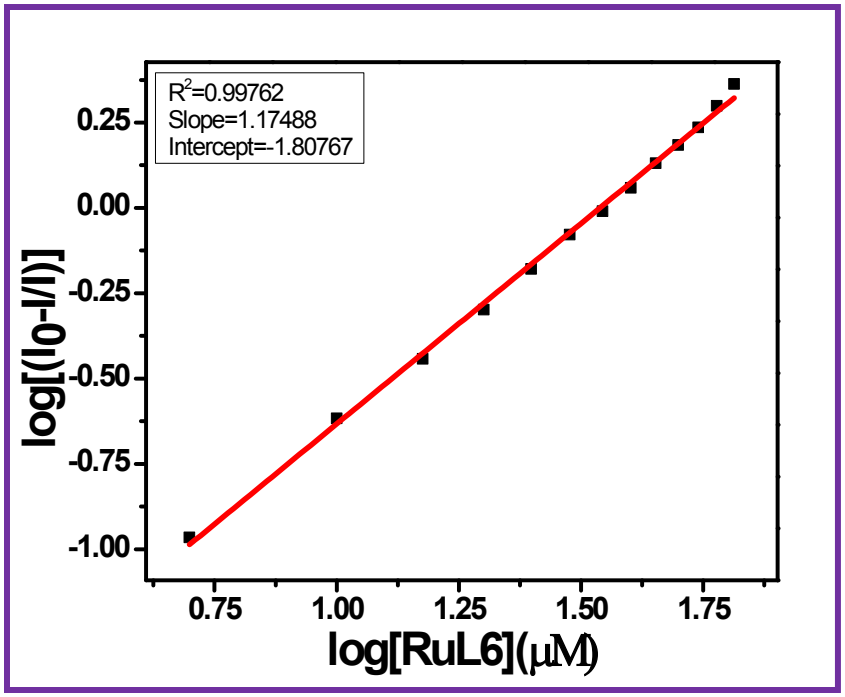

(e)

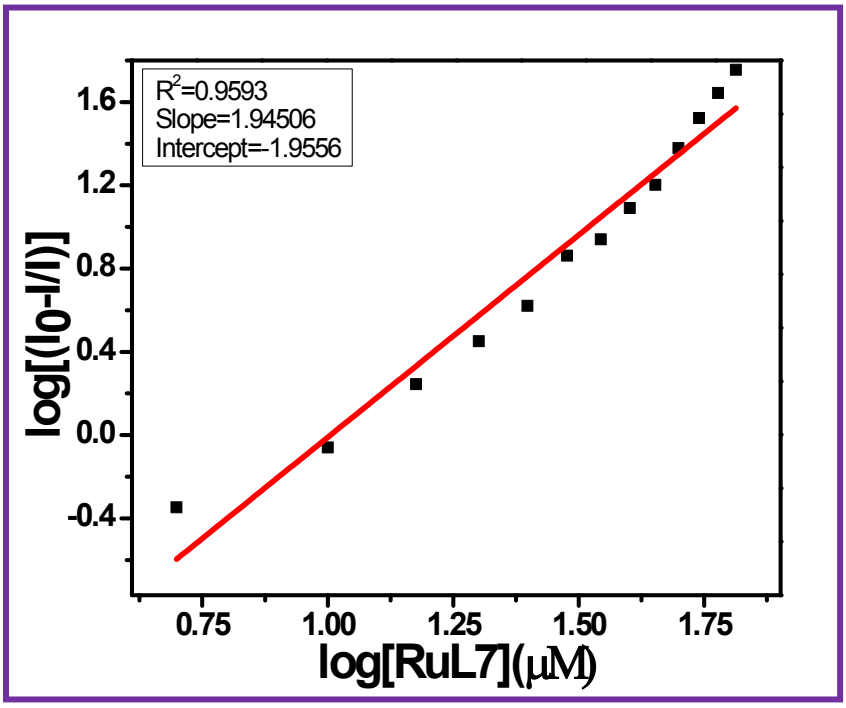

(f)

Fig. S9 Interaction of complexes (a) RuL6 and (b) RuL7 with BSA. Stern-Volmer Plot of I_0/I vs. concentration of complex (c) RuL6 and (d) RuL7. Scatchard Plot of log[$(I_0-I)/I$] vs. log[Complex] for BSA in the presence of for complex (e) RuL6 (f) RuL7.

Table S1 Photophysical characterisation at π - π* and MLCT region, solubility, lipophilicity and conductivity study of the complexes RuL1-RuL7

Samples	λ_a(nm)[a]		λ_e(nm)[b]	Stoke's shift	O.D[c]	ε($M^{-1}cm^{-1}$)[d]	(ϕ_f)[e]	log $P_{o/w}$[f]	Λ_M (Sm^2M^{-1})[g]	
	π - π*	MLCT							DMSO	10% DMSO
RuL1	280	410	348	68	0.358	11933	0.022	0.0327	7.3	35
RuL2	280	412	349	69	1.089	36300	0.030	-0.1001	6.6	22
RuL3	387	412	452	40	0.420	14000	0.045	0.2105	8.6	23
RuL4	283	360	350	67	1.660	55333	0.003	-0.3494	5.3	26
RuL5	330	414	375	45	1.179	39300	0.003	0.9452	4.6	41
RuL6	284	387	349	65	1.367	45566	0.005	0.2795	6.2	15
RuL7	278	409	454	45	2.036	67866	0.008	-0.1643	7.6	16
Quinine Sulphate	350		452	102	0.26	8000	0.546	-	-	

[a]Absorption maxima. [b]Emission wavelength. [c]Optical density. [d]Extinction coefficient. [e]Quantum yield. [f]n-Octanol/water partition coefficient. [g]Conductance in DMSO and 10% aqueous DMSO.

Table S2 Binding parameters for complexes **RuL6** and **RuL7** with ct-DNA.

Complex	λ_{max} [nm]	Change in absorbance intensity	[a]Δε (%)	[b]K_b($\times 10^6 M^{-1}$)	[c]K_{SV}($\times 10^6$ M^{-1})	[d]K_{app}($\times 10^6$ M^{-1})
RuL6	284	Hypochromism	32	0.323	0.0194	1.60
RuL7	300	Hypochromism	28	0.153	0.4684	2.28

[a]Δε, % of change in hypochromism. [b]k_b, intrinsic DNA binding constant from UV-Vis absorption titration. [c]K_{SV}, Stern-Volmer quenching constant. [d]K_{app}, apparent DNA binding constant from competitive displacement.

Table S3 Binding parameters for interaction of complexes **RuL6** and **RuL7** with BSA.

Complex	K_{BSA} [M^{-1}][a]	k_q[$M^{-1}s^{-1}$][b]	K [M^{-1}][c]	n[d]
RuL6	0.043 x10^6	0.431 x10^{13}	1.55 x10^4	1.18
RuL7	0.068 x10^6	0.685 x10^{13}	1.108 x10^4	1.95

[a]K_{BSA}, Stern-Volmer quenching constant; [b]K_q, quenching rate constant; [c]K, binding constant with BSA; [d]n, number of binding sites.

Experimental Section

Materials and method

Throughout the entire experiment, the reagents and solvents employed were of highest grade of purity and of best commercial quality. All organic solvents used for the purpose of chemical synthesis as well as in chromatography were of analytical grade which had been used without further purification and were acquired from E. Merck (India). 1,10-phenanthroline-5,6-dione, 2-hydroxybenzaldehyde, 2-hydroxy-3-methoxybenzaldehyde, 2-hydroxy-4-methylbenzaldehyde, 2,4-dihydroxybenzaldehyde, 5-bromo-2-hydroxybenzaldehyde, 2-hydroxy-3-(trifluoromethyl)benzyldehyde, 2-hydroxy-5-nitrobenzyldehyde, ammonium acetate, ruthenium-(dichloro)-p-cymene dimer, iridium-(dichloro)-pentamethylcyclopentadienyl dimer, o-phenylenediamine, 4-chloro-o-phenylenediamine, 2,3-diaminonaphthalene, 4,5-dimethyl-o-phenylenediamine, 4-trifluoromethyl-o-phenylenediamine, 4-fluoro-o-phenylenediamine and 4-chloro-5-fluoro-o-phenylenediamine and ammonium hexafluorophosphate were obtained from Sigma Aldrich, E-Merck and Spectrochem. Thin layer chromatography was performed on pre-coated silica gel 60 F254 aluminum sheets (E. Merck, Germany) and the solvent system was Ethyl-acetate-Methanol mixture. Bovine serum albumin (BSA) was purchased from Sigma Aldrich Chemical Limited. HeLa, HEK-293 and Human colon cancer cell line (HT-29) was procured from the National center for cell science (NCCS), Pune. Caco-2 cell line was purchased from ATCC (Sigma Aldrich). ^{1}H NMR, ^{13}C NMR, ^{19}F NMR and ^{31}P NMR spectra were recorded on a 400 MHz Advanced Bruker DPX spectrometer with tetramethylsilane (TMS) as internal standard. The chemical shifts (δ) were reported in ppm units. Abbreviations are as follows: s, singlet; brs, broad singlet; d, doublet; dd, double doublet; t, triplet; m, multiplet. The melting points of the complexes was measured on Elchem Microprocessor based DT apparatus using an open capillary tube. Viscosity experiment was carried out with the help of Ostwald viscometer and conductivity of the complexes was measured by TDS conductometer-307. Infrared spectra (IR) were recorded on a Shimadzu Affinity FT-IR spectrometer in the range of 4000-400 cm^{-1}. The mass spectra of the synthesized compounds were recorded on Shimadzu ESI-MS-4000 Mass Spectroscopic instrument, having 4000 triple quadrupole MS, using Methanol as the solvent. UV-Visible spectra were recorded on a JASCO V-730 spectrophotometer using 1 cm quartz cell and fluorescence spectra on Hitachi F7000

fluorescence spectrophotometer equipped with a xenon lamp. For cytotoxicity (MTT) assay, Elisa reader and 96-well plate were used. PerkinElmer instrument has been used for elemental analysis.

Chemistry

General Synthetic procedure of imidazophenanthroline analogues [L1- L7]:

Initially, 50 mg of 1,10-phenanthroline-5,6-dione (0.238 mmole, 1 eqv.) was thoroughly dissolved in minimum volume of glacial acetic acid in a 50 ml pear shaped round-bottom flask, followed by the addition of equimolar amount of different 2-hydroxybenzaldehyde analogues (1 eqv.) and 8 molar equivalent of ammonium acetate (146.69 mg, 1.903 mmole) in same mixture. The reaction mixture was kept under reflux condition for 30 h with constant stirring at 120°C. The reaction was monitored by using TLC in pure methanol to evaluate product formation. After the completion of the reaction, the reaction mixture was poured into ice-cold water in a beaker and ammonia solution was added drop-wise with constant stirring to neutralize the solution and induce precipitation. The precipitate was allowed to settle for 12hr in a refrigerator and then it was filtered and dried overnight. After that it was purified by repeated hexane wash. Then pure crystalline products were obtained with 92%-98% yield, displaying various shades of yellow and brown colour. The structures of products were confirmed by ^{1}H NMR spectroscopy, IR spectroscopy and ESI-MS.

2-(1H-imidazo[4,5-f][1,10]phenanthrolin-2-yl)phenol (L1): Yield: 92 %; Colour: Brown Yellow; Mp: 210˚C; R_f (pure methanol): 0.58; IR (cm^{-1}): υ Ar O-H stretching (3321), N-H stretching (3134), Ar C-H stretching (3043), C=N stretching (1604), Ar C=C stretching (1460), Ar C-H bending (721); ^{1}H NMR (DMSO-d6, 400MHz): δ 9.05 (d, 1H, J = 4.0 Hz), 8.94 (d, 2H, J = 8.0 Hz), 8.19 (t, 1H, J = 8.0 Hz), 7.83-7.86 (m, 2H), 7.38 (t, 1H, J=8.0 Hz), 7.09 (d, 2H, J=8.0 Hz), 6.76 (d, 1H, J=7.6 Hz); ESI-MS (MeOH): m/z = 313 $M+H]^{+}$.

2-(1H-imidazo[4,5-f][1,10]phenanthrolin-2-yl)-6-methoxyphenol (L2): Yield: 96 %; Colour: Brown; Mp: 250˚C; R_f (pure methanol): 0.50; IR (cm^{-1}): υ Ar O-H stretching (3626), N-H stretching (3340), Ar C-H stretching (3045), C=N stretching (1627), Ar C=C stretching (1427), C-N stretching (1371), C-O stretching (1253 and 1056), Ar C-H bending (721); ^{1}H NMR (DMSO-d_6, 400MHz): δ 9.02 (d, 2H, *J* = 2.4 Hz), 8.90 (d, 2H, *J* = 8.0 Hz), 7.79-7.83 (m, 3H), 7.05 (d, 1H, *J* = 7.6 Hz), 6.96 (t, 1H, *J*=8.0 Hz), 3.85 (s, 3H); ESI-MS (MeOH): m/z = 343.2 $[M+H]^+$.

2-(1H-imidazo[4,5-f][1,10]phenanthrolin-2-yl)-5-methylphenol (L3): Yield: 90 %; Colour: Dark Brown; Mp: 270˚C, R_f (pure methanol): 0.42; IR (cm^{-1}): υ Ar O-H stretching (3660), N-H stretching (3360), Ar C-H stretching (3043), C=N stretching (1629), Ar C=C stretching (1404), Ar C-H bending (723); ^{1}H NMR (DMSO-d_6, 400MHz): δ 8.83-9.17 (m, 4H), 8.08 (s, 1H), 7.92 (d, 2H, *J*=25.6 Hz), 6.99 (d, 2H, *J* = 28.4 Hz), 2.35 (s, 3H); ESI-MS (MeOH): m/z = 327 $[M+H]^+$.

4-(1H-imidazo[4,5-f][1,10]phenanthrolin-2-yl)benzene-1,3-diol (L4): Yield: 92 %; Colour: Black; Mp: 230˚C; R_f (pure methanol): 0.39; IR (cm^{-1}): υ Ar O-H stretching (3618), N-H stretching (3130), Ar C-H stretching (3043), C=N stretching (1620), Ar C=C stretching (1404), C-N stretching (1325), Ar C-H bending (721); ^{1}H NMR (DMSO-d_6, 400MHz): δ 9.98 (s, 1H), 9.05 (s, 2H), 8.92 (t, 2H, *J*=5.2 Hz), 7.83-8.00 (m, 4H), 6.52 (t, 2H, *J*=8.0 Hz); ESI-MS (MeOH): m/z = 329.2 $[M+H]^+$.

4-bromo-2-(1H-imidazo[4,5-f][1,10]phenanthrolin-2-yl)phenol (L5): Yield: 85 %; Colour: Dark Yellow; Mp: 280˚C; R_f (pure methanol): 0.34; IR (cm^{-1}): υ Ar O-H stretching (3439), N-H stretching (3390), Ar C-H stretching (3078), C=N stretching (1606), Ar C=C stretching (1467), C-N stretching (1369), Ar C-H bending (721), C-Br stretching (626); ^{1}H NMR (DMSO-d6, 400MHz): δ 9.01 (s, 2H), 8.83 (d, 2H, J = 7.2 Hz), 8.33 (s, 1H), 7.79 (t, 2H, J = 4.4 Hz), 7.48 (d, 1H, J=8.0 Hz), 7.02 (d, 1H, J=8.0 Hz); ESI-MS (MeOH): m/z = 391 [M+H]+.

2-(1H-imidazo[4,5-f][1,10]phenanthrolin-2-yl)-6-(trifluoromethyl)phenol (L6): Yield: 90 %; Colour: Brown; Mp: 330˚C (dp) (lit. Mp: 240˚C); R_f (pure methanol): 0.55; IR (cm^{-1}): υ Ar O-H

stretching (3626), N-H stretching (3323), Ar C-H stretching (3050), C=N stretching (1622), Ar C=C stretching (1411), C-F stretching (1055), Ar C-H bending (713); ^{1}H NMR (DMSO-d_6, 400MHz): δ 9.19 (s, 1H), 9.14 (d, 1H, *J* = 7.6 Hz), 8.87-9.02 (m, 3H), 8.47 (t, 1H, *J* = 7.2 Hz), 7.77-7.95 (m, 3H); ESI-MS (MeOH): m/z = 381.1 $[M+H]^+$.

2-(1H-imidazo[4,5-f][1,10]phenanthrolin-2-yl)-4-nitrophenol (L7): Yield: 95 %; Colour: Chrome Yellow; Mp: 270˚C (lit. Mp: 240˚C); R_f (pure methanol): 0.63; IR (cm^{-1}): υ Ar O-H stretching (3610), N-H stretching (3450), Ar C-H stretching (3103), C=N stretching (1612), Ar C=C stretching (1591), N=O stretching (1469), C-N stretching (1336), N-O stretching (1298), Ar C-H bending (723); ^{1}H NMR (DMSO-d_6, 400MHz): δ 8.89-9.11 (m, 6H), 8.10 (d, 1H, *J* = 8.4 Hz), 7.81 (s, 2H), 6.92 (d, 1H, *J* = 8.0 Hz); ESI-MS (MeOH): m/z = 358.2 $[M+H]^+$.

General procedure for the synthesis of Ru(II)-*p*-cymene imidazophenanthroline complexes [RuL1-RuL7]:

At first, 20mg (0.033 mmole, 1 eqv.) of dichloro(*p*-cymene)Ruthenium (II) dimer was dissolved in minimum volume of methanol and few drops of DCM in a 50 ml round-bottom flask and was stirred continuously for 10 min to dissolve the reactant. After the complete dissolution, 2.1 equivalents of the previously synthesized ligands (**L1-L7**) were added and kept sonication for 2 h at room temperature. After that, 2.5 equivalents of ammonium hexafluorophosphate (13.3 mg, 0.082 mmole) was added again sonicated for another 90 min at room temperature. The progress of reaction was monitored by TLC. After completion of the reaction, the product formed was filtered, washed with hexane and further recrystallized from diethyl ether/Methanol (1:1) solvent system. Finally, the complexes (**RuL1-RuL7**) were obtained as yellow-brown crystals with high yield (92% -95%). The structures of products were confirmed by NMR spectroscopy, FT-IR spectroscopy and ESI-MS.

[(η^6-p-cymene)RuCl(K^2-N,N-4-(1H-imidazo[4,5-f][1,10]phenanthrolin-2-yl)phenol]PF$_6$ (RuL1): Yield: 94 %; Colour: Lemon Yellow; Mp: 185˚C; R_f (pure methanol): 0.73; IR (cm^{-1}): υ Ar O-H stretching (3321), N-H stretching (3134), Ar C-H stretching (3043), sp^3 C-H stretching (2966), C=N stretching (1604), Ar C=C stretching (1460), sp^3 C-H bending (1406), P-F stretching (831), Ar C-H bending (721); ^{1}H NMR (DMSO-d_6, 400MHz): δ 9.85 (d, 2H, H-1, H-10, *J* = 5.2 Hz, ArH), 9.35 (d, 1H, H-8, *J* = 7.6 Hz, ArH), 8.19-8.26 (m, 3H, H-2, H-3, H-9, ArH), 7.43 (t, 3H, H-15, H-16, H-17, *J* = 7.2 Hz, ArH), 6.80-6.84 (m, 1H, H-18, ArH), 6.33 (d, 1H, H-c, *J* = 6.4 Hz, *p*-cymene ArH), 6.09 (d, 1H, H-d, *J* = 8.0 Hz, *p*-cymene ArH), 5.81(d, 2H, H-e, H-f, *J* = 6.0 Hz, *p*-cymene ArH), 2.77-2.84 (m, 1H, H-h, *p*-cymene aliphatic proton), 2.19 (s, 3H, H-a, *p*-cymene aliphatic proton), 0.89 (d, 6H, H-i, H-j, *J* = 6.8 Hz, *p*-cymene aliphatic proton); ^{13}C NMR (DMSO-d_6, 100 MHz): δ 157.5, 154.4, 143.6, 138.5, 133.2, 130.6, 129.3, 126.8, 122.2, 120.0, 117.9, 116.6, 115.9, 107.0, 100.7 (*p*-cymene ArC); 86.8 (*p*-cymene ArCH), 86.7 (*p*-cymene ArCH), 85.9 (*p*-cymene ArCH), 84.3 (*p*-cymene ArCH), 30.5 (CH), 22.1(isopropyl –CH_3), 21.9 (isopropyl –CH_3), 18.3 (-CH_3); ^{19}F NMR (DMSO-d_6, 376 MHz): δ -71.03 (PF_6), -69.14 (PF_6); ^{31}P NMR (DMSO-d_6, 162 MHz): δ -153.02 to -131.07 (PF_6); ESI-MS (MeOH): m/z = 583.60 $[M\text{-}PF_6]^+$; Anal. Calcd for $C_{29}H_{26}N_4OClF_6PRu$: C, 47.84; H, 3.60; N, 7.70. Found: C, 47.56; H, 3.26; N, 7.44.

[(η^6-p-cymene)RuCl(K^2-N,N-4-(1H-imidazo[4,5-f][1,10]phenanthrolin-2-yl)-6 methoxyphenol]PF$_6$ (RuL2): Yield: 93 %; Colour: Yellow; Mp: 178˚C; R_f (pure methanol): 0.61; IR (cm^{-1}): υ Ar O-H stretching (3626), N-H stretching (3340), Ar C-H stretching (3045), sp^3 C-H stretching (2875), C=N stretching (1627), Ar C=C stretching (1427), C-N stretching (1371), C-O stretching (1253 and 1056), P-F stretching (829), Ar C-H bending (721); ^{1}H NMR (DMSO-d_6, 400MHz): δ 10.0 (t, 1H, -NH proton, *J* = 5.2 Hz), 9.86 (d, 3H, H-1, H-10, H-3, *J* = 4.8 Hz, ArH), 9.40 (d, 2H, H-8, H-15, *J* = 8.4 Hz, ArH), 8.28-8.33 (m, 1H, -OH proton), 8.2 (t, 3H, H-2, H-9, H-16, *J* = 7.2 Hz, ArH), 7.97 (d, 1H, H-17, *J* = 8.0 Hz, ArH), 6.35 (d, 2H, H-c, H-d, *J* = 6.0 Hz, *p*-cymene ArH), 6.13 (d, 2H, H-e, H-f, *J* = 6.0 Hz, *p*-cymene ArH), 3.9 (s, 1H, H-20), 2.59-2.65 (m, 1H, H-h, *p*-cymene aliphatic proton), 2.2 (s, 3H, H-a, *p*-cymene aliphatic proton), 0.92 (d, 6H, H-i, H-j, *J* = 6.8 Hz, *p*-cymene aliphatic proton); ^{13}C NMR (DMSO-d_6, 100 MHz): δ 155.4, 153.8, 149.1, 148.2, 143.5, 141.6, 137.8, 133.2, 129.3, 127.7, 126.8, 124.6, 120.8, 119.4, 118.9, 114.9, 110.4, 104.9, 101.8 (*p*-cymene ArC), 86.8 (*p*-cymene ArCH), 86.7 (*p*-cymene ArCH), 86.0 (*p*-cymene ArCH),

84.4 (*p*-cymene ArCH), 56.4 (-OMe), 30.9 (-CH), 22.1 (isopropyl –CH_3), 18.7 (-*p*-cymene -CH_3); ^{19}F NMR (DMSO-d_6, 376 MHz): δ -71.07 (PF_6), -69.18 (PF_6); ^{31}P NMR (DMSO-d_6, 162 MHz): δ -152.98 to -135.43 (PF_6); ESI-MS (MeOH): m/z = 613.6 $[M\text{-}PF_6]^+$; Anal. Calcd for $C_{30}H_{28}N_4O_2ClF_6PRu$: C, 47.53; H, 3.72; N, 7.39. Found: C, 47.11; H, 3.39; N, 7.98.

[(η^6-p-cymene)RuCl(K^2-N,N-4-(1H-imidazo[4,5-f][1,10]phenanthrolin-2-yl)benzene-1,3-diol]PF_6 (RuL3): Yield: 95 %; Colour: Dark Yellow; Mp: 180˚C; R_f (pure methanol): 0.65; IR (cm^{-1}): υ Ar O-H stretching (3660), N-H stretching (3360), Ar C-H stretching (3043), sp^3 C-H stretching (2910), C=N stretching (1629), Ar C=C stretching (1404), P-F stretching (833), Ar C-H bending (723); ^{1}H NMR (DMSO-d_6, 400MHz): δ 9.85 (d, 2H, H-1, H-10, *J* = 4.8 Hz, ArH), 9.26 (d, 2H, H-3, H-8, *J* = 8.0 Hz, ArH), 8.17-8.20 (m, 2H, H-2, H-9, ArH), 8.08 (t, 1H, H-15, *J* = 4.0 Hz, ArH), 6.92 (s, 2H, H-16, H-18, ArH), 6.34 (d, 2H, H-c, H-d, *J* = 6.4 Hz, *p*-cymene ArH), 6.11 (d, 2H, H-e, H-f, *J* = 6.0 Hz, *p*-cymene ArH), 2.58-2.64 (m, 1H, H-h, *p*-cymene aliphatic proton), 2.35 (s, 3H, H-20), 2.19 (s, 3H, H-a), 0.90 (d, 6H, H-i, H-j, *J* = 6.8 Hz, *p*-cymene aliphatic proton); ^{13}C NMR (DMSO-d_6, 100 MHz): δ 157.6 (ArC), 154.0, 152.3, 149.3, 143.4, 134.7, 132.9, 127.1, 126.6, 121.7, 121.1, 119.0, 117.9, 115.1, 104.2, 103.5 (*p*-cymene ArC), 86.7 (*p*-cymene ArCH), 85.6 (*p*-cymene ArCH), 85.0 (*p*-cymene ArCH), 84.4 (*p*-cymene ArCH), 30.9 (-CH); 22.1 (isopropyl –CH_3), 21.6 (isopropyl –CH_3); 21.0 (-CH_3); 18.7 (*p*-cymene -CH_3); ^{19}F NMR (DMSO-d_6, 376 MHz): δ -71.07 (PF_6), -69.18 (PF_6); ^{31}P NMR (DMSO-d_6, 162 MHz): δ -157.38 to -135.43 (PF_6); ESI-MS (MeOH): m/z = 597.80 $[M\text{-}PF_6]^+$. Anal. Calcd for $C_{30}H_{28}N_4OClF_6PRu$: C, 48.56; H, 3.80; N, 7.55. Found: C, 48.79; H, 3.48; N, 7.71.

[(η^6-p-cymene)RuCl(K^2-N,N-4(1H-imidazo[4,5-f][1,10]phenanthrolin-2-yl)-5 methylphenol]PF_6 (RuL4): Yield: 92 %; Colour: Greenish Yellow; Mp: 182˚C; R_f (pure methanol): 0.67; IR (cm^{-1}): υ Ar O-H stretching (3618), N-H stretching (3130), Ar C-H stretching (3043), sp^3 C-H stretching (2968), C=N stretching (1620), Ar C=C stretching (1404), C-N stretching (1325), P-F stretching (831), Ar C-H bending (721); ^{1}H NMR (DMSO-d_6, 400MHz): δ 12.28 (s, 1H, -NH proton), 10.17 (d, 1H, H-15, *J* = 9.2 Hz, ArH), 9.87 (d, 2H, H-1, H-10, *J* = 6.4 Hz, ArH), 9.52, 9.25 (s, 2H, -OH protons), 8.21 (d,

4H, H-2, H-3, H-8, H-9, *J* = 8.8 Hz, ArH), 6.53 (t, 2H, H-16, H-18, *J* = 8.8 Hz, ArH), 5.83 (d, 2H, H-c, H-d, *J* = 6.0 Hz, *p*-cymene ArH), 5.79 (d, 2H, H-e, H-f, *J* = 6.0 Hz, *p*-cymene ArH), 2.80-2.87 (m, 1H, H-h, *p*-cymene aliphatic proton), 2.2 (s, 3H, H-a, *p*-cymene aliphatic proton), 0.92 (d, 6H, H-i, H-j, *J* = 6.8 Hz, *p*-cymene aliphatic proton); ^{13}C NMR (DMSO-d_6, 100 MHz): δ 158.4, 156.1, 155.5, 153.8, 148.2, 139.7, 136.5, 129.1, 128.2, 127.6, 122.4, 121.8, 120.4, 112.4, 105.4, 103.2 (*p*-cymene ArC); 86.6 (*p*-cymene ArCH), 86.5 (*p*-cymene ArCH), 85.3 (*p*-cymene ArCH), 84.7 (*p*-cymene ArCH), 30.9 (-CH); 22.2 (isopropyl –CH_3), 22.1 (isopropyl –CH_3), 18.7 (-*p*-cymene CH_3); ^{19}F NMR (DMSO-d_6, 376 MHz): δ -71.06 (PF_6), -69.17 (PF_6); ^{31}P NMR (DMSO-d_6, 162 MHz): δ -152.98 to -135.42 (PF_6); ESI-MS (MeOH): m/z = 599.70 $[M\text{-}PF_6]^+$. Anal. Calcd for $C_{29}H_{26}N_4O_2ClF_6PRu$: C, 46.81; H, 3.52; N, 7.53. Found: C, 46.78; H, 3.31; N, 7.50.

[(η^6-p-cymene)RuCl(K^2-N,N-4-bromo-2-(1H-imidazo[4,5-f][1,10]phenanthrolin-2-yl)phenol]PF_6 (RuL5): Yield: 93 %; Colour: Bright Yellow; Mp: 196˚C; R_f (pure methanol): 0.65; IR (cm^{-1}): υ Ar O-H stretching (3439), N-H stretching (3390), Ar C-H stretching (3078), sp^3 C-H stretching (2970), C=N stretching (1606), Ar C=C stretching (1467), sp^3 C-H bending (1411), C-N stretching (1369), P-F stretching (840), Ar C-H bending (721), C-Br stretching (626); ^{1}H NMR (DMSO-d_6, 400MHz): δ 9.84 (d, 2H, H-1, H-10, *J* = 5.2 Hz, ArH), 9.24 (d, 2H, H-3, H-8, *J* = 8.0 Hz, ArH), 8.37 (s, 1H, H-17, ArH), 8.17 (t, 2H, H-2, H-9, *J* = 7.6 Hz, ArH), 7.5 (d, 1H, H-15, *J* = 8.4 Hz, ArH), 7.03 (d, 1H, H-18, *J* = 8.8 Hz, ArH), 6.34 (d, 2H, H-c, H-d, *J* = 8.0 Hz, *p*-cymene ArH), 6.11 (d, 2H, H-e, H-f, *J* = 4.0 Hz, *p*-cymene ArH), 2.57-2.64 (m, 1H, H-h, *p*-cymene aliphatic proton), 2.2 (s, 3H, H-a, *p*-cymene aliphatic proton), 0.90 (d, 6H, H-i, H-j, *J* = 4.0 Hz, *p*-cymene aliphatic proton); ^{13}C NMR (DMSO-d_6, 100 MHz): δ 153.7, 150.6 , 147.5, 145.6, 137.1, 133.8, 129.9, 129.3, 127.6, 127.4, 122.1, 118.3, 115.9, 112.1, 104.4, 102.6 (*p*-cymene ArC); 86.3 (*p*-cymene ArCH), 85.5 (*p*-cymene ArCH), 83.9 (*p*-cymene ArCH), 82.9 (*p*-cymene ArCH), 30.2 (-CH); 22.8 (isopropyl –CH_3), 20.8 (isopropyl –CH_3); 19.7 (-CH_3); ^{19}F NMR (DMSO-d_6, 376 MHz): δ -71.09 (PF_6), -69.13 (PF_6); ^{31}P NMR (DMSO-d_6, 162 MHz): δ -152.51 to -134.99 (PF_6); ESI-MS (MeOH): m/z = 661.8$[M\text{-}PF_6]^+$. Anal. Calcd for $C_{29}H_{25}N_4OBrClF_6PRu$: C, 43.16; H, 3.12; N, 6.94. Found: C, 43.23; H, 3.19; N, 7.05.

[(η^6-p-cymene)RuCl(K^2-N,N-4(1H-imidazo[4,5-f][1,10]phenanthrolin-2-yl)-6-(trifluoromethyl)phenol]PF_6 (RuL6): Yield: 95 %; Colour: Chrome Yellow; Mp: 190˚C; R_f (pure methanol): 0.71; IR (cm^{-1}): υ Ar O-H stretching (3626), N-H stretching (3323), Ar C-H stretching (3050), sp^3 C-H stretching (2950), C=N stretching (1622), Ar C=C stretching (1411), C-F stretching (1055), P-F stretching (825), Ar C-H bending (713); ^{1}H NMR (DMSO-d_6, 400MHz): δ 10.11 (t, 5H, H-1, H-3, H-8, H-9, H-10, *J* = 5.2 Hz, ArH), 10.02 (d, 1H, -NH proton, *J* = 4.8 Hz, ArH), 8.41 (t, 3H, H-2, H-15, H-17, *J* = 5.6, ArH), 8.35 (t, 1H, H-16, *J* = 5.2 Hz, ArH), 6.45 (d, 2H, H-c, H-d, *J* = 6.0 Hz, *p*-cymene ArH), 6.2 (d, 2H, H-e, H-f, *J* = 6.0 Hz, *p*-cymene ArH), 2.69-2.76 (m, 1H, H-h, *p*-cymene aliphatic proton), 2.2 (s, 3H, H-a, *p*-cymene aliphatic proton), 1.0 (d, 6H, H-i, H-j, *J* = 8.0 Hz, *p*-cymene aliphatic proton); ^{13}C NMR (DMSO-d_6, 100 MHz): δ 156.7, 154.3, 148.5, 144.5, 143.7, 133.1, 129.4, 126.7, 125.9, 120.1, 110.9, 106.9, 103.2, 100.5 (*p*-cymene ArC); 86.8 (*p*-cymene ArCH), 86.7 (*p*-cymene ArCH), 85.9 (*p*-cymene ArCH), 84.4 (*p*-cymene ArCH); 30.9 (-CH); 22.1 (isopropyl –CH_3), 21.9 (isopropyl –CH_3); 18.3 (-*p*-cymene CH_3); ^{19}F NMR (DMSO-d_6, 376 MHz): δ -71.07 (PF_6), -69.19 (PF_6), -61.41 (-CF_3); ^{31}P NMR (DMSO-d_6, 162 MHz): δ -152.99 to -135.43 (PF_6); ESI-MS (MeOH): m/z = 651.8 $[M\text{-}PF_6]^+$. Anal. Calcd for $C_{30}H_{25}N_4OClF_9PRu$: C, 45.26; H, 3.17; N, 7.04. Found: C, 45.16; H, 3.11; N, 7.08.

[(η^6-p-cymene)RuCl(K^2-N,N-4(1H-imidazo[4,5-f][1,10]phenanthrolin-2-yl)-4-nitrophenol]PF_6 (RuL7): Yield: 92 %; Colour: Dark Greenish Yellow; Mp: >200˚C; R_f (pure methanol): 0.56; IR (cm^{-1}): υ Ar O-H stretching (3610), N-H stretching (3450), Ar C-H stretching (3103), sp^3 C-H stretching (2990), C=N stretching (1612), Ar C=C stretching (1591), N=O stretching (1469), sp^3 C-H bending (1413), C-N stretching (1336), N-O stretching (1298), P-F stretching (837), Ar C-H bending (723); ^{1}H NMR (DMSO-d_6, 400MHz): δ 9.89 (d, 2H, H-1, H-10, *J* = 5.2 Hz, ArH), 9.29 (d, 2H, H-3, H-8, *J* = 8.0 Hz, ArH), 9.14 (d, 1H, H-15, *J* = 2.4 Hz, ArH), 8.19-8.26 (m, 3H, H-2, H-9, H-17, ArH), 7.22 (d, 1H, H-18, *J* = 8.4 Hz, ArH), 6.37 (d, 2H, H-c, H-d, *J* = 6.4 Hz, *p*-cymene ArH), 6.14 (d, 2H, H-e, H-f, *J* = 6.4 Hz, *p*-cymene ArH), 2.6-2.67 (m, 1H, H-h, *p*-cymene aliphatic proton), 2.2 (s, 3H, H-a, *p*-cymene aliphatic proton), 0.93 (d, 6H, H-i, H-j, *J* = 6.8 Hz, *p*-cymene aliphatic proton); ^{13}C NMR (DMSO-d_6, 100 MHz): δ 159.6, 154.5, 153.2, 151.2, 143.6, 133.2, 128.9, 126.6, 119.9, 119.4, 114.9, 106.9, 104.6, 100.5 (*p*-cymene ArC); 86.8 (*p*-cymene ArCH), 86.7 (*p*-cymene ArCH), 85.9 (*p*-cymene ArCH), 84.4 (*p*-cymene ArCH); 30.8 (-CH); 22.1 (isopropyl

–CH_3), 21.9 (isopropyl –CH_3); 18.7 (-*p*-cymene CH_3); ^{19}F NMR (DMSO-d_6, 376 MHz): δ -71.07 (PF_6), -69.18 (PF_6); ^{31}P NMR (DMSO-d_6, 162 MHz): δ -152.98 to -135.43 (PF_6); ESI-MS (MeOH): m/z = 628.6 $[M\text{-}PF_6]^+$. Anal. Calcd for $C_{29}H_{25}N_5O_3ClF_6PRu$: C, 45.06; H, 3.26; N, 9.06. Found: C, 45.11; H, 3.02; N, 9.07.

Biology

Cell culture:

In pursuit of doing the cell culture the cells were retained in DMEM media (Gibco), added with 10% fetal bovine serum (Himedia, India), 1% penicillin and streptomycin and 1% of Glutmax (Gibco, Thermo Scientific, USA) at 37°C in 5% CO_2. When the cells reached 70%-80% confluency they were trypsinized using 0.25% trypsin-EDTA (Thermo Fisher Scientific, USA).

***In vitro* cytotoxic study**

The standard MTT assay protocol was properly followed to do the In Vitro cytotoxicity study.[1] First the prepared complexes (**RuL1-RuL7**) were dissolved in 0.1% DMSO followed by dilution with DMEM medium. Two cancer cell lines *i.e*. human Epithelioid Cervix Carcinoma (HeLa), human epithelial colorectal adenocarcinoma cells (Caco-2), and one normal kidney cell (HEK 293) were used for this assay. Approximately 1×10^4 cells per well were cultured in 100 µL of a growth medium in 96-well plates and then incubated under 5% CO_2 atmosphere at 37°C temperature. Then the incubated cells were treated with different concentrations of the complexes (0-300 µM for HeLa cell and 0-150 µM for Caco-2 cell) in the volume of 100 µM/well. The cisplatin was taken as standard positive control for this experiment. The Cells which were in the control wells, also engaged the same volume of medium containing 0.1% DMSO. After 48 h, the medium was superfluous and cell cultures were again incubated with 100 µL of MTT reagent (1 mg/mL) for 5 h at 37^o C. Then the resultant suspension was kept on micro vibrator for 10 min and the absorbance was recorded at λ = 570 nm in ELISA plate reader. Similar experiment was performed in excess GSH (1mM). The experiment was also performed in triplicate. The data were represented as the growth inhibition percentage i.e. % growth inhibition = 100 − [(AD ×

100)/AB], where AD, measured absorbance in wells which contain samples and AB, measured absorbance for blank wells (cells with a medium and a vehicle).

Stability study

The stability of the Ru(II) complexes were tested in aqueous DMSO (H_2O: DMSO = 9:1), GSH medium.

Viscosity measurement

For finding out the binding mode of complexes, using compound **RuL6, RuL7** and EtBr treated DNA with respect to cisplatin; a hydrodynamic method like viscosity study was performed using Ostwald Viscometer.

DNA binding study

Electronic absorption spectroscopy was used to study the binding capacity of the complexes with calf-thymus DNA (CT-DNA) and competitive binding assay as studied using EtBr as quencher by fluorescence spectroscopy.

UV–visible studies[2]

DNA binding assay was carried out by using complexes **RuL6** and **RuL7** in Tris-HCl buffer (5 mM Tris-HCl in water, pH 7.4) in aqueous medium. The concentration of CT-DNA was calculated from its absorbance intensity at 260 nm and its known molar absorption coefficient value of 6600 $M^{-1}cm^{-1}$. Equal amount of DNA was added in both the sample and reference in cuvettes. Titration was carried out by increasing concentration of CT-DNA (0-50 µM). On the eve of each measurement, sample was equilibrated with CT-DNA for about 5 min and then absorbance of the complex was measured. The intrinsic DNA binding constant (K_b) was calculated using the equation (i):

$$\frac{[DNA]}{(\varepsilon_a - \varepsilon_f)} = \frac{[DNA]}{(\varepsilon_b - \varepsilon_f)} + \frac{1}{K_b(\varepsilon_a - \varepsilon_f)} \quad (i)$$

Where [DNA] is the concentration of DNA in the base pairs, ε_a is the apparent extinction coefficient observed for the complex, the term ε_f correspond to the extinction coefficient of the complex in its free form and ε_b refers to the extinction coefficient of the complex when fully bound to DNA. The

resultant data were plotted using Origin Lab, version 8.5 to obtain the [DNA]/(ε_a-ε_f) vs. [DNA] linear plot. The ratio of the slope to intercept from the linear fit gave the values of the intrinsic binding constants (K_b).

UV and Fluorescence study

UV and Fluorescence study of all these Ru(II) complexes were executed in 10 % DMSO solution. Then the fluorescence quantum yields (Φ) were calculated by applying the comparative William's method which involves the use of well-characterized standard with known quantum yield value using 10% DMSO solution.[3] Quinine sulphate was used as a standard. Quantum yield was calculated according to the equation (ii):

$$\varphi = \varphi_R \times \frac{I_S}{I_R} \times \frac{OD_R}{OD_S} \times \frac{\eta_S}{\eta_R} \cdots\cdots\cdots (ii)$$

Where, φ = quantum yield, I = peak area, OD = absorbance at λ_{max}, η = refractive index of solvent (s) and reference (R). Here, we have used quinine sulphate as a standard for calculating the quantum yield.

Ethidium bromide displacement assay

Ethidium bromide (EtBr) displacement assay was carried out to illustrate the mode of binding between the potent compounds with DNA.[4] The apparent binding constant (K_{app}) of the complexes **RuL6** and **RuL7** to CT-DNA were calculated using EtBr as a spectral probe in 5 mM Tris-HCl buffer (pH 7.4). EtBr was not able to exhibit any fluorescence in its free state as its fluorescence was quenched by the solvent molecules. But its fluorescence intensity was started to increase in presence of CT-DNA, which suggested the intercalative mode of binding of EtBr with DNA grooves. The fluorescence intensity was found to decrease with further increase in concentration of the complexes. Thus it can be said that the complexes displaced EtBr from CT-DNA grooves and the complexes themselves got bound to the DNA base pairs. The values of the apparent binding constant (K_{app}) were obtained by using the equation (iii):

$$K_{app} \times [Complex]_{50} = k_{EtBr} \times [EtBr] \cdots\cdots\cdots (iii)$$

Where K_{EtBr} is the EtBr binding constant (K_{EtBr} = 1.0 × 10^7 M^{-1}), and [EtBr] = 8 × 10^{-6} M. Stern-Volmer equation was followed for quantitative determination of the Stern-Volmer quenching constant (K_{SV}).[5] Origin 8.5 software was used to plot the fluorescence data to obtain linear plot of I_0/I vs. [complex]. The value of K_{SV} was calculated from the following equation.

$$I_0/I = 1 + \mathrm{K}_{SV}[Q] \quad (iv)$$

Where I_0 = fluorescence intensity in absence of complex and I = fluorescence intensities in presence of complex of concentration [Q].

Protein binding studies

We know that serum albumin proteins are the main component in blood plasma proteins and plays important roles in drug transport and metabolism interaction of the drug with bovine serum albumin (BSA), a structural homologue of human serum albumin (HSA) was studied from tryptophan emission quenching experiment.[6] Tryptophan emission quenching experiment was performed to detect the interaction of the ruthenium complex **RuL6** and **RuL7** with protein BSA. Initially, BSA solution (2 × 10^{-6} M) was prepared in Tris-HCl/NaCl buffer. The aqueous solutions of the complexes were subsequently added to BSA solution with gradual increase of their concentrations. After each addition, the solutions were shaken slowly for 5 min before recording the fluorescence at a wavelength of 295 nm (λ_{ex} = 295 nm). A gradual decrease in fluorescence intensity of BSA at λ = 340 nm was observed upon increasing the concentration of complex, which confirmed that the interaction between the complex and BSA was happened. Stern-Volmer equation was employed to quantitatively determine the quenching constant (K_{BSA}). Origin Lab, version 8.5 was used to plot the emission spectral data to obtain linear plot of I_0/I vs. [complex] using the equation (v) given below:

$$I_0/I = 1 + \mathrm{K}_{BSA}[Q] = 1 + k_q\tau_0[Q] \quad (v)$$

Where I_0 is the fluorescence intensity of BSA in absence of complex and I indicates the fluorescence intensity of BSA in presence of complex of concentration [Q], τ_0 = lifetime of the tryptophan in BSA

found as 1×10^{-8} and k_q is the quenching constant. Scatchard equation (vi) gives the binding properties of the complexes.[7] Where K = binding constant and n = number of binding sites.

$$\log\left(I_0 - I/I\right) = \log K + n\log\left[Q\right] \quad (vi)$$

Conductivity measurement[8]

For validating the interaction of the complexes with DMSO, aqueous DMSO, GSH and Ct-DNA solutions, conductivity of the prepared complexes were performed using conductivity-TDS meter-307 (Systronics, India) and cell constant 1.0 cm^{-1}. Complex concentration was taken as 3×10^{-5} M.

n-Octanol-water partition coefficient (log $P_{o/w}$)

The log $P_{o/w}$ of the ruthenium complexes were followed shake flask method using the previously published procedure.[9] A known amount of each complex (**RuL1-RuL7**) was suspended in water (pre-saturated with n-octanol) and shaken for 48 h on an orbital shaker. To allow the phase separation, the solution was centrifuged for 10 min at 3000 rpm. Then the amount of ruthenium present in saturated aqueous solution was measured by ICP-MS. To obtain the partition coefficient, different ratios (0.5:1, 1:1, and 2:1) of the saturated solutions were shaken with pre-saturated n-octanol for 20 min on an orbital shaker and followed the same procedure.

Notes and References

1. Liu,P.; Wu,B.; Liu,J.; Dai,Y.; Wang, Y.; Wang, K.; DNA Binding and Photocleavage Properties, Cellular Uptake and Localization, and in-Vitro Cytotoxicity of Dinuclear Ruthenium(II) Complexes with Varying Lengths in Bridging Alkyl Linkers, *Inorg. Chem.* **2016**, *55*, 1412−1422.
2. Sirajuddin, M.; Ali, S.; Badshah, A.; Drug–DNA interactions and their study by UV–Visible, fluorescence spectroscopies and cyclic voltammetry, *J. Photochem. Photobio. B*., **2013**, *124*, 1–19.
3. Shamsi-Sani, M.; hirini, F.; Abedini, SM.; Seddighi, M.; Synthesis of benzimidazole and quinoxaline derivatives using reusable sulfonated rice husk ash (RHA-SO3H) as a green and efficient solid acid catalyst, *Res. Chem. Intermed*., **2016**, *42*, 1091–1099.

4. Dasari, S.; Patra, A. K.; Luminescent europium and terbium complexes of dipyridoquinoxaline and dipyridophenazine ligands as photosensitizing antennae: structures and biological perspectives, *Dalton Trans*., **2015**, *44*, 19844-19855.
5. Keizer, J.; Nonlinear fluorescence quenching and the origin of positive curvature in Stern-Volmer plots, *J. Am. Chem. Soc*., **1983**, *105*, 1494–1498.
6. Suryawanshi, V. D.; Walekar, L. S.; Gore, A. H.; Anbhule, P. V.; Kolekar, G. B. Spectroscopic analysis on the binding interaction of biologically active pyrimidine derivative with bovine serum albumin, *J. Pharm. Anal*., **2016**, *6*, 56–63.
7. Jeyalakshmi, K.; Haribabu, J.; Balachandran, C.; Swaminathan, S.; Bhuvanesh, N. S. P.; Karvembu,R.; Coordination Behavior of N,N′,N″-Trisubstituted Guanidine Ligands in Their Ru–Arene Complexes: Synthetic, DNA/Protein Binding, and Cytotoxic Studies, *Organometallics***2019**, *38*, 753−770.
8. Nikolić, S.; Rangasamy, L.; Gligorijević, N.; Aranđelović, S.; Radulović, S.; Gasser, G.; Grgurić-Šipka, S.; Synthesis, characterization and biological evaluation of novel Ru(II)–arene complexes containing intercalating ligands, *J. Inorg. Biochem.***2016**, *160*, 156–165.
9. Kubanik, M.; Holtkamp, H.; Söhnel, T.; Jamieson, S. M. F.; Hartinger,C. G.; Impact of the Halogen Substitution Pattern on the Biological Activity of Organoruthenium 8-Hydroxyquinoline Anticancer Agents, *Organometallics*, **2015**, *34*, 5658–5668.